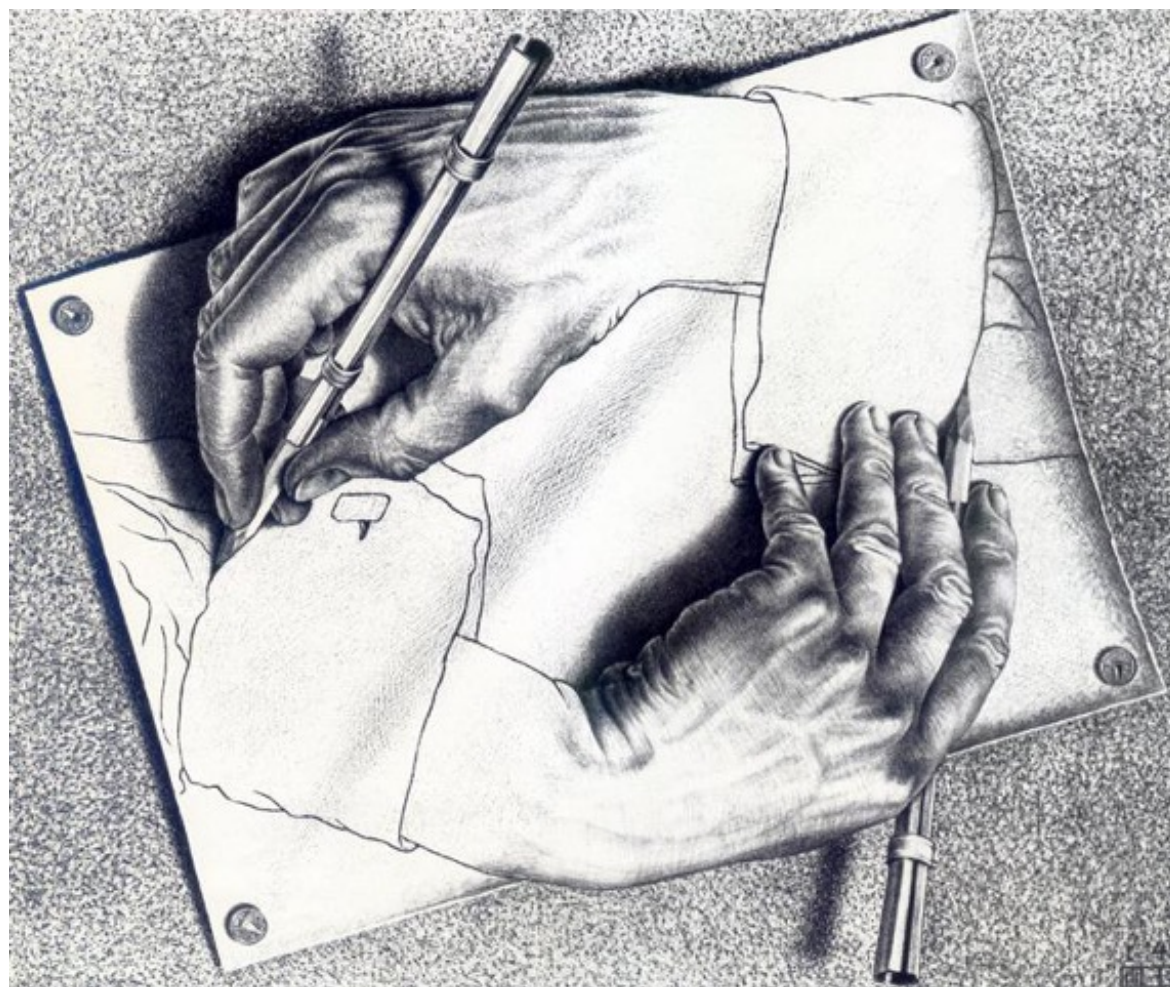

Fundamental Symmetries

David Kawall, University of Massachusetts Amherst



- Ramsey's method of Separated Oscillatory Fields for EDM searches
- Statistical Sensitivity of typical EDM experiment
- CeNTREX experiment
- ACME experiment

- How do we measure an EDM? We place the particles in parallel (or anti-parallel) electric and magnetic fields and measure their Larmor precession frequency.
- The energy of the states depends on the relative orientation of the spin and the fields:

$$h\nu = 2\mu B \pm 2dE$$

The Experimental Protocol:

1. Measure the precession frequency $\nu_{\uparrow\uparrow}$ with \vec{E} parallel to \vec{B} .
2. Reverse the electric field direction so \vec{E} is anti-parallel to \vec{B} .
3. Measure the new precession frequency $\nu_{\uparrow\downarrow}$.

The difference in frequency isolates the EDM contribution:

$$\Delta\nu = \nu_{\uparrow\uparrow} - \nu_{\uparrow\downarrow} = \frac{4dE}{h} \quad \Longrightarrow \quad \boxed{d = \frac{h\Delta\nu}{4E}}$$

Challenge: We need to measure $\Delta\nu$ with extraordinary precision.

Before Ramsey, the standard technique was I.I. Rabi's method (1938).

- Atoms pass through a *single* continuous oscillating field region of length L .
- The interaction time is $\tau = L/v$.
- The transition probability is given by the Rabi formula:

$$P(\delta) = \frac{\Omega^2}{\Omega^2 + \delta^2} \sin^2 \left(\frac{\sqrt{\Omega^2 + \delta^2} \tau}{2} \right)$$

- The linewidth (FWHM) of the central resonance is $\Delta\nu \approx \Omega/\pi \approx 1/\tau$.

Limitations of the Rabi Method

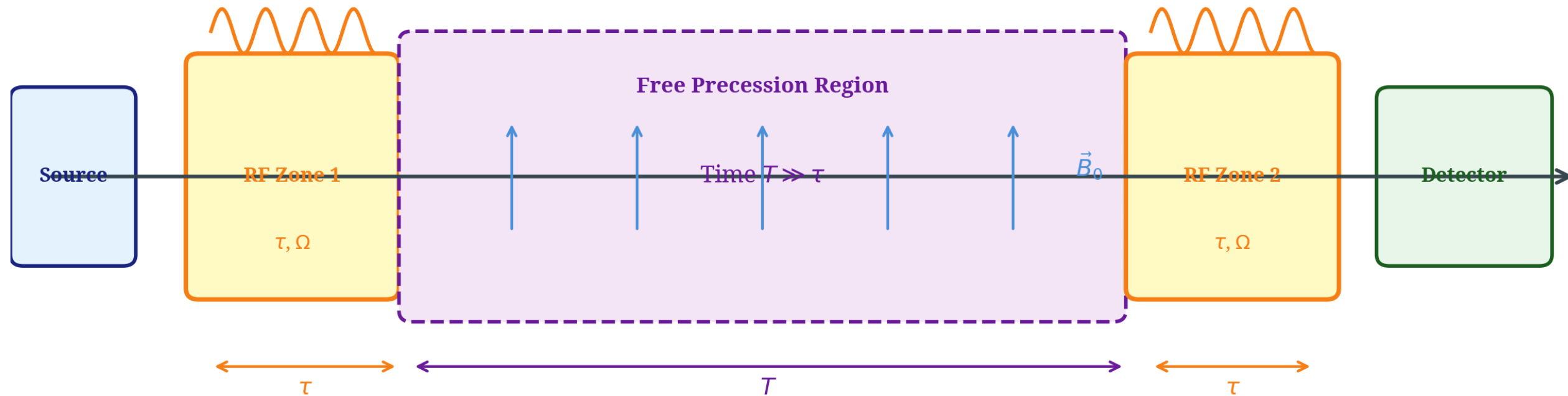
- Linewidth is $\delta \approx \pi/\tau \approx \pi v/L$
- Narrower linewidth requires long interaction time τ and/or L
- This requires making the RF cavity very long.
- Difficult to maintain a perfectly uniform B_0 field over a large spatial volume. Field inhomogeneities broaden and wash out the resonance line.
- Tradeoff between resolution and systematic errors

Ramsey's Insight (1949/1950)

- Replace single long zone with two short zones separated by a long field-free region. Precision is set by drift time T .

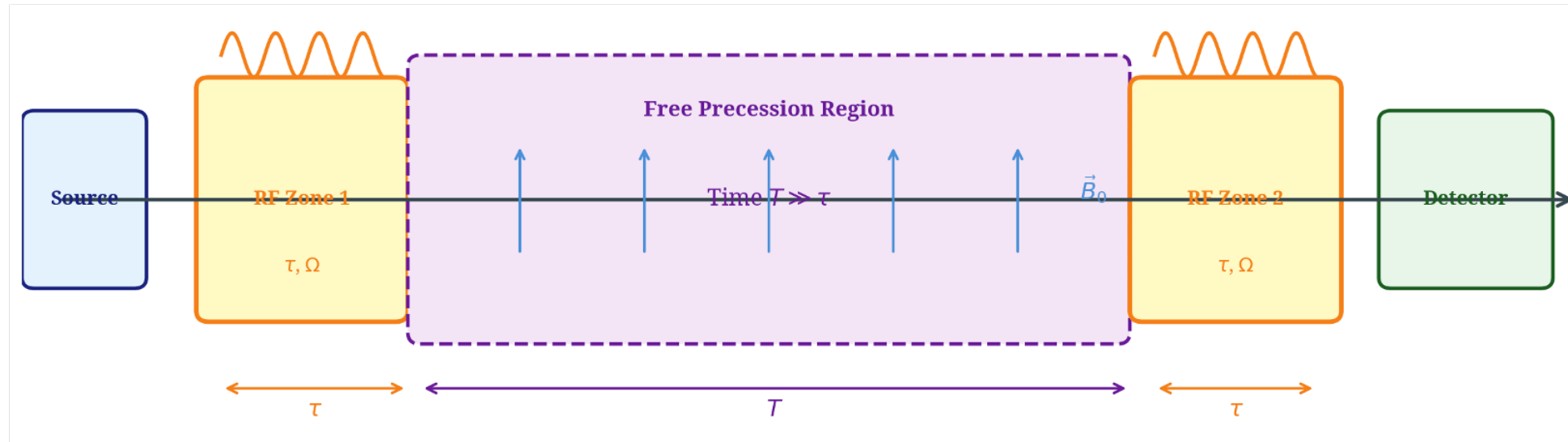
Norman Ramsey (1949) solved this by separating the oscillatory field into two short regions, separated by a long field-free region.

Ramsey Separated Oscillatory Fields — Apparatus Schematic



- **Zone 1:** First RF pulse of duration τ creates a coherent superposition (a $\pi/2$ pulse).
- **Free Precession:** Spins precess in B_0 (and E) for a long time $T \gg \tau$.
- **Zone 2:** Second RF pulse of duration τ recombines the states (interferometry).

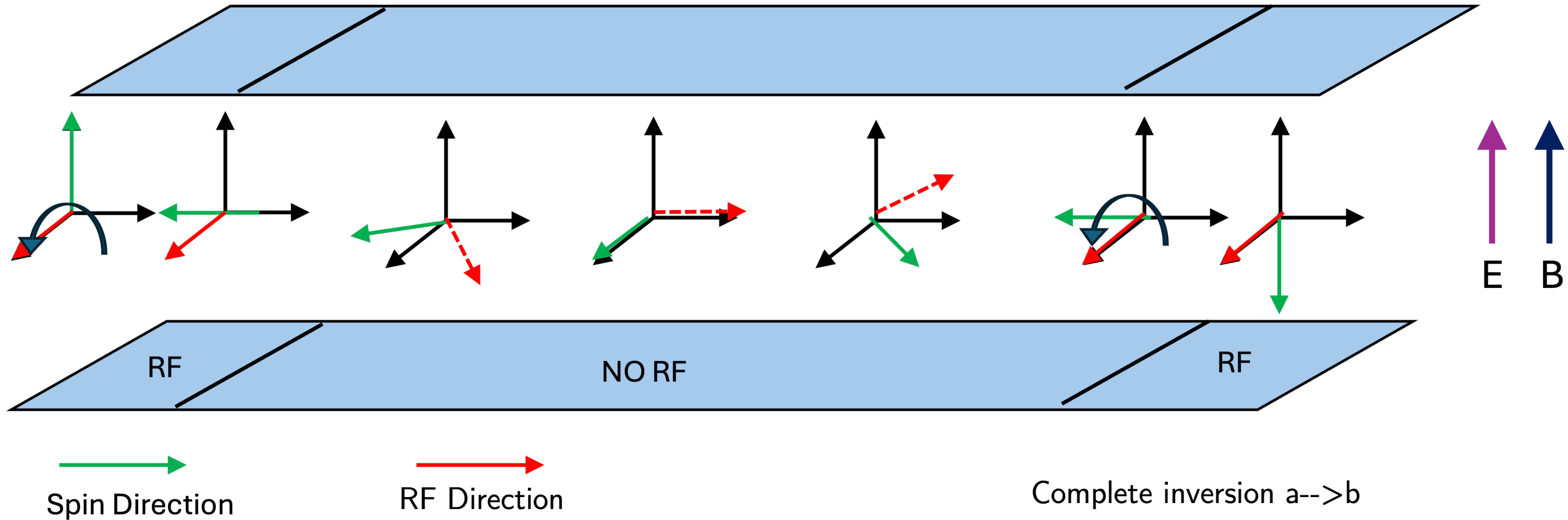
Ramsey's Method of Separated Oscillatory Fields: Physical Setup



Region	Duration	Field Applied
First interaction zone	τ	Oscillating field $\mathbf{B}_{\perp} \cos(\omega t)$
Free-precession (drift)	$T \gg \tau$	Static field \mathbf{B}_{\parallel} only
Second interaction zone	τ	Oscillating field (phase-coherent)

- Key requirement is **phase coherence** between the two oscillating fields — both driven by the same oscillator.
- In the free-precession zone, the magnetic moment precesses at Larmor frequency $\omega_0 = \mu B_{\parallel} / \hbar$. Accumulated phase difference is $\phi = (\omega_0 - \omega)T = \delta T$.
- **Physical picture:** The first pulse creates a superposition state ($\pi/2$ rotation). The atom freely accumulates phase for time T . The second pulse reads out this phase.

Ramsey Separated Oscillatory Fields



Note: if we had π phase shift between two RF regions, we would return $|a\rangle \rightarrow |a\rangle$

Consider a two-level atom $\{|a\rangle, |b\rangle\}$ with transition frequency ω_0 . In the rotating frame (RWA), the Hamiltonian is:

$$\hat{H} = \frac{\hbar}{2} \begin{pmatrix} \delta & \Omega \\ \Omega & -\delta \end{pmatrix}$$

Solution to the Schrödinger equation for initial conditions $a(t_0) = a_0, b(t_0) = b_0$:

$$a(t + t_0) = a_0 \left[\cos \frac{\Omega_g t}{2} - \frac{i\delta}{\Omega_g} \sin \frac{\Omega_g t}{2} \right] - b_0 \frac{i\Omega}{\Omega_g} \sin \frac{\Omega_g t}{2}$$
$$b(t + t_0) = -a_0 \frac{i\Omega}{\Omega_g} \sin \frac{\Omega_g t}{2} + b_0 \left[\cos \frac{\Omega_g t}{2} + \frac{i\delta}{\Omega_g} \sin \frac{\Omega_g t}{2} \right]$$

In the free-precession zone ($\Omega = 0$): pure phase accumulation, $a \rightarrow a e^{-i\delta T/2}, b \rightarrow b e^{+i\delta T/2}$.

- **Note:** This uses oscillating field Ω along \hat{x}
- Using $\Omega e^{i\phi}$ changes this direction. Can use this freedom to make phase shifts between the two RF regions

- The full sequence is a product of three propagators. For the interaction zones:

$$U_{\text{int}}(\tau) = \begin{pmatrix} \cos\frac{\Omega_g\tau}{2} - \frac{i\delta}{\Omega_g} \sin\frac{\Omega_g\tau}{2} & -\frac{i\Omega}{\Omega_g} \sin\frac{\Omega_g\tau}{2} \\ -\frac{i\Omega}{\Omega_g} \sin\frac{\Omega_g\tau}{2} & \cos\frac{\Omega_g\tau}{2} + \frac{i\delta}{\Omega_g} \sin\frac{\Omega_g\tau}{2} \end{pmatrix}$$

- For the free-precession zone ($\Omega = 0$):

$$U_{\text{free}}(T) = \begin{pmatrix} e^{-i\delta T/2} & 0 \\ 0 & e^{+i\delta T/2} \end{pmatrix}$$

- The total evolution operator is:

$$U_{\text{Ramsey}} = U_{\text{int}}(\tau) \cdot U_{\text{free}}(T) \cdot U_{\text{int}}(\tau)$$

- Matrix multiplication produces cross terms — interference between transitions in the *first* vs. *second* zone.
- This is the origin of **Ramsey fringes**.

- Assuming the system starts in the ground state $|g\rangle = \begin{pmatrix} 0 \\ 1 \end{pmatrix}$, we compute the final amplitude $c_e = (U_{\text{total}})_{12}$.
- After multiplying the matrices and taking the absolute square $P(\delta) = |c_e|^2$, we obtain the exact Ramsey transition probability $P = |b(2\tau + T)|^2$:

$$P_{\text{Ramsey}}(\delta, T, \tau) = \frac{4\Omega^2}{\Omega_g^2} \sin^2\left(\frac{\Omega_g\tau}{2}\right) \left[\cos\frac{\Omega_g\tau}{2} \cos\frac{\delta T}{2} - \frac{\delta}{\Omega_g} \sin\frac{\Omega_g\tau}{2} \sin\frac{\delta T}{2} \right]^2$$

Physical Interpretation

- **Rabi envelope:** The prefactor is the transition probability for a single zone.
- **Interference factor:** The bracketed term contains the cosine of the accumulated phase $\delta T/2$.

The $\pi/2$ -Pulse Limit

- For $\Omega_g\tau = \pi/2$ and $|\delta| \ll \Omega$:

$$P_{\text{Ramsey}} \approx \cos^2\left(\frac{\delta T}{2}\right)$$

- This is the **ideal Ramsey fringe** — a pure cosine-squared oscillation with period $\Delta\delta = 2\pi/T$.

- The state vector $\mathbf{r} = (\langle\sigma_x\rangle, \langle\sigma_y\rangle, \langle\sigma_z\rangle)$ traces a path on the unit sphere.

- **Step 1: First $\pi/2$ Pulse**

Starting from south pole $|a\rangle$, rotate by $\pi/2$ about x-axis.

State becomes equatorial superposition:

$$\frac{1}{\sqrt{2}}(|a\rangle - i|b\rangle)$$

- **Step 2: Free Precession**

Precess about z-axis at detuning rate δ . Accumulated angle $\phi = \delta T$:

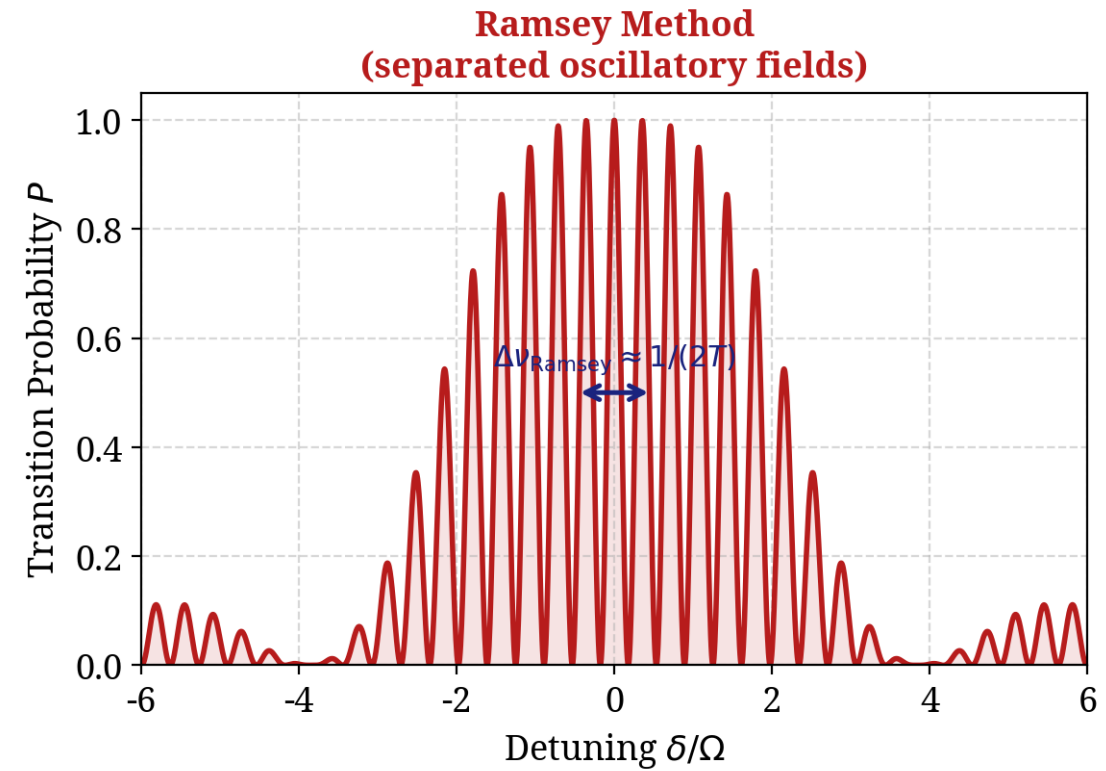
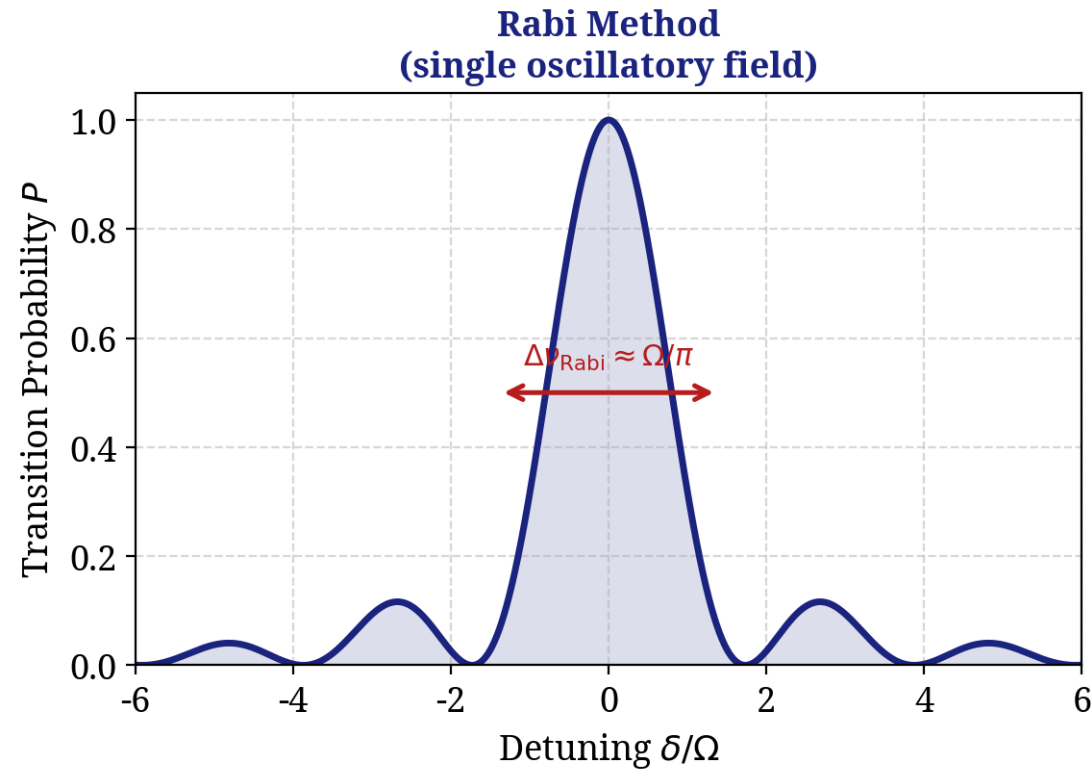
- If $\delta = 0$: no precession.
- If $\delta \neq 0$: rotates by δT .

- **Step 3: Second $\pi/2$ Pulse**

Rotate by $\pi/2$ about x-axis. Final z-projection depends on δT :

- If $\delta T = 0$: reaches $|b\rangle$, $P = 1$.
- If $\delta T = \pi$: returns to $|a\rangle$, $P = 0$.

- **Oscillation between $P = 0$ and $P = 1$ produces the Ramsey fringes.**

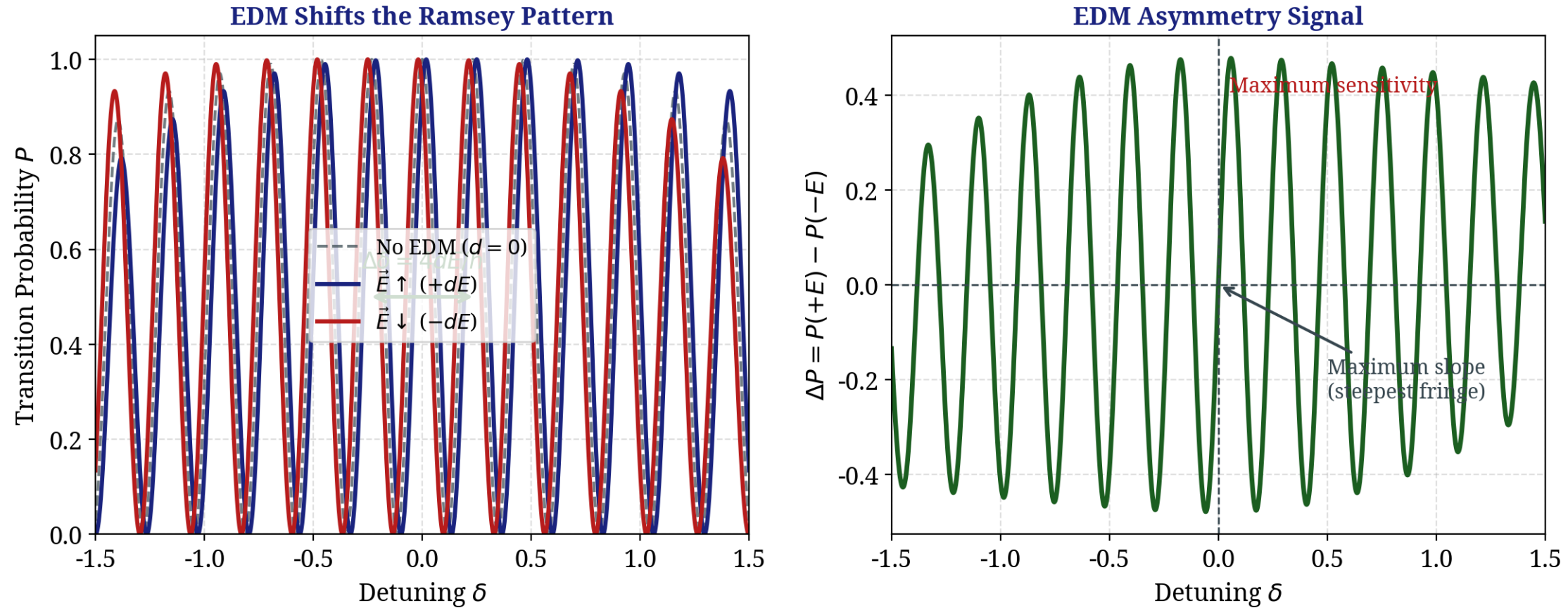


Rabi Method

- Linewidth determined by total time in the RF field.
- Highly sensitive to B -field inhomogeneity over the entire RF cavity.

Ramsey Method

- Linewidth determined by the *free precession* time T .
- RF zones can be very short; only the *average* B -field in the free region matters.
- Central fringe FWHM $\Delta\nu \approx 1/(2T)$



The EDM Shift

- Reversing the E-field shifts the entire Ramsey fringe pattern by $\Delta\delta = 4dE/\hbar$
- Park the laser/RF frequency at the steepest part of the central fringe (maximum slope).
- A small horizontal shift $\Delta\delta$ translates into a large change in transition probability ΔP .

Ramsey Transition Probability

In ideal Ramsey separated oscillatory fields experiment using $\pi/2$ pulses, transition probability from $|g\rangle$ to $|e\rangle$ given by:

$$P(\delta) = \frac{1}{2} [1 + \cos(\delta T)]$$

where:

- T is the free precession time between the two RF zones.
 - $\delta = \omega - \omega_0$ is detuning of applied RF frequency ω from Larmor precession frequency ω_0 .
-

In actual experiment, fringe contrast reduced by:

- Imperfect polarization
- Decoherence
- Velocity spread
- Background counts

Account for this with **visibility parameter** $\alpha \leq 1$:

$$P(\delta) = \frac{1}{2} [1 + \alpha \cos(\delta T)]$$

To measure EDM tiny shift in resonance frequency, want probability P to change as much as possible for a small change in δ .

Want to sit on maximum of fringe slope

- The slope of the fringe is:

$$\frac{dP}{d\delta} = -\frac{\alpha T}{2} \sin(\delta T)$$

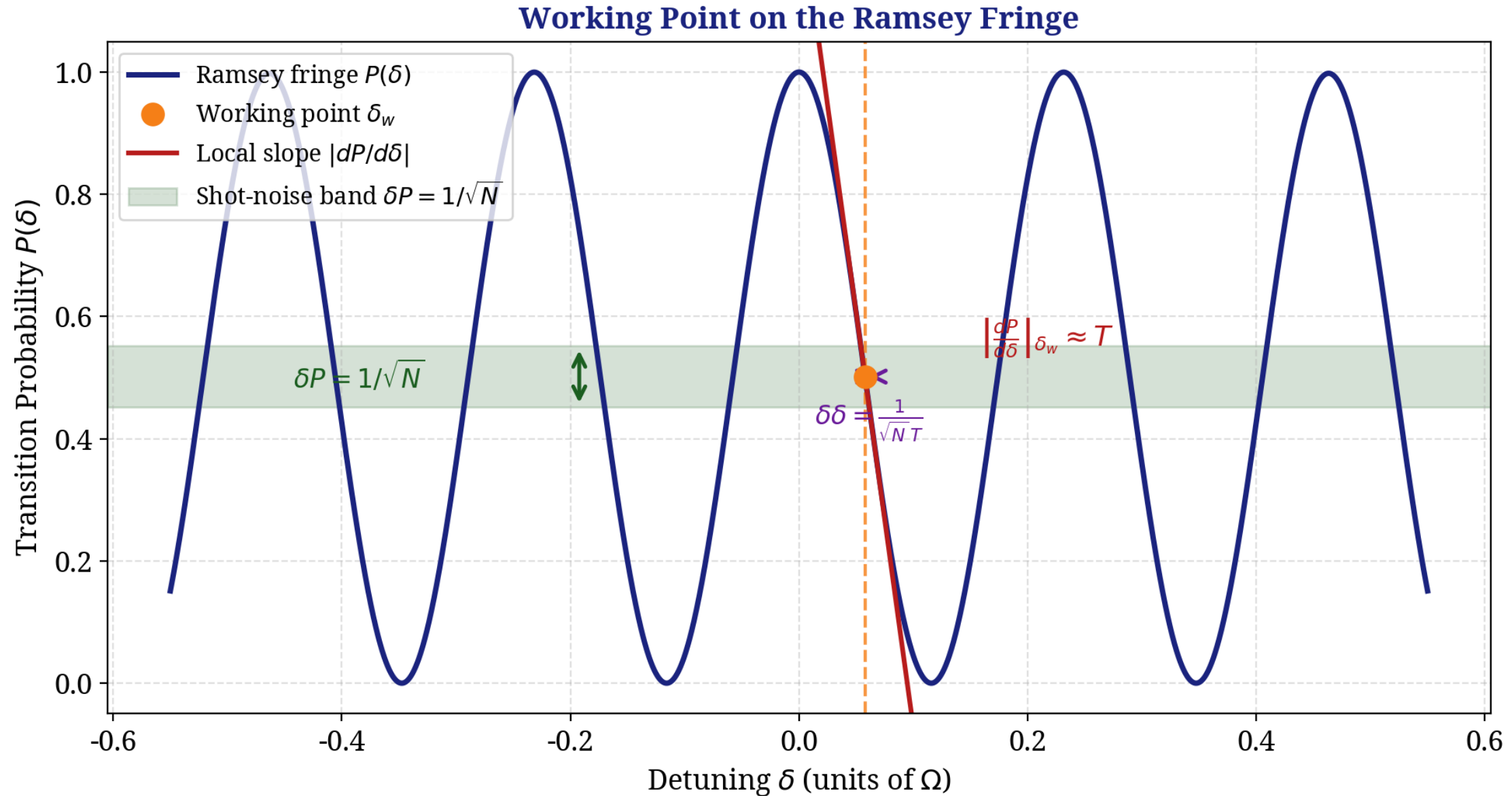
- Slope maximized when $\sin(\delta T) = \pm 1$, which occurs at detunings:

$$\delta_w = \pm \frac{\pi}{2T}, \pm \frac{3\pi}{2T}, \dots$$

- At this optimal working point, the magnitude of the slope is:

$$\left| \frac{dP}{d\delta} \right|_{\max} = \frac{\alpha T}{2}$$

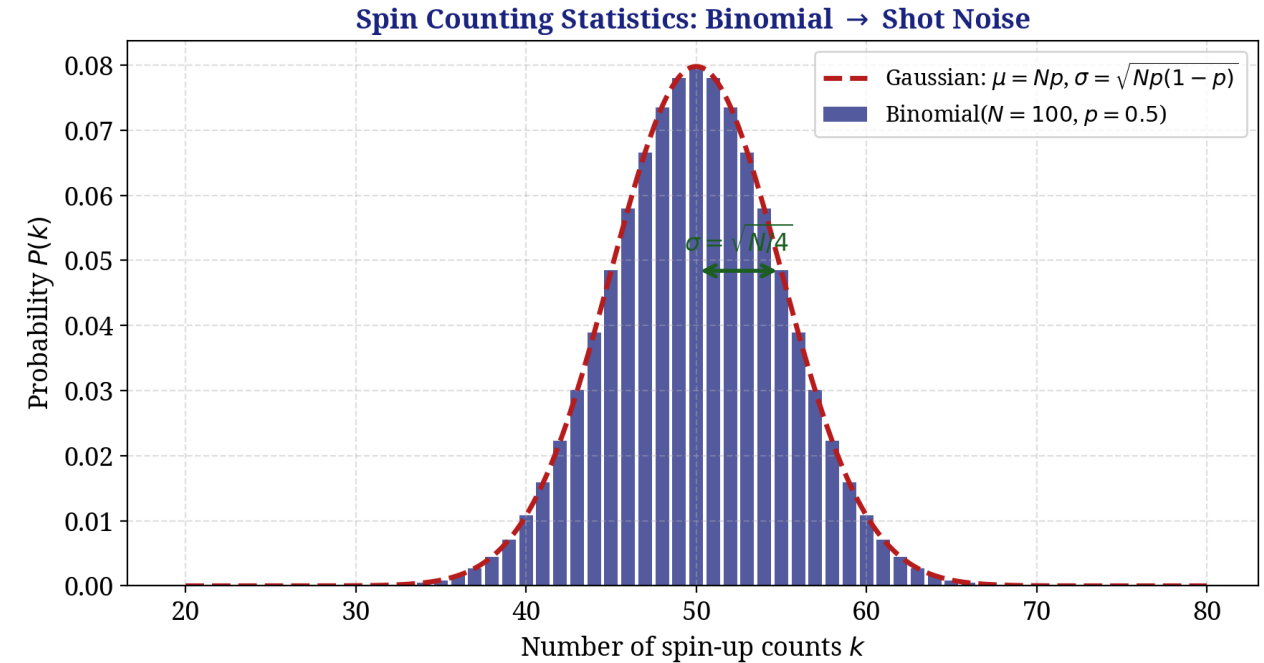
⇒ Notice the importance of maximizing coherence time T



- Tuning RF frequency to δ_w , shifts in precession frequency ($\delta\delta$) translate linearly into a change in transition probability (δP).

- Count N total particles per measurement cycle
- Number of particles detected in state $|e\rangle$ is N_e .
- Since each particle detection is an independent Bernoulli trial with probability P , N_e follows a binomial distribution
- Variance in the number of counts is:

$$\sigma_{N_e}^2 = NP(1 - P)$$



At working point $\delta_w = \pi/(2T)$, the probability is $P = 1/2$. This yields:

$$\sigma_{N_e}^2 = N \binom{1}{2} \binom{1}{2} = \frac{N}{4}$$

The uncertainty in the *measured probability* $P = N_e/N$ is the **shot noise**.

⇒ Shot-Noise Uncertainty in Probability:

$$\delta P = \frac{\sigma_{N_e}}{N} = \frac{\sqrt{N/4}}{N} = \frac{1}{2\sqrt{N}}$$

- We know uncertainty in measured probability (δP)
- We know how probability relates to frequency detuning via the slope at the working point

$$\delta P = \left| \frac{dP}{d\delta} \right| \Delta\omega$$

- Substituting our known expressions:

$$\frac{1}{2\sqrt{N}} = \left(\frac{\alpha T}{2} \right) \Delta\omega$$

- Solving for shot-noise limited frequency resolution $\Delta\omega$:

$$\Delta\omega = \frac{1}{\alpha T \sqrt{N}} \text{ rad/s}$$

- Relate the frequency resolution $\Delta\omega$ to the EDM
- Larmor precession frequency shifts when electric field \vec{E} reversed relative to magnetic field \vec{B}_0 :

$$\hbar\omega_{\uparrow\uparrow} = 2\mu B_0 + 2dE \quad \text{and} \quad \hbar\omega_{\uparrow\downarrow} = 2\mu B_0 - 2dE$$

- The difference between the two configurations is:

$$\hbar\Delta\omega = 4dE \implies d = \frac{\hbar\Delta\omega}{4E}$$

- Since we measure ω twice (once for $+E$, once for $-E$), the variance doubles, adds factor of $\sqrt{2}$. However, for *total* of N particles across both measurements, the standard form is:

$$\text{Shot-Noise Limited EDM Sensitivity: } \sigma_d = \frac{\hbar}{2E\alpha T\sqrt{N}}$$

- **Maximize E**: use higher voltages or polar molecules with large internal E_{eff}
- **Maximize T**: use UCN, slow molecular beams, trapped molecules
- **Maximize N**: increase source intensity, detection efficiency

- Use external electric field to polarize the electron cloud of atom or molecule
- Equal superposition of states of opposite parity yields largest polarization, largest internal electric field
- In atoms, states of opposite parity (s and p) typically of order 1 eV apart = $1.6 \times 10^{-19} \text{ J} \leftrightarrow 100 \text{ THz}$
- Very hard to make large admixture of s and p , need huge electric fields
- Apply external field \mathbf{E}_0 , with Stark interaction $H' = -e\mathbf{r} \cdot \mathbf{E}_0$, estimate admixture

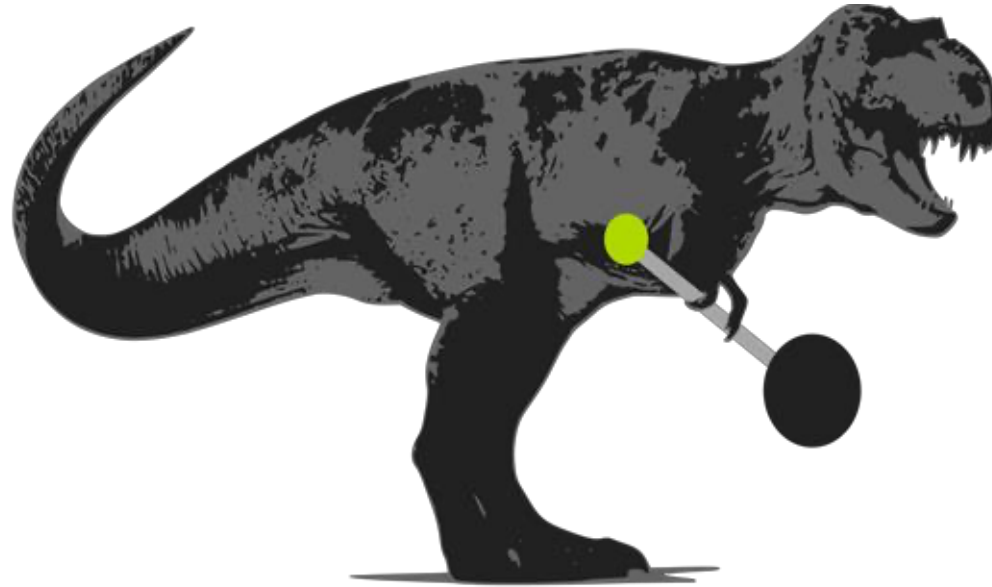
$$\begin{aligned} \Delta E_{edm} &= \langle \tilde{\Psi} | H' | \tilde{\Psi} \rangle \approx \langle j | \mathbf{d}_e \cdot \mathbf{E}_{int} | i \rangle \frac{\langle j | e\mathbf{r} \cdot \mathbf{E}_0 | i \rangle}{E_i - E_j} \\ &\approx d_e E_{int} \frac{\langle j | e\mathbf{r} \cdot \mathbf{E}_0 | i \rangle}{E_i - E_j} \approx d_e E_{eff} \end{aligned}$$

- For atom:

$$\frac{\langle j | e\mathbf{r} \cdot \mathbf{E}_0 | i \rangle}{E_i - E_j} \approx \frac{1.6 \times 10^{-19} \text{ C} \cdot 5.3 \times 10^{-11} \text{ m} \cdot 1 \text{ MV/m}}{6.6 \times 10^{-34} \text{ J} \cdot 100 \text{ THz}} \approx 10^{-4}$$

- Can get near full polarization if $E_i - E_j \approx 10 \text{ GHz}$, typical rotational splitting in heavy diatomic molecule!
 - Some molecules have Ω -doublets with $E_i - E_j \approx 10 \text{ MHz}$ or less
 - Fully polarized in fields of $< 1 \text{ kV/cm}$, access internal electric fields $\gg 10 \text{ GV/cm}$
 - Dysprosium, radium, Ytterbium have accidental near degeneracies
- \Rightarrow EDM signal much larger when opposite parity states closely spaced in energy and in large electric fields

Progress towards a measurement of the Schiff moment of ^{205}Tl in
TlF Molecules with CeNTREX



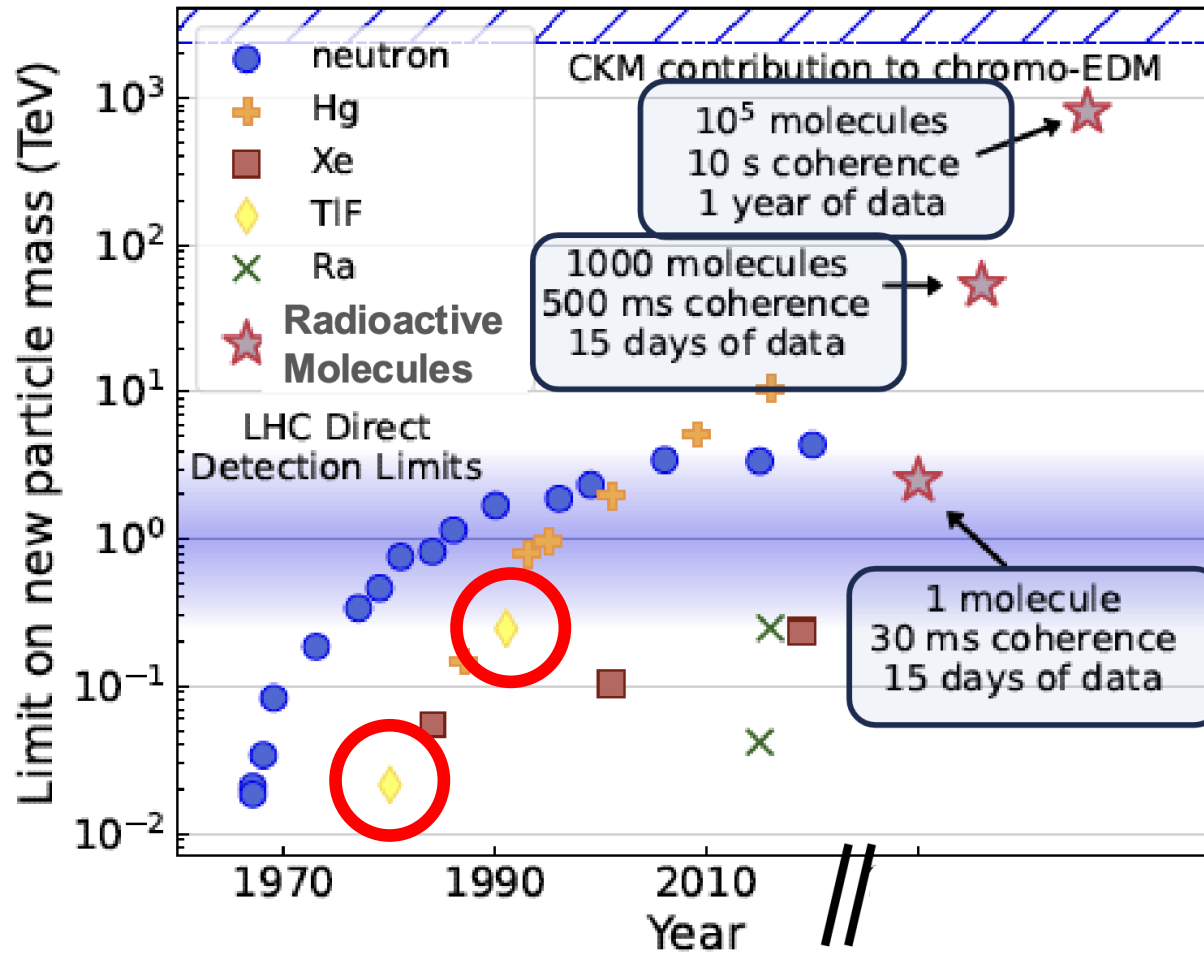
CeNTREX

Cold molecule **Nuclear Time Reversal EX**periment

Dave Kawall, University of Massachusetts Amherst

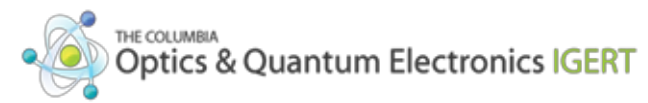
Fundamental Symmetries, APR 05 2024, UW

Progress towards a measurement of the Schiff moment of ^{205}Tl in TIF Molecules with CeNTREX



From Ronald Garcia Ruiz

CeNTREX Team



Principal Investigators

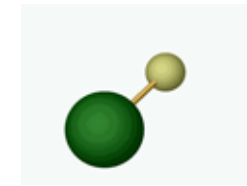


David DeMille
Argonne,
U Chicago,
Johns Hopkins U

David Kawall
UMass,
Amherst

Tanya Zelevinsky
Columbia

DeMille



Group



Research Scientist



Olivier Grasdijk
Argonne

Ph.D. students



Jianhui Li
Columbia



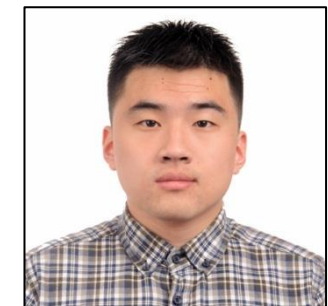
Yuanhang Yang
UChicago



Perry Zhou
Columbia



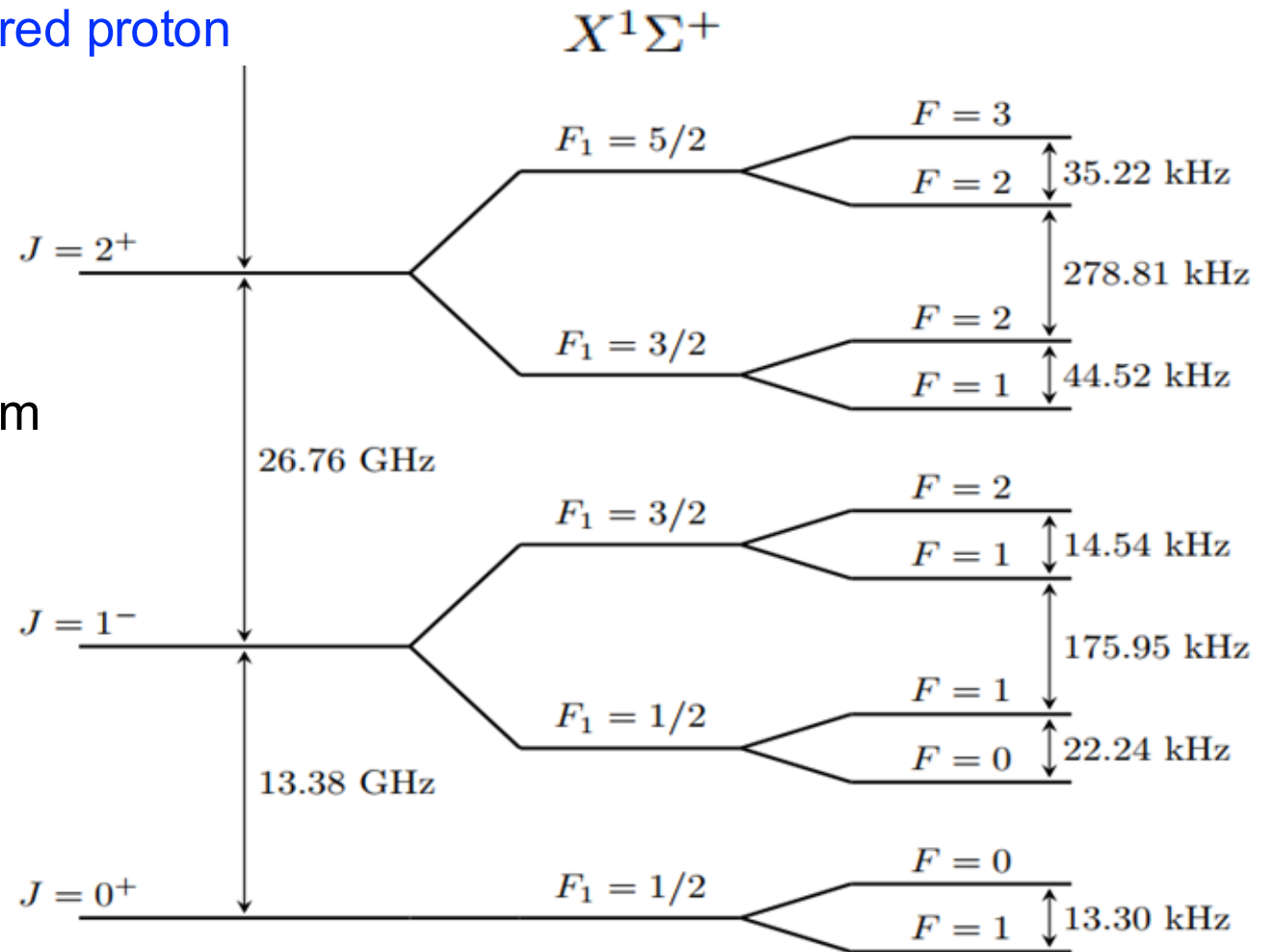
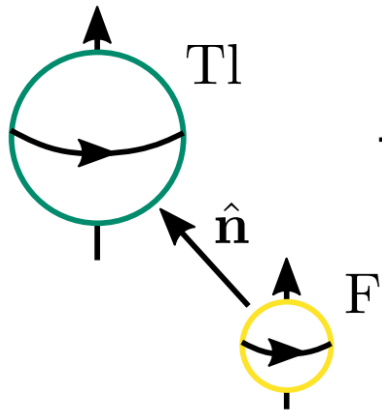
Emma McClure
UChicago



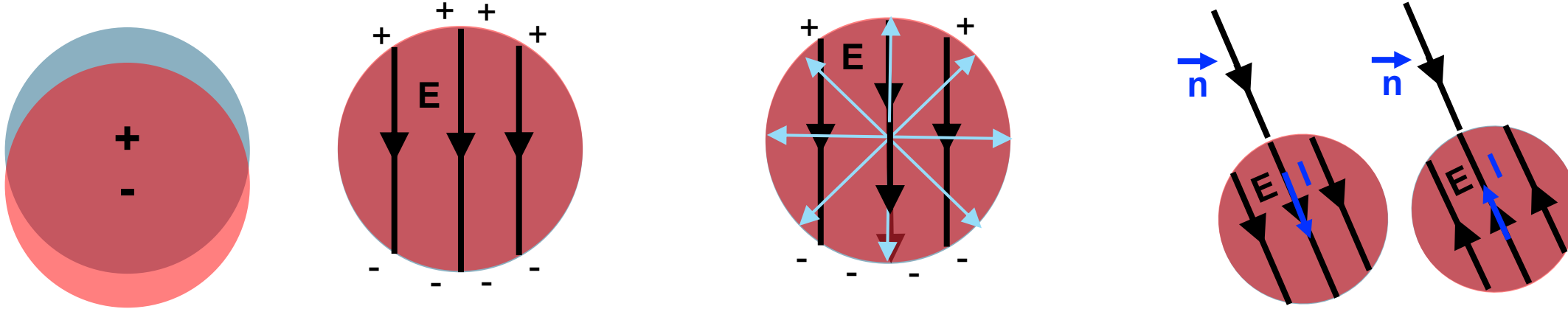
Junlin Wu
UMass Amherst

Introduction to Thallium Fluoride

- ^{205}Tl : 81 protons, 124 neutrons, so **one unpaired proton**
- ^{205}Tl : nuclear spin $I_1 = \frac{1}{2}$
- ^{19}F : nuclear spin $I_2 = \frac{1}{2}$
- Molecular ground state: $X^1\Sigma^+$ ($v = 0$)
- No electronic spin or orbital angular momentum
- Rotation J and two nuclear spins, I_1 and I_2
- Couple $\mathbf{F}_1 = \mathbf{J} + \mathbf{I}_1$, and $\mathbf{F} = \mathbf{F}_1 + \mathbf{I}_2$
- Each rotational level J has $4 \times (2J+1)$ magnetic sublevels



Schiff Moment: Simple-minded view



Nuclear EDM
polarizes nucleus

Surface charge $\cos(\theta)$.
from EDM

Adds and subtracts
from Coulomb field

- Electric field due to nuclear EDM distribution
- EDM polarizes the nucleus, creates uniform E field along nuclear spin
- This field adds to regular nuclear Coulomb field on one side of nucleus, subtracts in the other
- Electrons spend some time inside nucleus
 - Energies are shifted if gradient in electron density over nucleus
- Larger nuclear charge \rightarrow electron spends more time inside nucleus: *Schiff moment* $\propto Z^2$
- ^{205}TI nucleus has unpaired proton
- Sensitive to p EDM; previous hadronic EDMs mostly sensitive to n EDM

Effective Hamiltonian Ground State Thallium Fluoride

$$\mathcal{H}_{\text{TlF}} = \mathcal{H}_{\text{rot}} + \mathcal{H}_{\text{sr}} + \mathcal{H}_{\text{ss}} + \mathcal{H}_{\text{S}},$$

$$\mathcal{H}_{\text{rot}} = B\mathbf{J}^2,$$

$$\mathcal{H}_{\text{sr}} = c_1(\mathbf{I}_1 \cdot \mathbf{J}) + c_2(\mathbf{I}_2 \cdot \mathbf{J}),$$

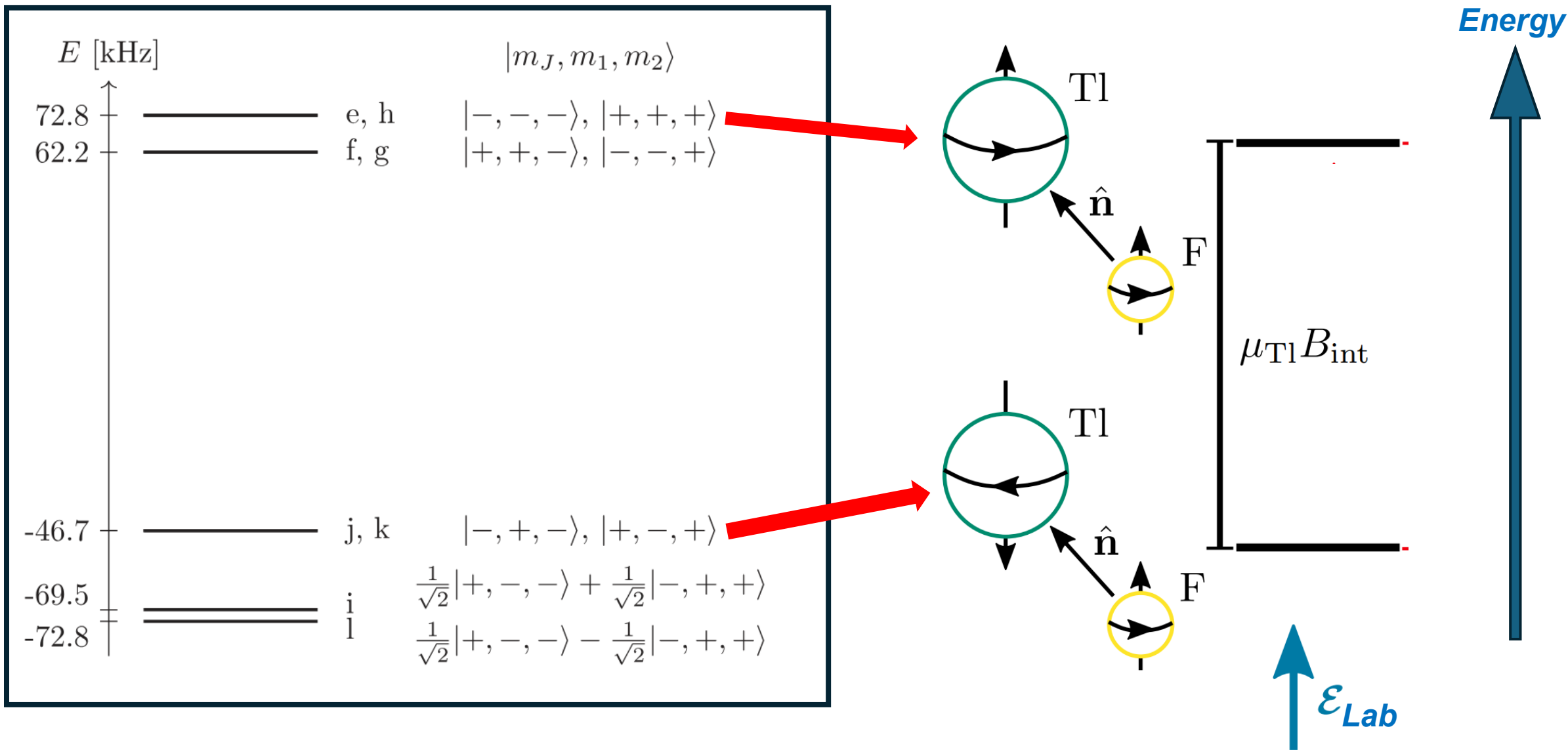
$$\mathcal{H}_{\text{ss}} = c_3 T^2(\mathbf{C}) \cdot T^2(\mathbf{I}_1, \mathbf{I}_2) + c_4(\mathbf{I}_1 \cdot \mathbf{I}_2),$$

$$\mathcal{H}_{\text{S}} = -\mu_e \cdot \boldsymbol{\mathcal{E}},$$

$B = 6.66733$	GHz	$\mu_e = 2.1285(4)$	MHz/V/cm
$c_1 = 126.03(12)$	kHz	$c_2 = 17.89(15)$	kHz
$c_3 = 0.70(3)$	kHz	$c_4 = -13.30(72)$	kHz

- Interesting feature: spin-rotation term behaves like internal magnetic field

^{205}TlF ground state energy levels at high electric field



- Rotation creates internal magnetic field along z

Effect of Schiff Moment in Thallium Fluoride

CP-Violating Effective Hamiltonian:

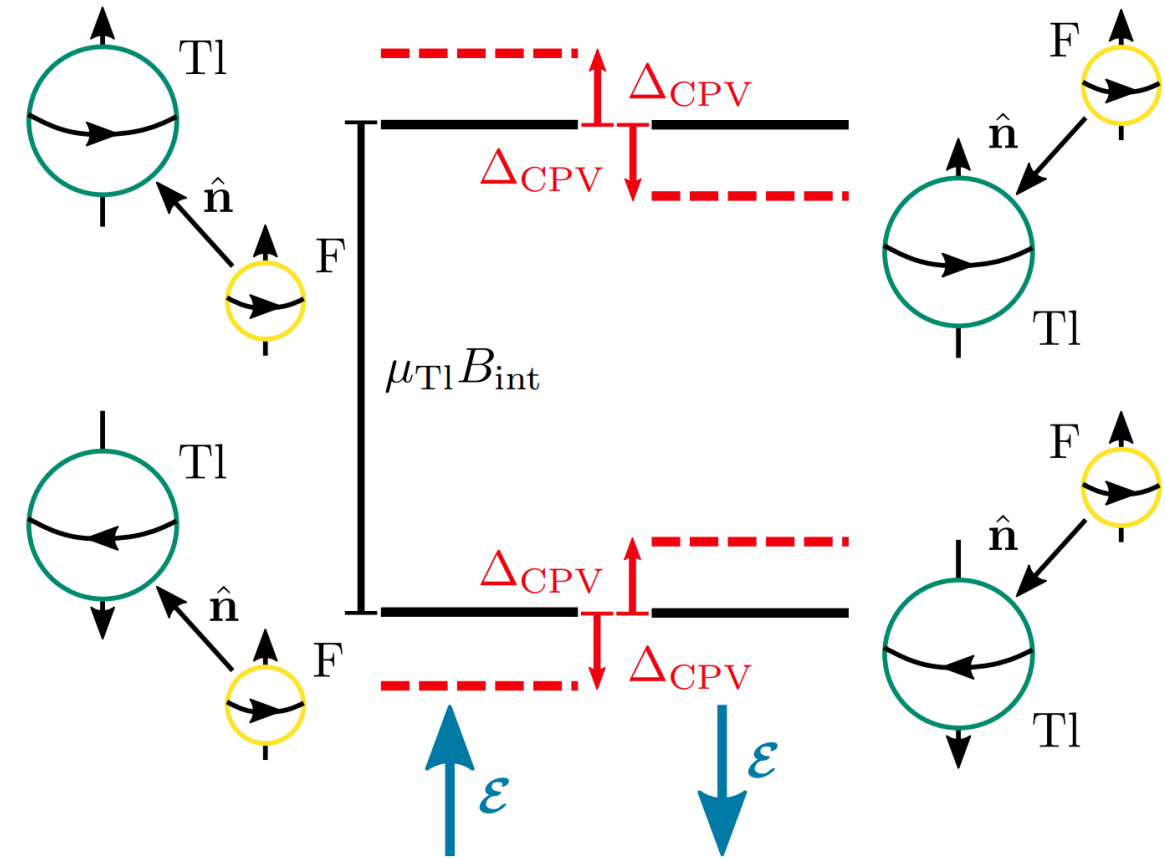
$$H_{\text{CPV}} = W_S S \frac{I}{I} \cdot \hat{n}$$

- W_S = intramolecular energy associated with NSM
- S = Schiff moment
- I = nuclear spin = 1/2

Energy shift due to CPV:

$$\Delta_{\text{CPV}} = W_S S \mathcal{P}$$

- \mathcal{P} = degree of polarization w.r.t \mathcal{E} ($\mathcal{P} = 0.547$ @ 30 kV/cm)
- $W_S = (1.8 \pm 0.2) \times 10^6 \text{ Hz} / (e \text{ fm}^3)$ (M. Hubert, Timo Fleig, Phys Rev A **106**, 022817 (2022))
- $S(^{205}\text{Tl}) = (3.9 \pm 6.8) \times 10^{-11} e \text{ fm}^3 \longleftrightarrow (1.4 \pm 2.4) \times 10^{-4} \text{ Hz}$. (D. Cho et al, Phys Rev A **44**, 2783 (1991))



Schiff Moment in Thallium has many possible sources

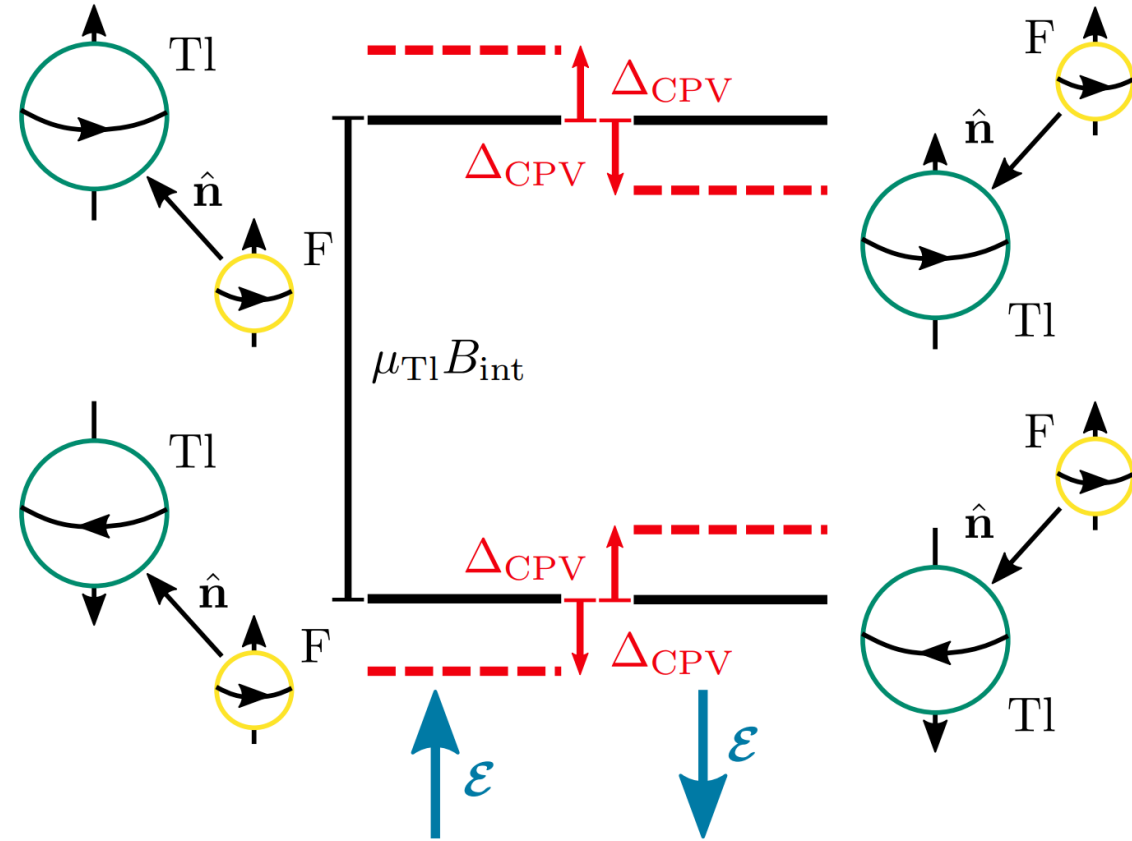
Extract S from $\Delta_{\text{CPV}} = W_S S \mathcal{P}$

$$S(^{205}\text{Tl}) \simeq (13g\bar{g}_0 - 0.04g\bar{g}_1 - 0.27g\bar{g}_2) e \text{ fm}^3$$

$$S(^{205}\text{Tl}) \simeq 0.027\bar{\theta} e \text{ fm}^3$$

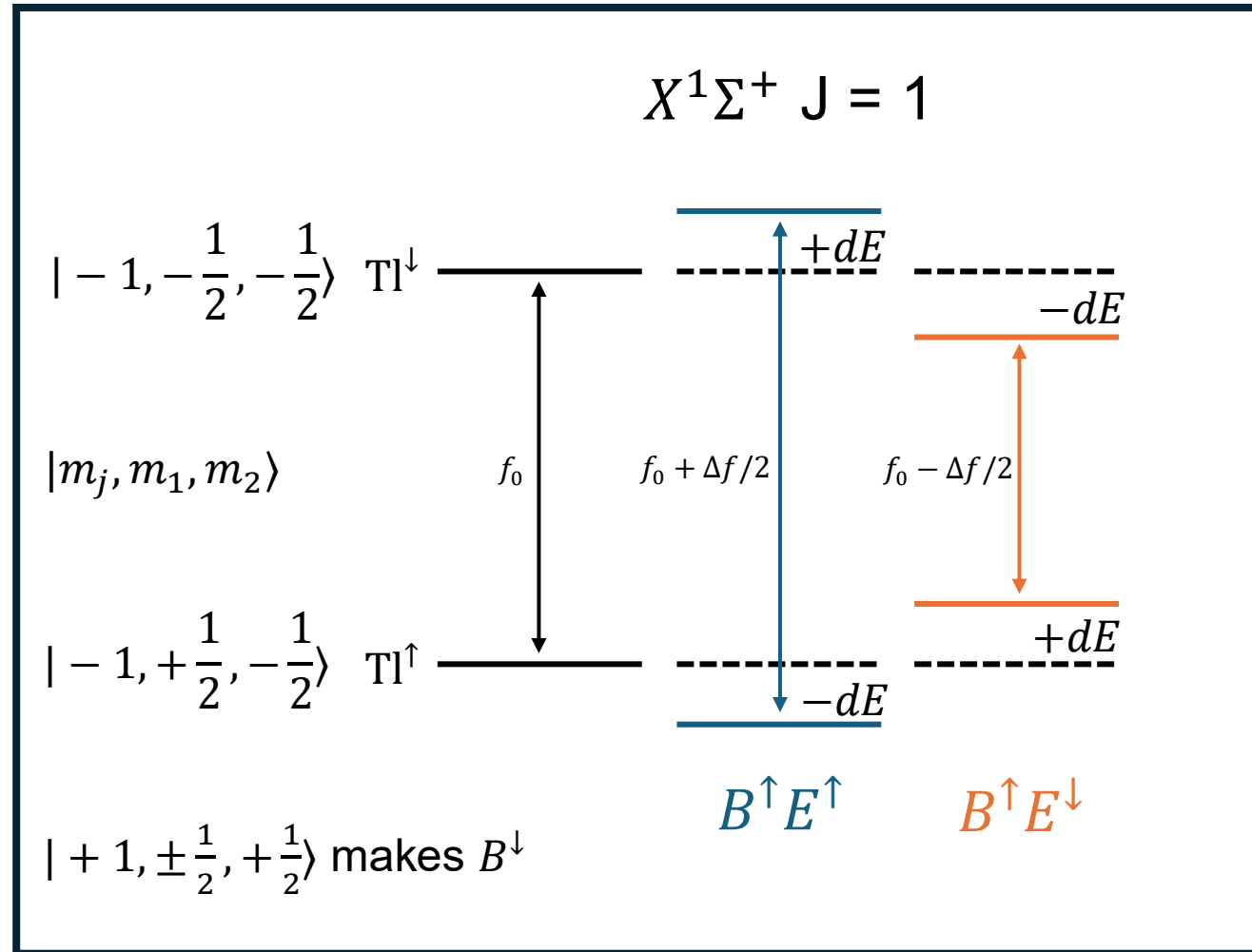
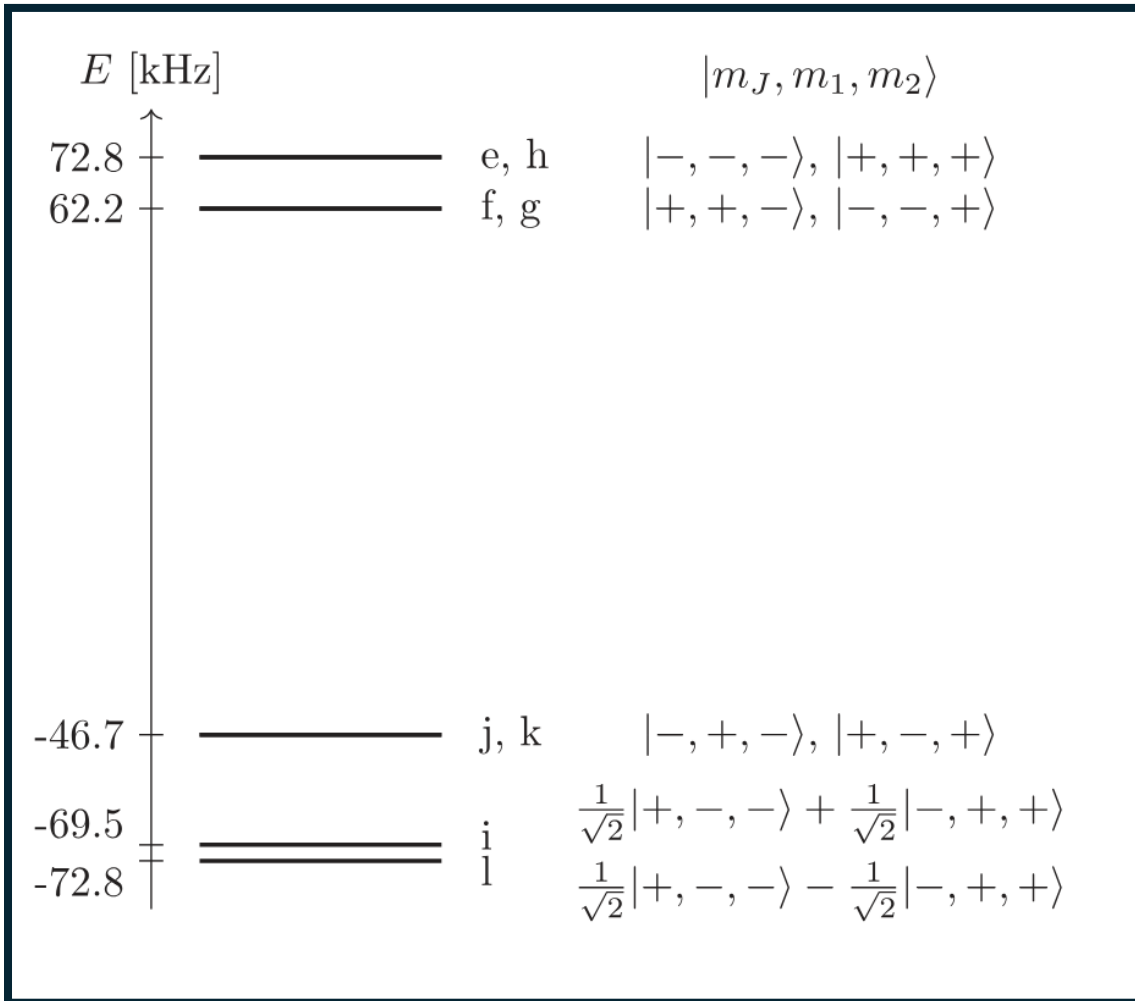
$$S(^{205}\text{Tl}) \simeq (12\tilde{d}_d + 9\tilde{d}_u) e \text{ fm}^2$$

$$S(^{205}\text{Tl}) \simeq 0.4d_p \text{ fm}^2$$



V.V. Flambaum and V.A. Dzuba, Cho et al, Phys Rev A **101**, 042504 (2020)

^{205}TlF ground state energy levels at high electric field

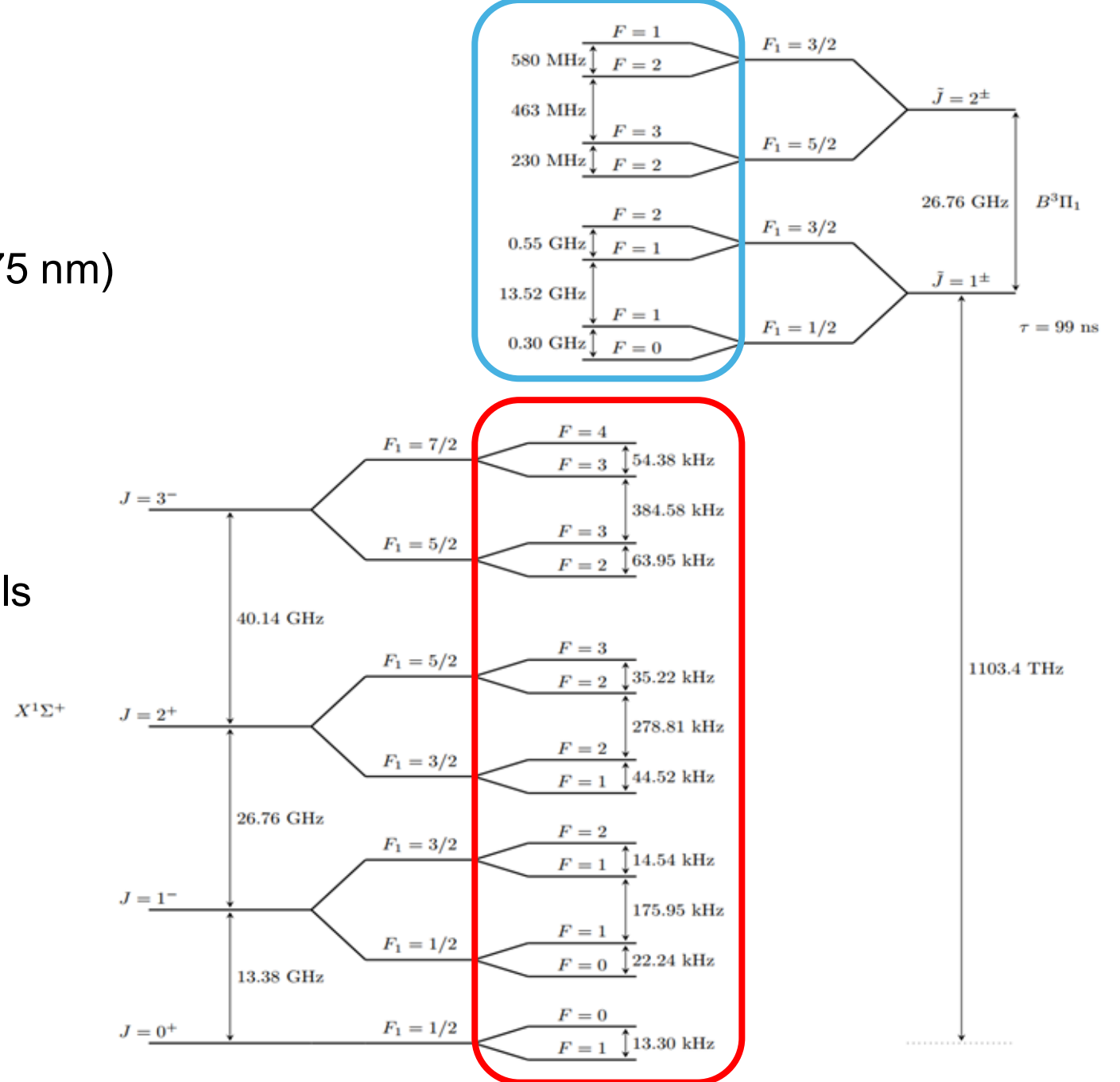


- EDM search uses e+j and/or h+k states in which Tl spin flips
- (e+j) and (h+k) have opposite signs of internal B field
- Need molecules in J=1, high electric field

^{205}TlF Energy Levels

Zero electric field

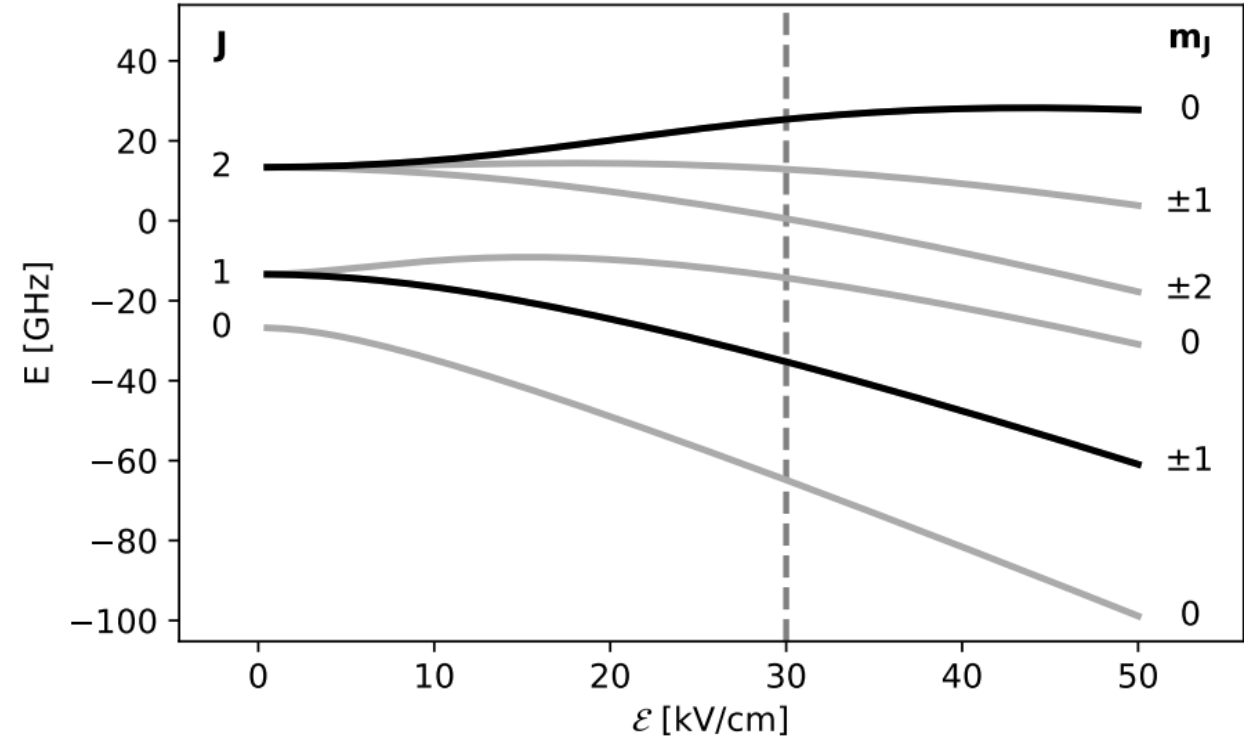
- Laser transitions are UV (1100 THz, 271.75 nm)
 - X ground state hfs ≤ 100 kHz
 - B excited state hfs ≥ 100 MHz
 - $\Gamma = 2\pi \times 1.6$ MHz
 - Dark states; $n_g \gg n_e$
- Use microwaves to change rotational levels



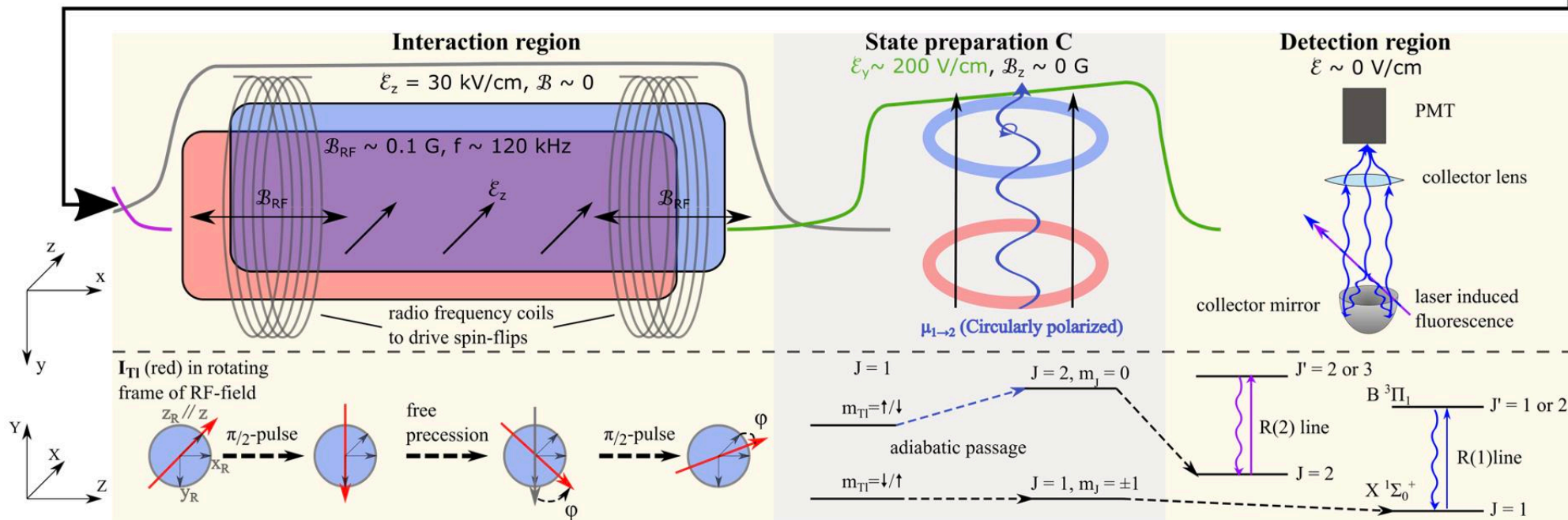
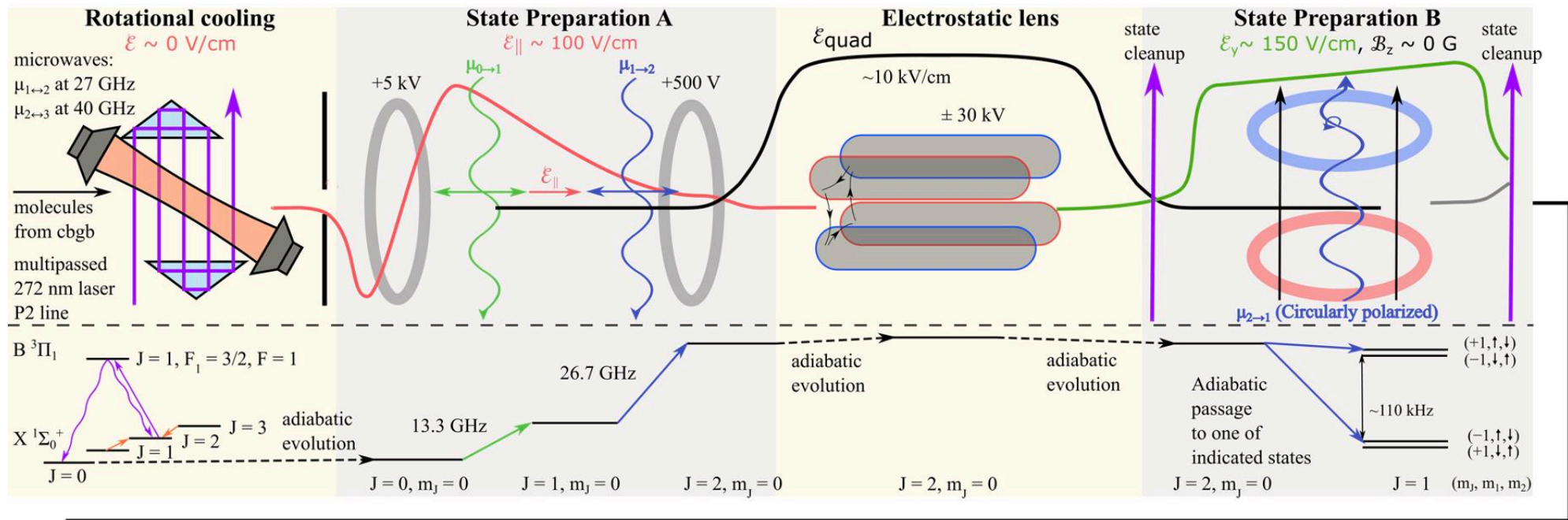
Ground State Energy Levels in Electric Field

$$\Delta_{\text{CPV}} = W_S S \mathcal{P}$$

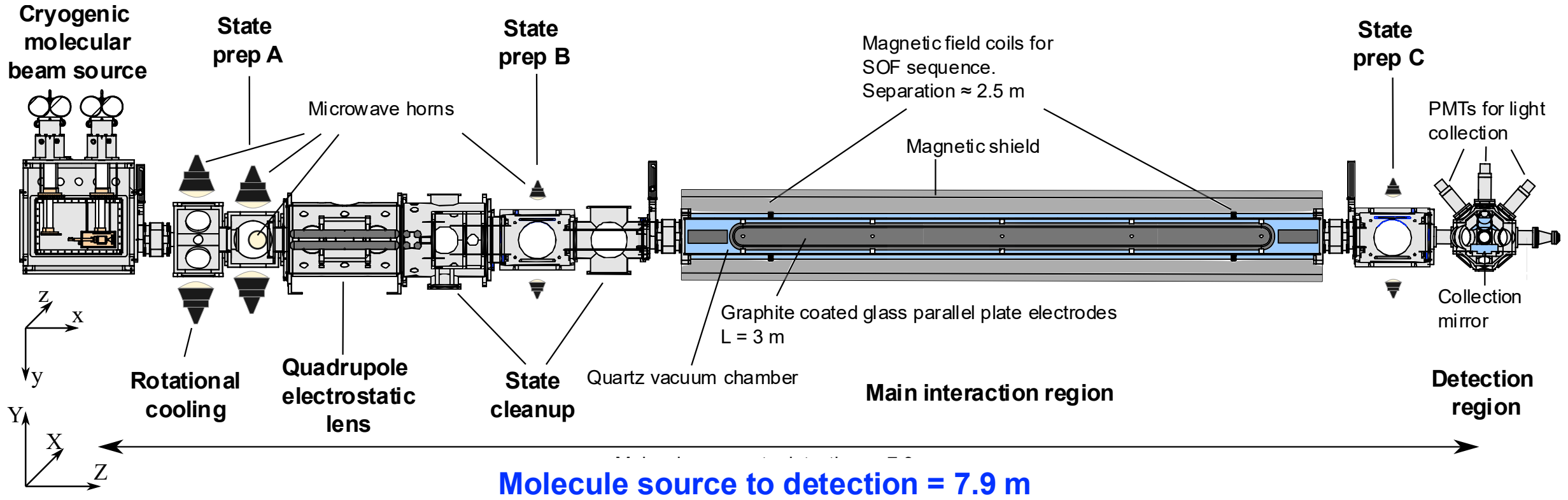
- \mathcal{P} larger for smaller J
 - \mathcal{P} arises from mixing between states with different parity, i.e. different J
 - J states closer together for smaller J
- systematics suppressed with strong spin-rotation
 - requires $m_J \neq 0$
 - 'effective' intra-molecular magnetic field \mathcal{B}_{int}
 - no external magnetic field required
- Schiff Moment measurement performed in $|\tilde{J} = 1, m_J = \pm 1\rangle$



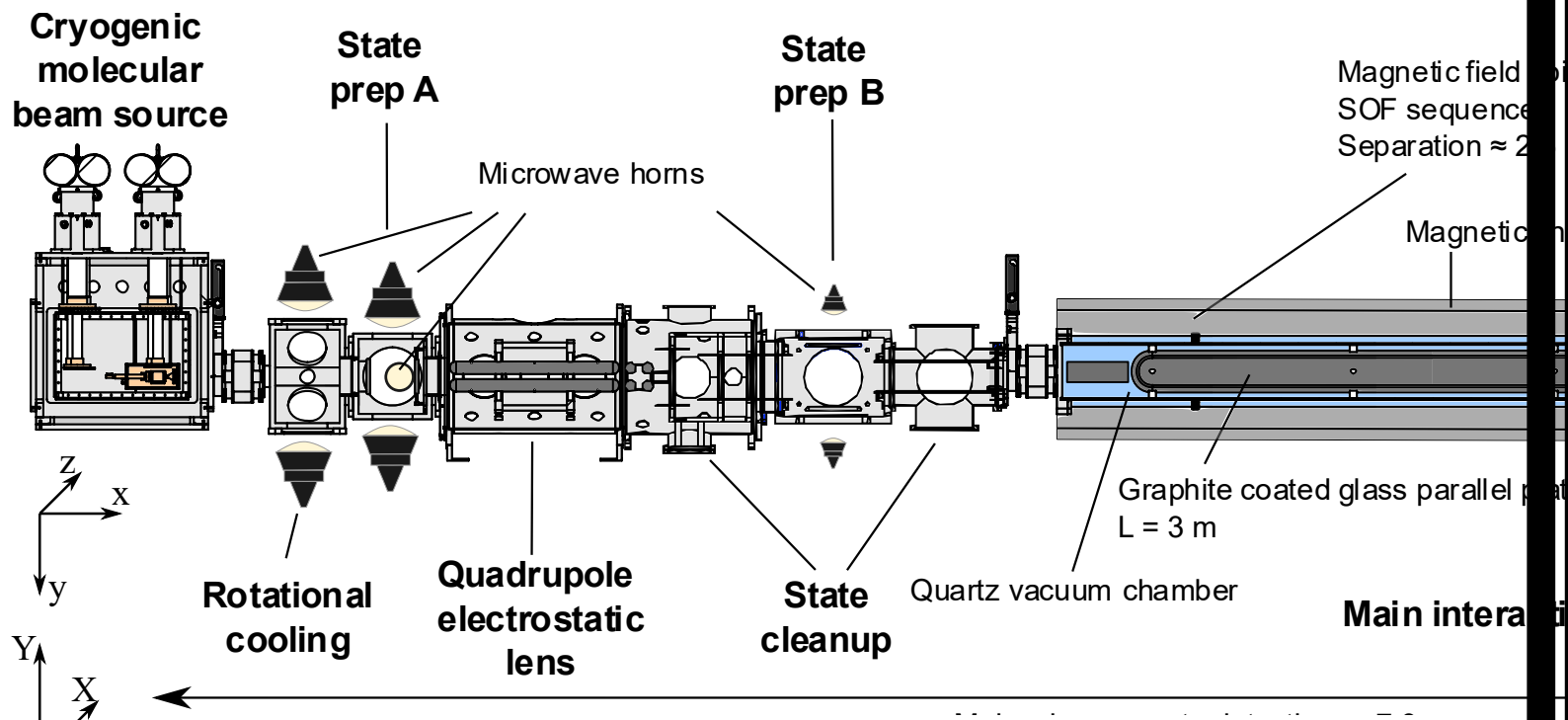
Experiment Overview



Experiment Overview: Beamline



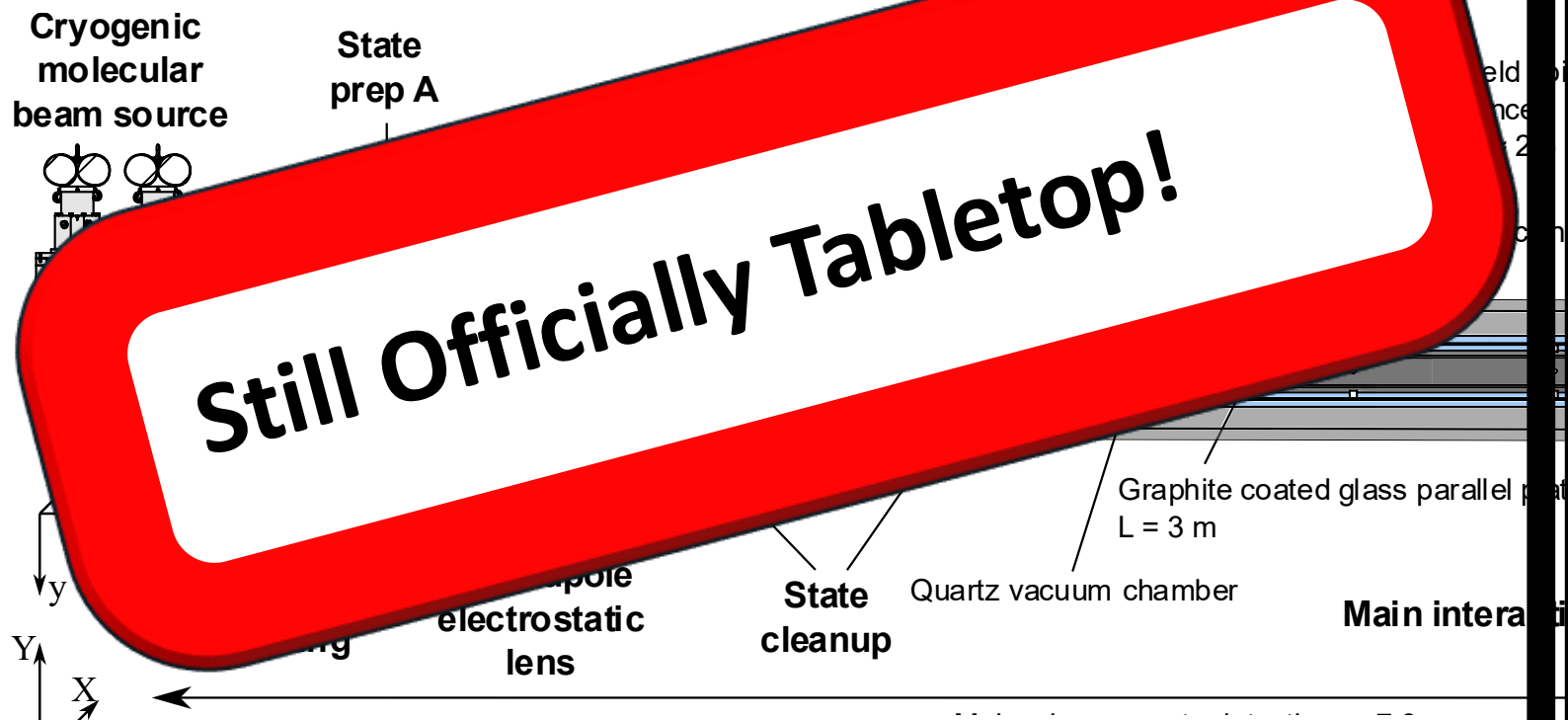
Experiment Overview: Beamline



Longest table: Taj Falaknuma Palace
33 meters long = 4 x CeNTREX !
Seats 100

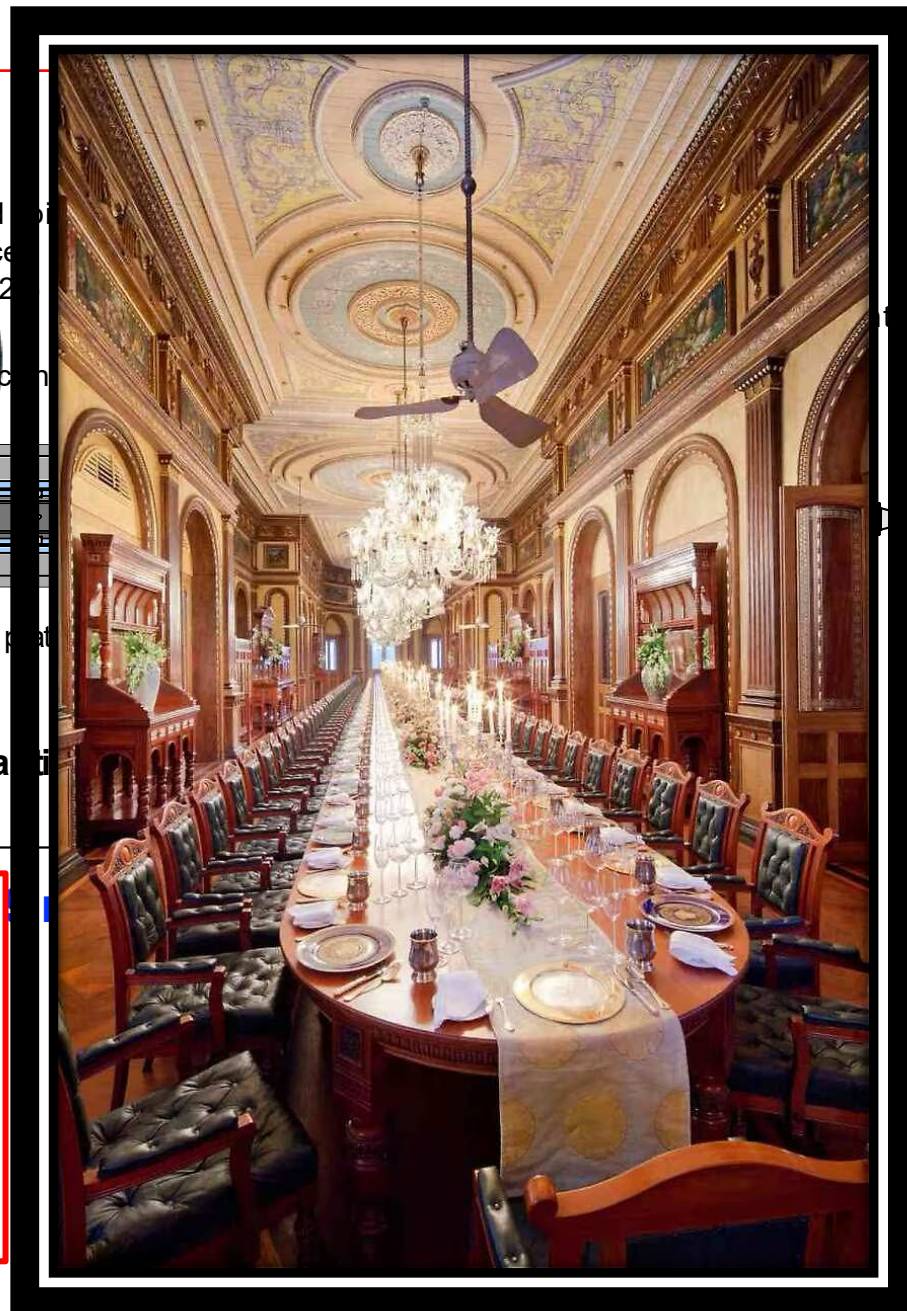


Experiment Overview: Beamline

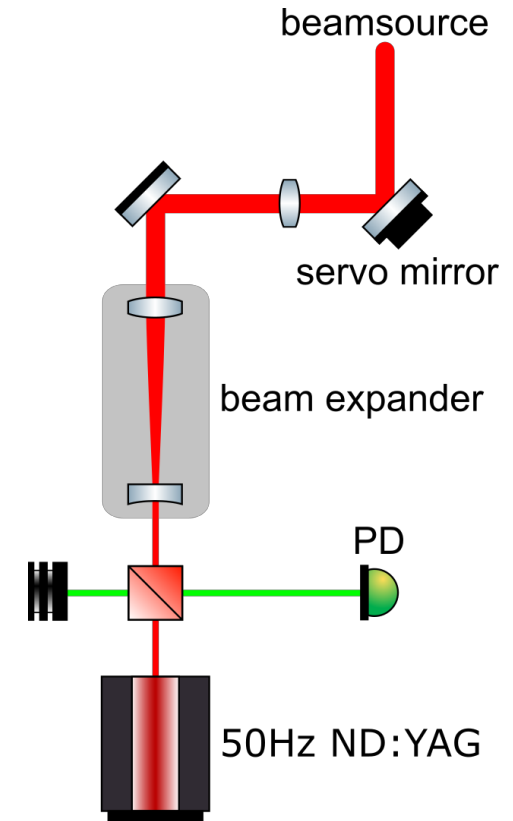
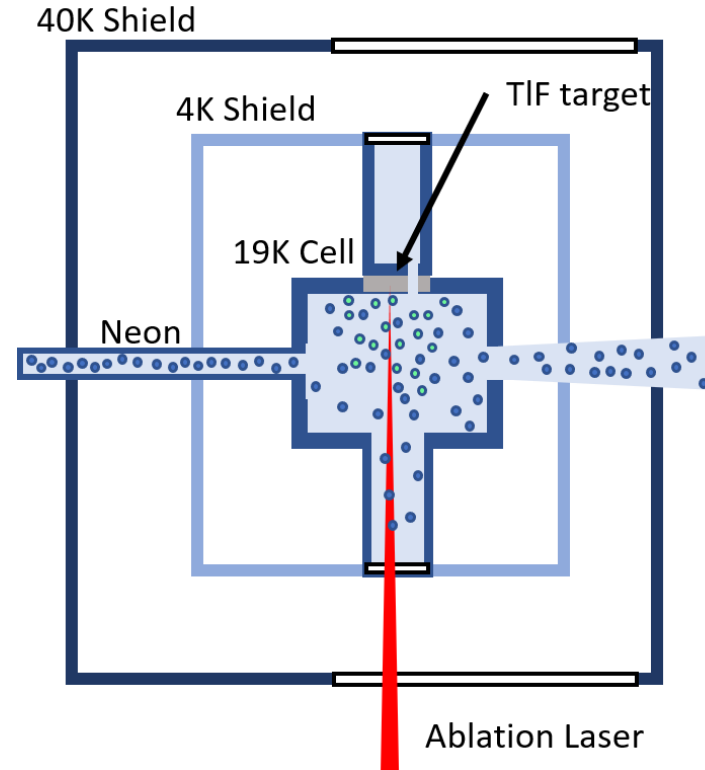
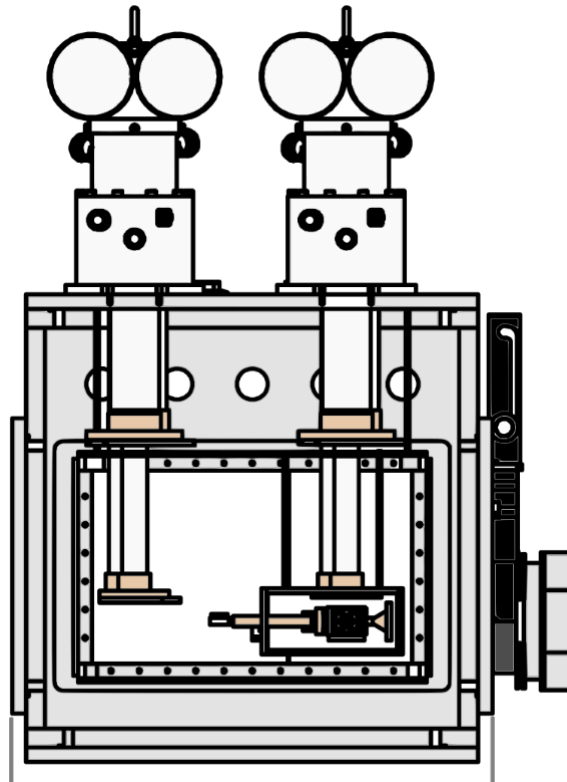


Still Officially Tabletop!

Longest table: Taj Falaknuma Palace
33 meters long = 4 x CeNTREX !
Seats 100

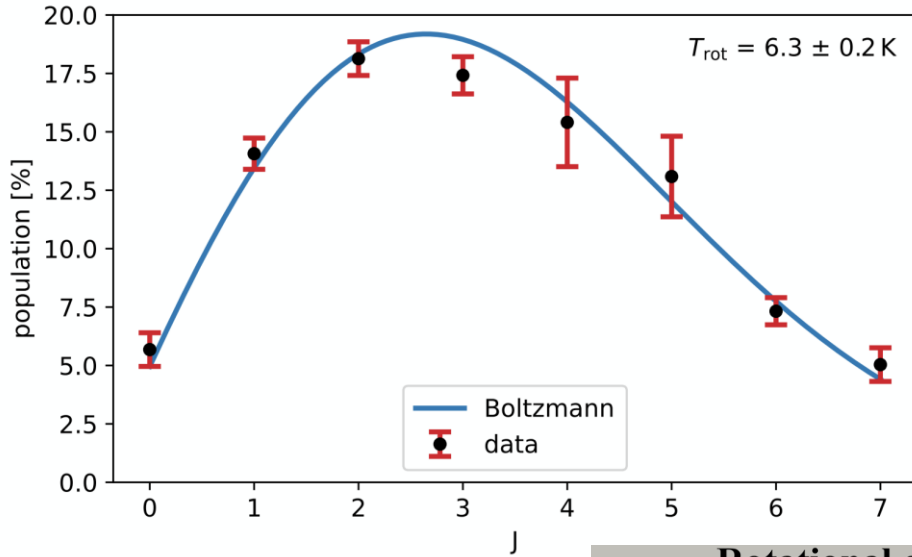


Cryogenic Buffer Gas Beam Source of TIF

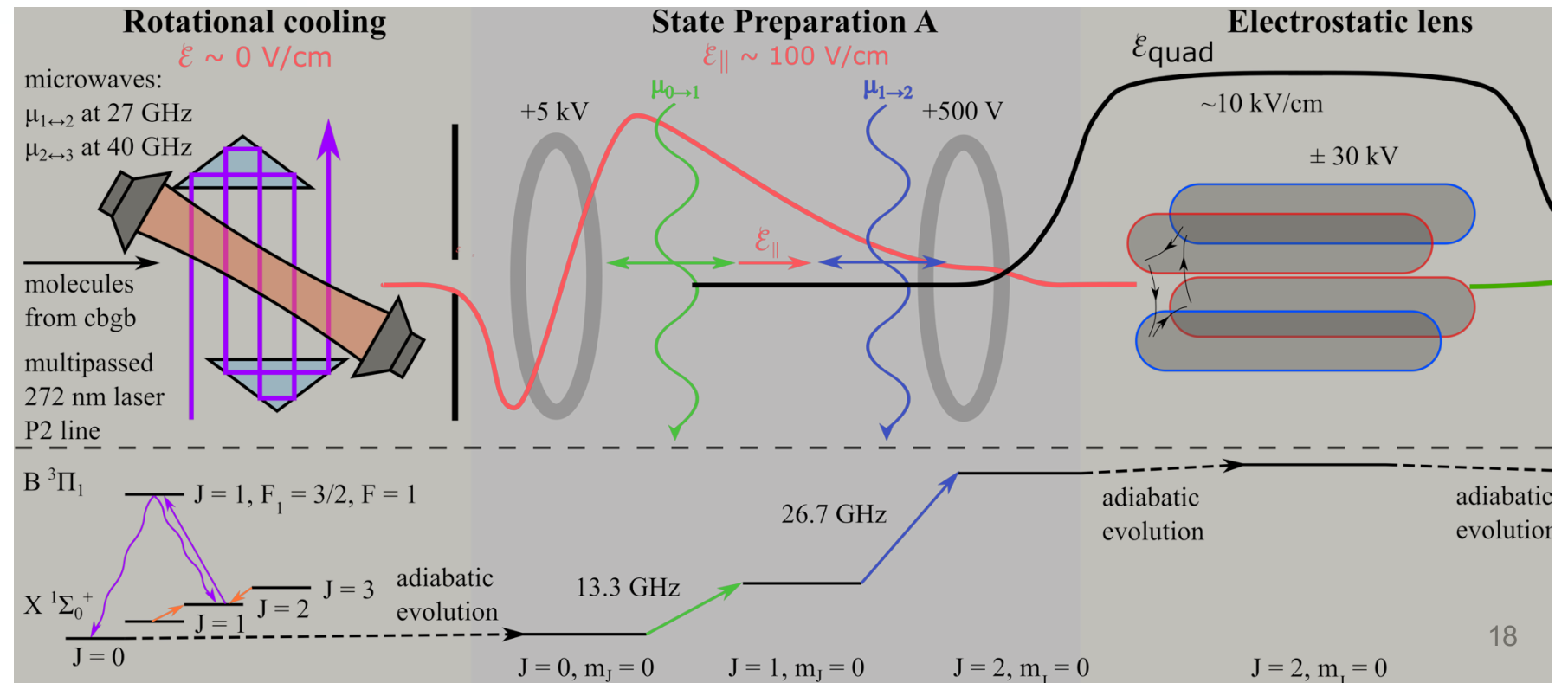


- Cold cell @19K cools down neon buffer gas
- YAG pulse ablates TIF target at 50 Hz
- Collisional cooling + supersonic expansion creates cold TIF beam
- 6.3(2) K rotational temperature, 184(16) m/s forward velocity, 5×10^{12} molecules/state/sr/s

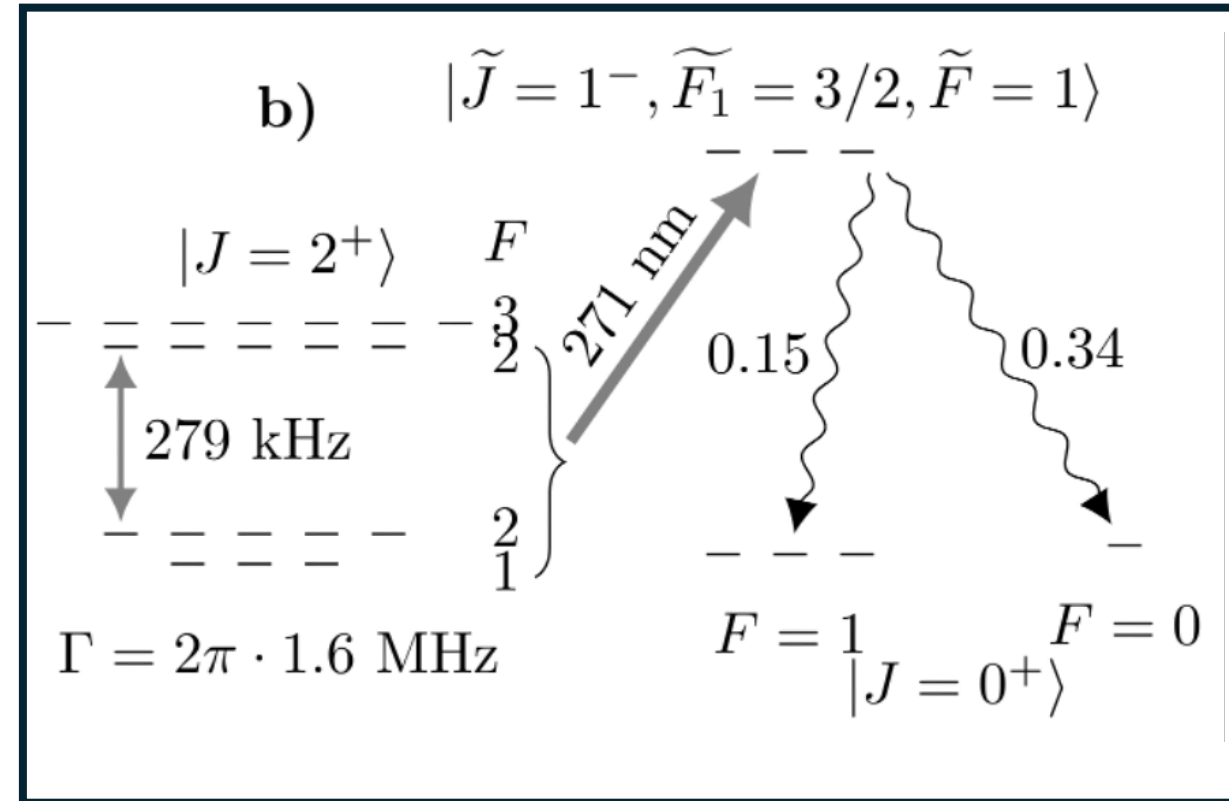
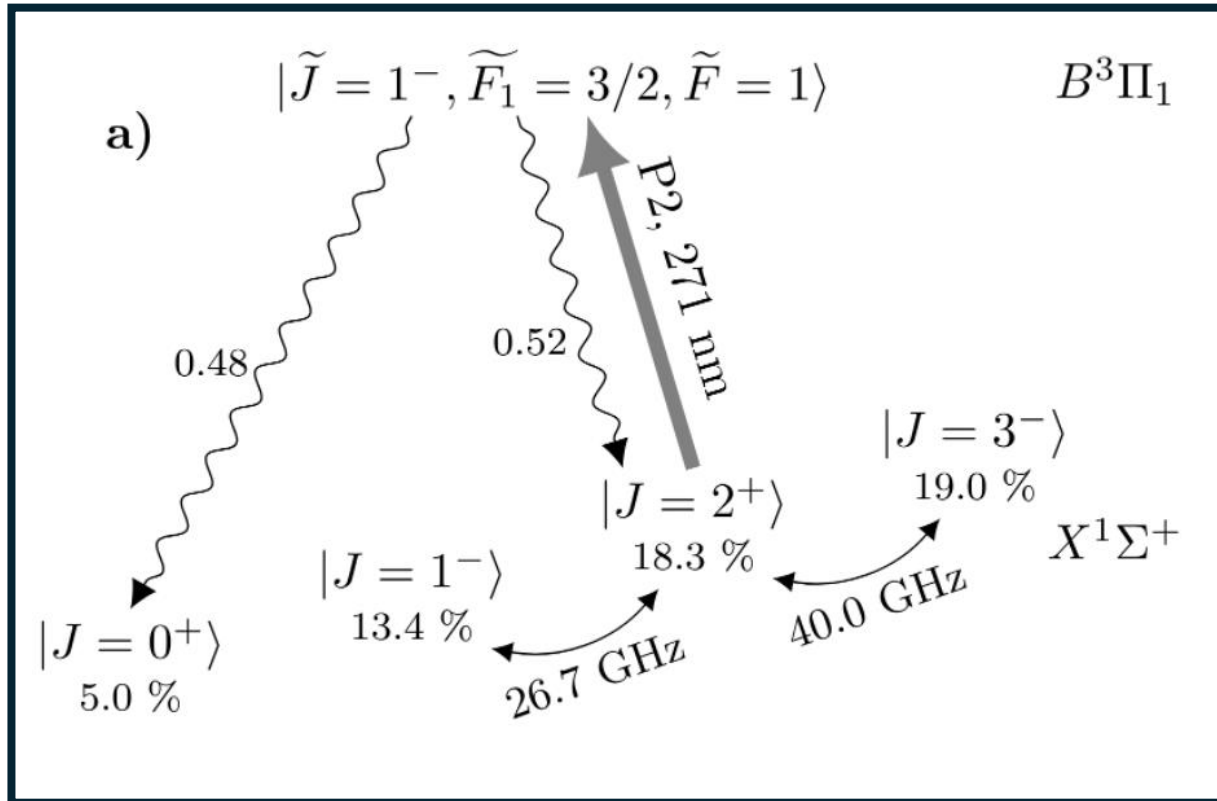
Rotational Cooling + Electrostatic Lens: Increase #molecules for measurement



- $T_{\text{rot}} = 6.3 \pm 0.2 \text{ K}$
- $\approx 56\%$ in lowest 4 rotational states
- Rotational cooling: transfer $J=3, 2, 1$ into $J=0$
- Electrostatic focusing

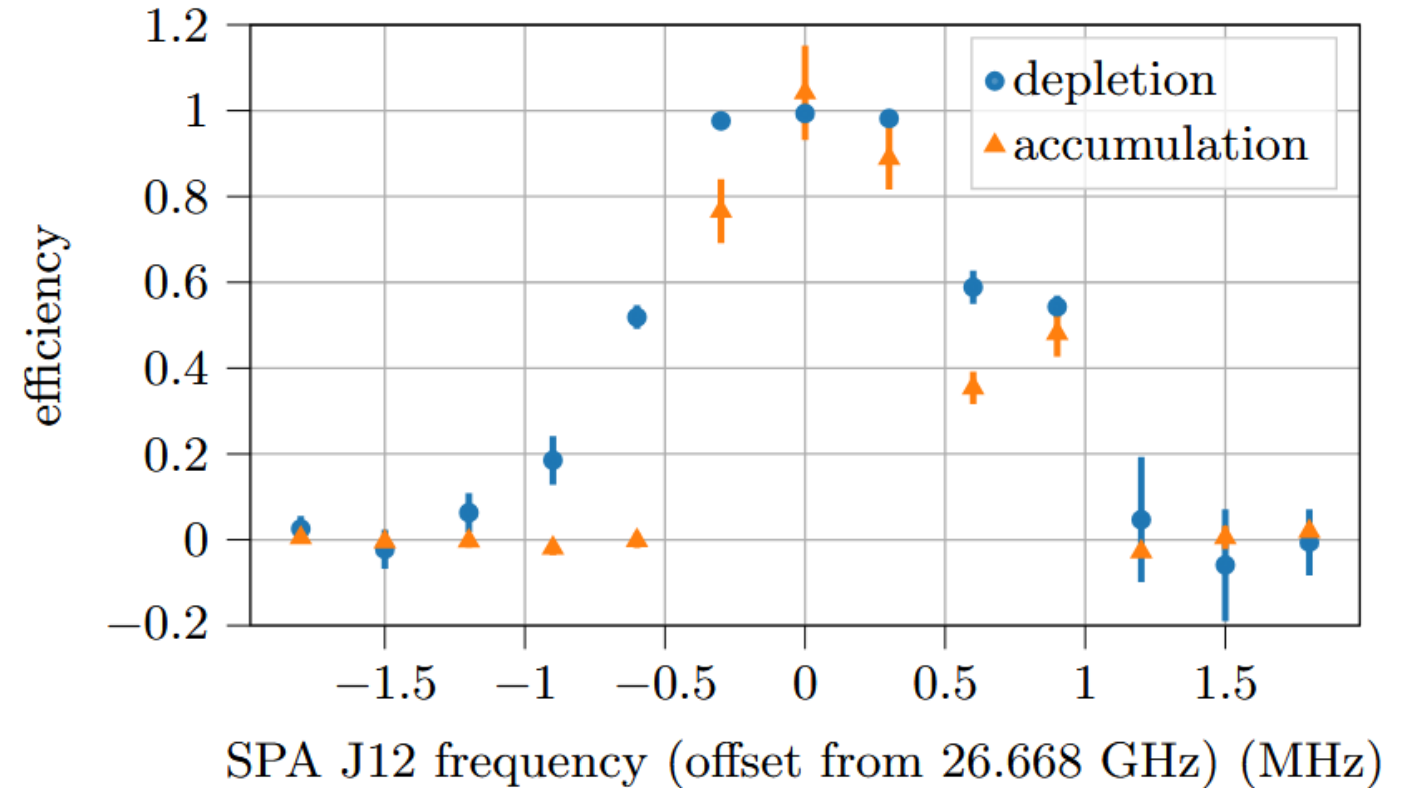
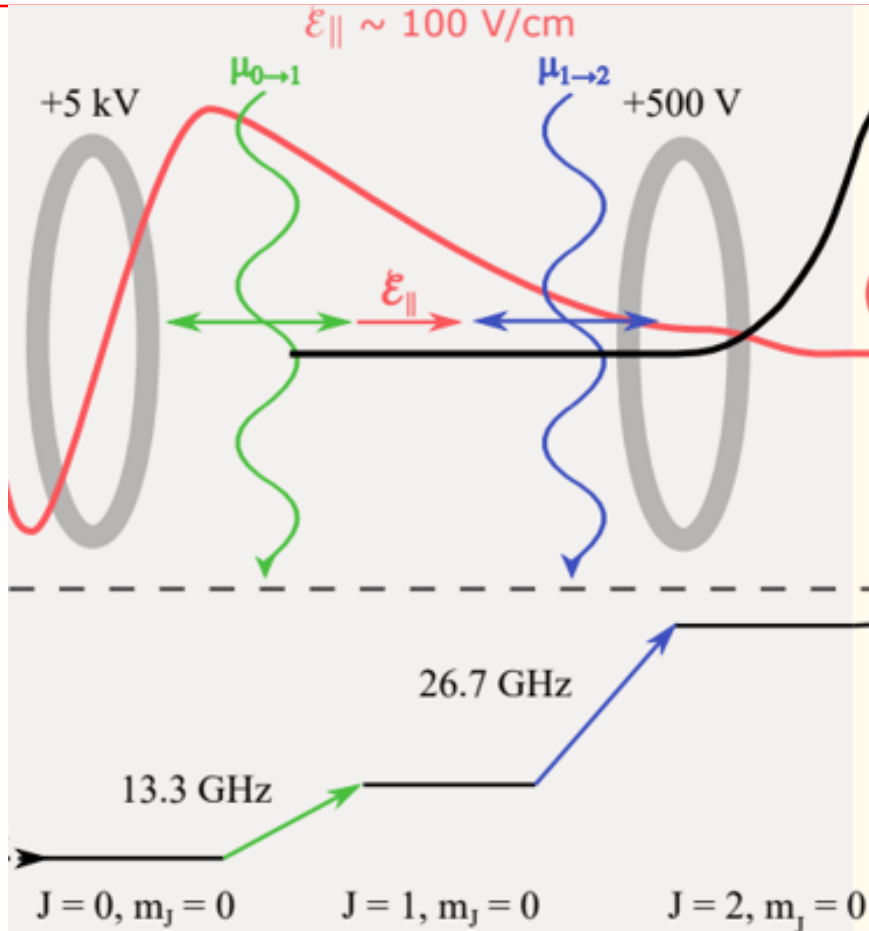


Rotational Cooling: Transfer population from $J=3, 2, 1$ to $J=0$



- Gain of 20.1(4) achieved (@ 6.3 K)
- Full rotational cooling in $J = 1, 2, 3$ would give ≈ 29 gain
- Limited by laser power; currently 90 mW @ 271 nm

State Preparation A: Transfer from $J=0, m_J=0$ to $J=2, m_J=0$ for electrostatic lens



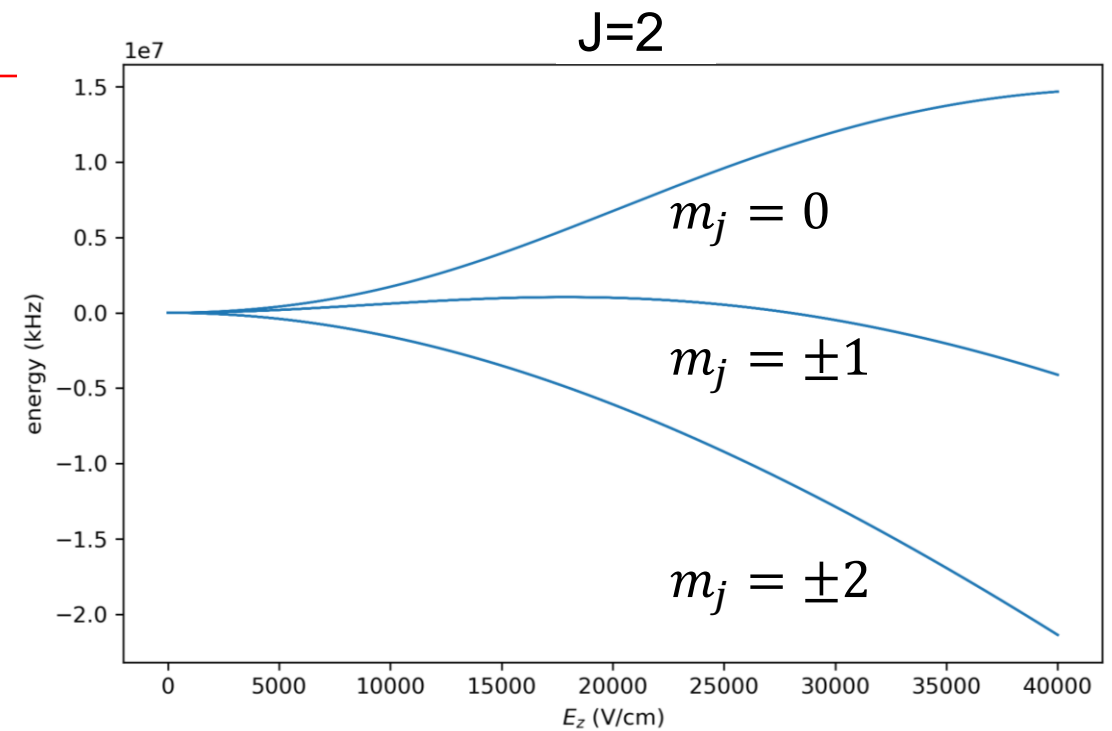
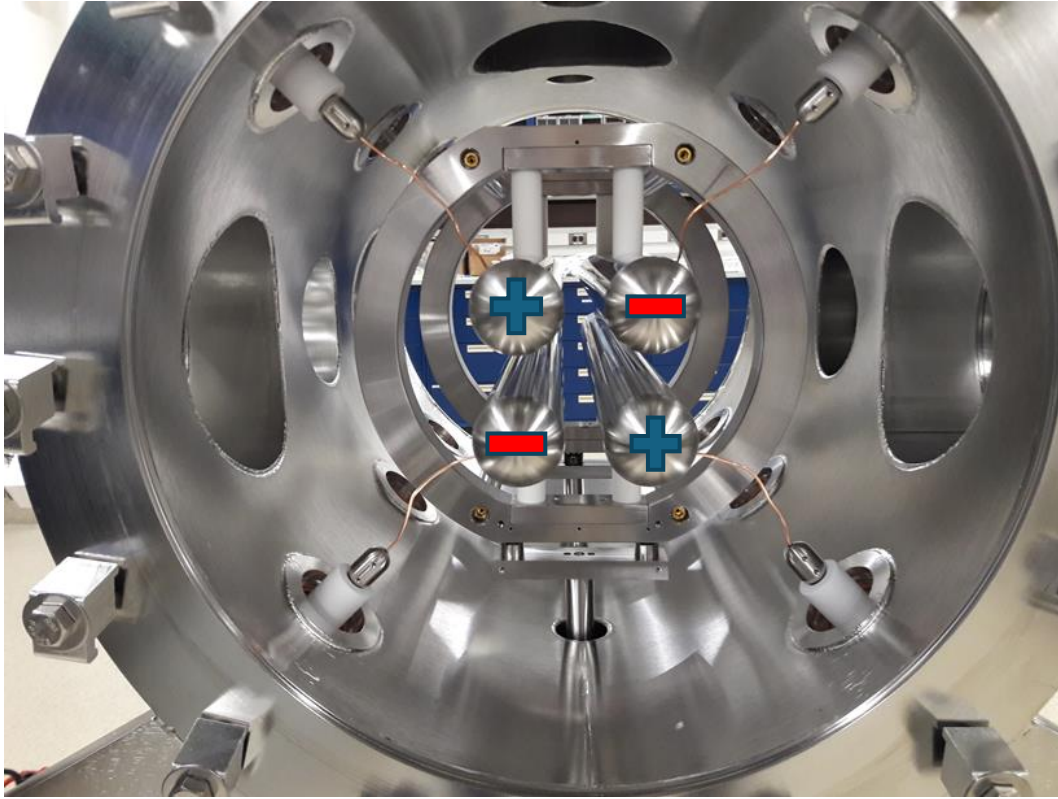
Adiabatic passage from $J = 0, I_{tot} = 0 \rightarrow J = 1 \rightarrow J = 2, I_{tot} = 0$

- Microwave driven with Gaussian focusing horns to localize fields
- Spatially-varying DC electric field yields Stark shift

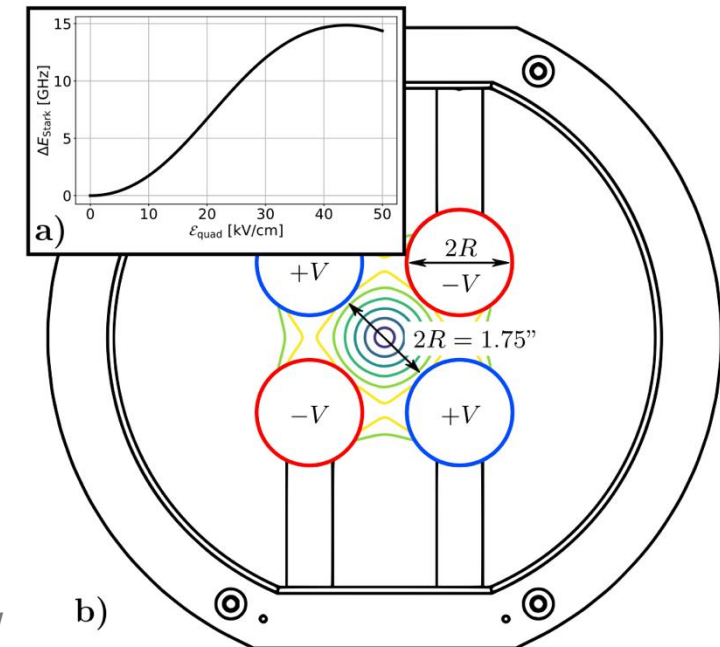
Efficiency

- $J = 0 \rightarrow J = 1 \Rightarrow 88(11)\%$
- $J = 1 \rightarrow J = 2 \Rightarrow 104(11)\%$

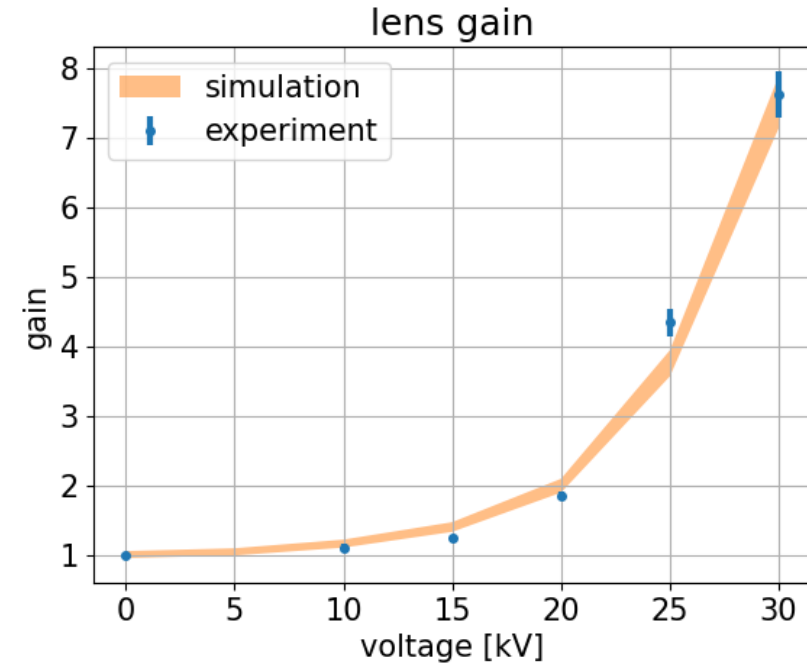
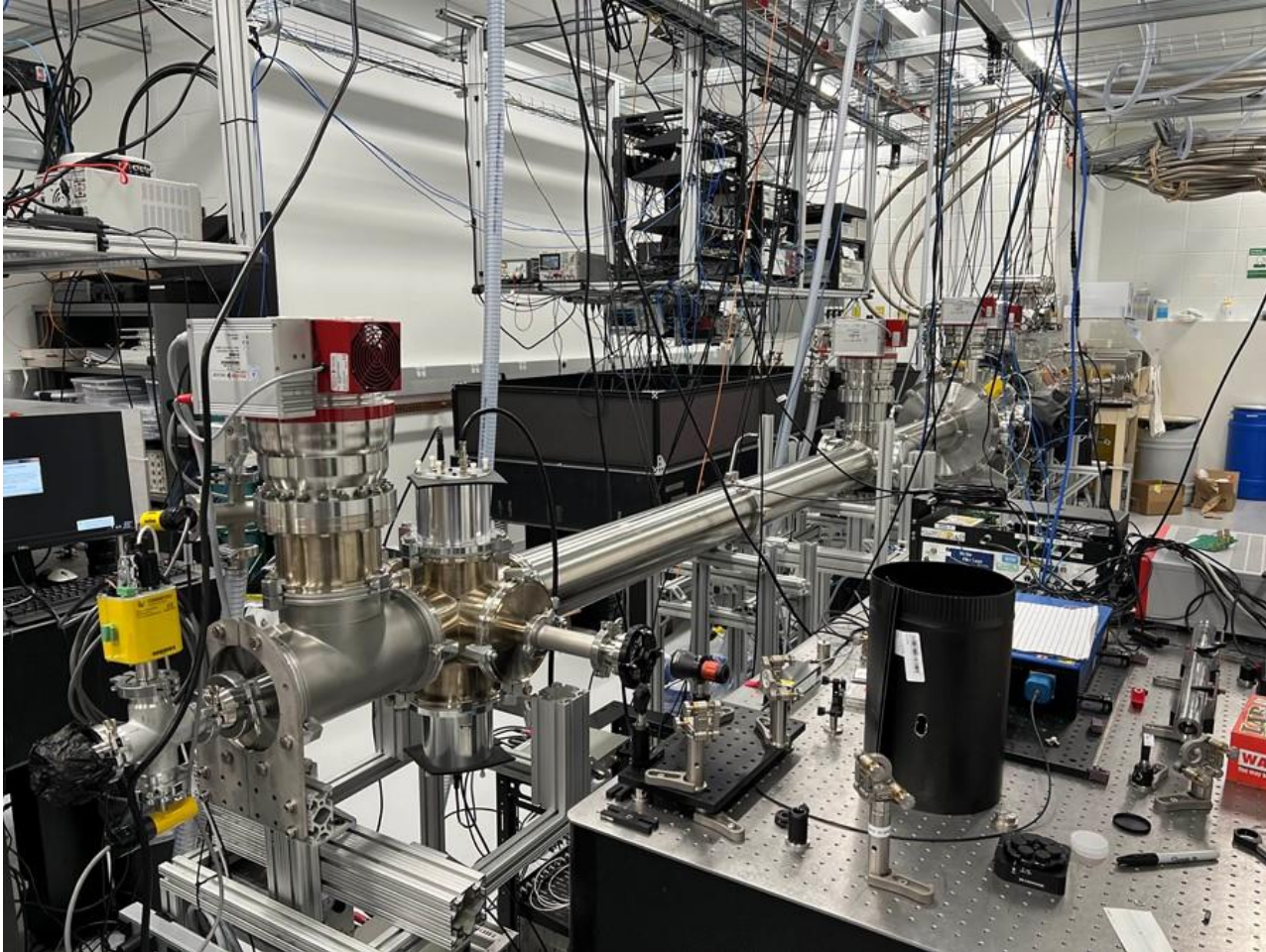
Electrostatic Focusing



- 4 rods, 60 cm long, rod diameter = separation=1.75"
- Quadrupole config makes linear radial electric field
- \approx quadratic Stark shift of low-field seeking state $J = 2, m_j = 0$
- Looks like harmonic potential, analogous to thick lens
- Measured gain at 1.26 m from lens of $\approx 7.5(7)$
- At full scale expect gain in lensing state of 23 {lens in/out}

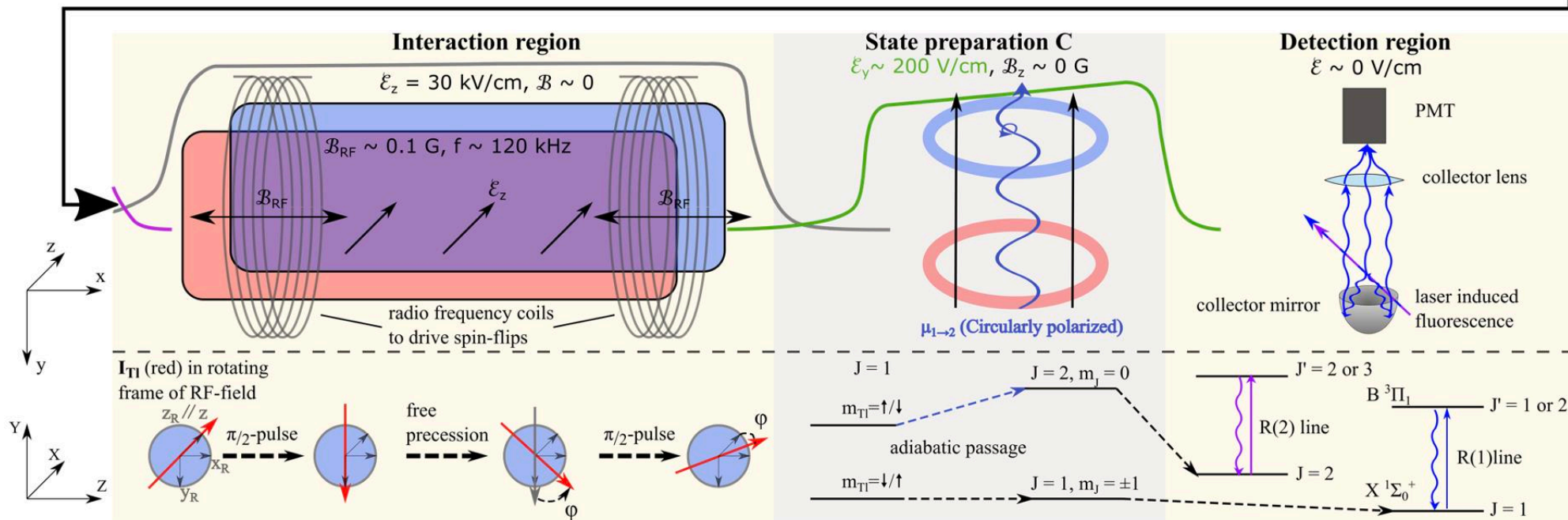
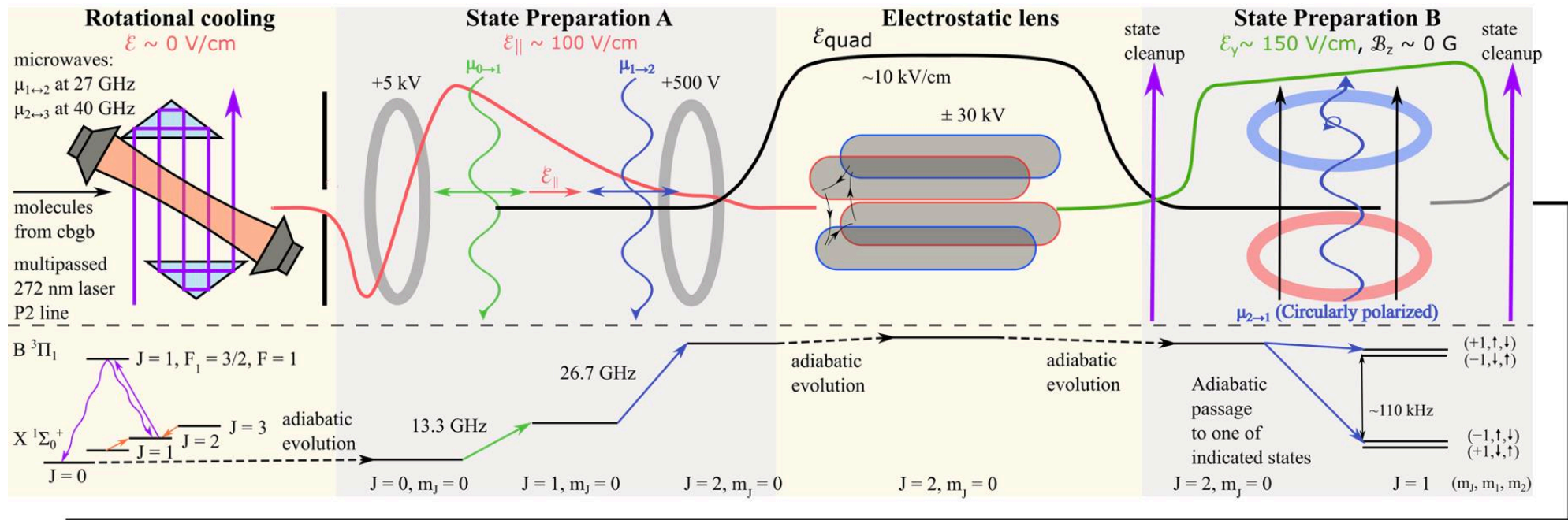


Electrostatic Focusing



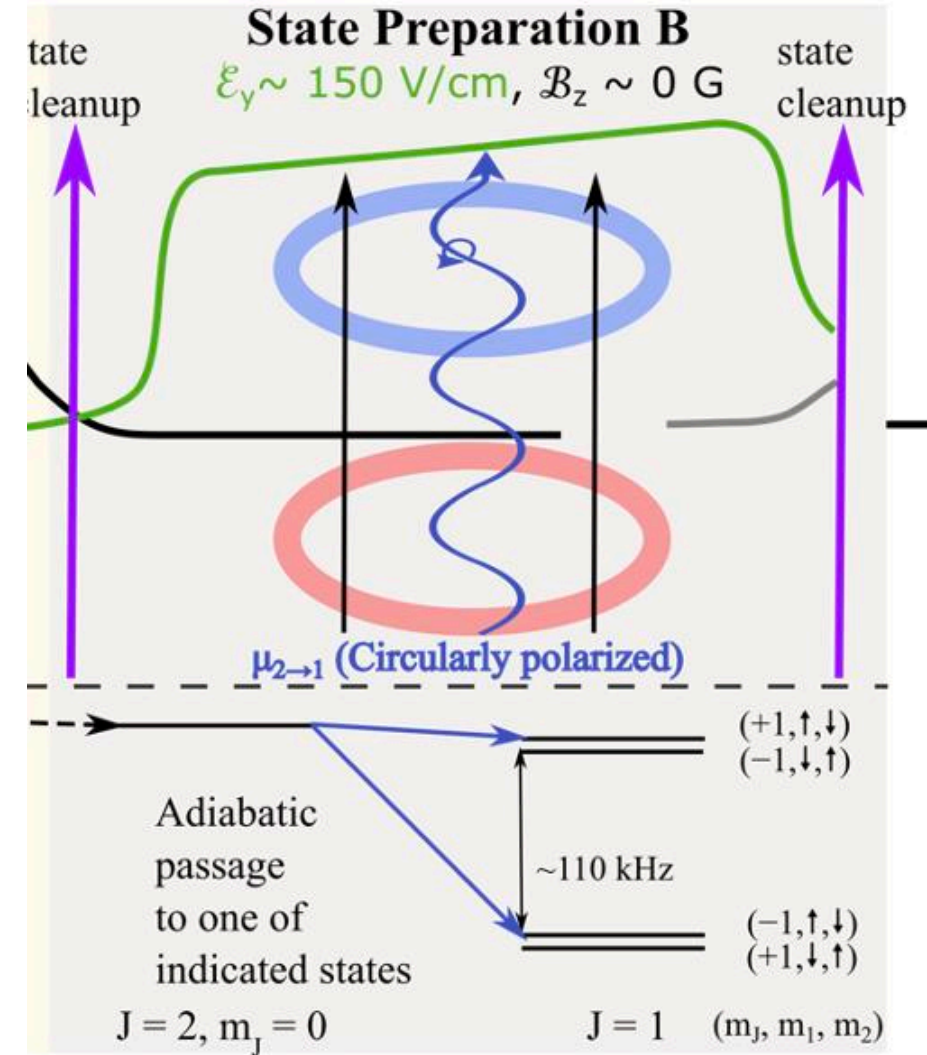
- Measured gain at 1.26 m from lens of $\approx 7.5(7)$
- At full scale expect gain in lensing state of 23 {lens in/out}

Experiment Overview

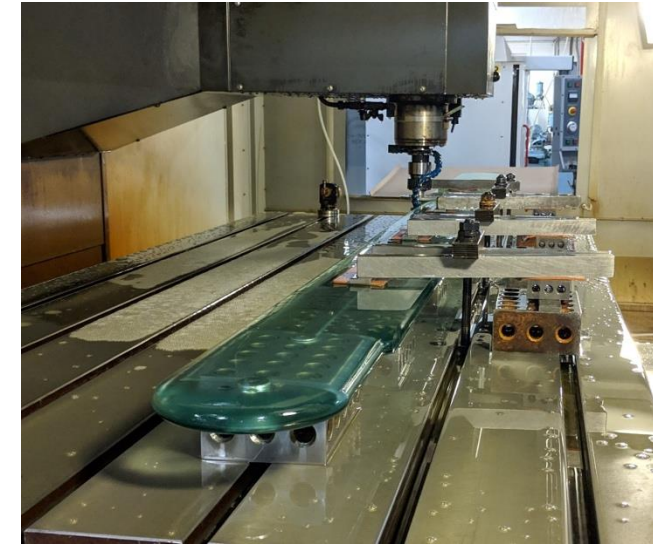
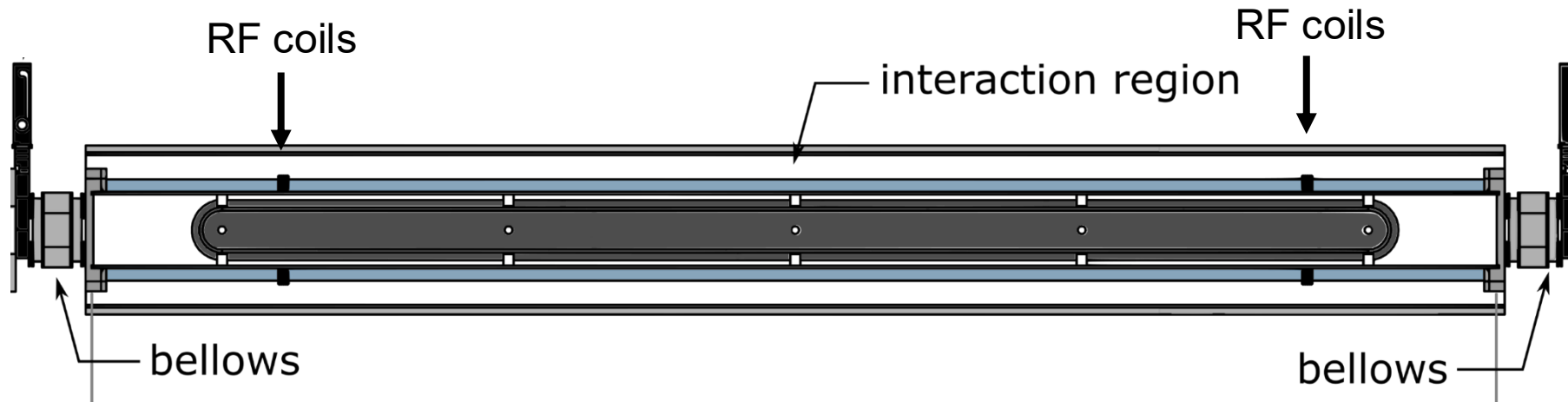


State Preparation B and State Cleanup

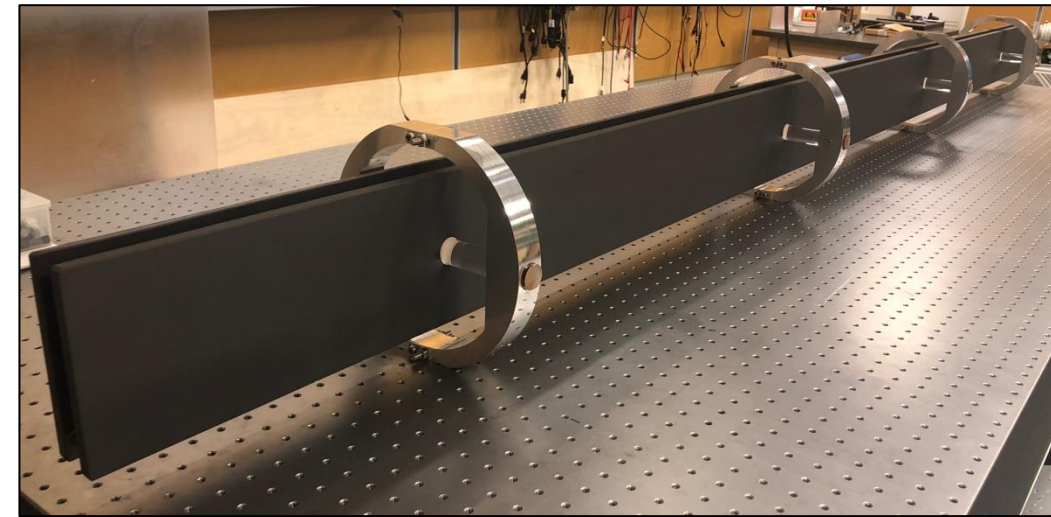
- Transfer from lens state to SM measurement state
 - $|J = 2, m_J = 0\rangle \rightarrow |J = 1, m_J = \pm 1\rangle$
- Microwave driven adiabatic passage
 - Analogous to SPA, except circular polarization
- Lasers remove remaining population in $J = 1$ & $J = 2$
 - Reduces potential systematics



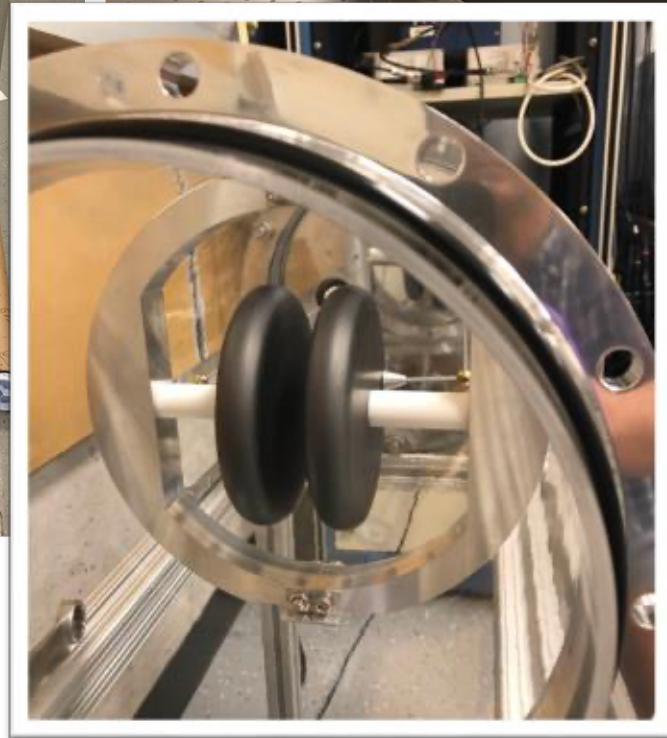
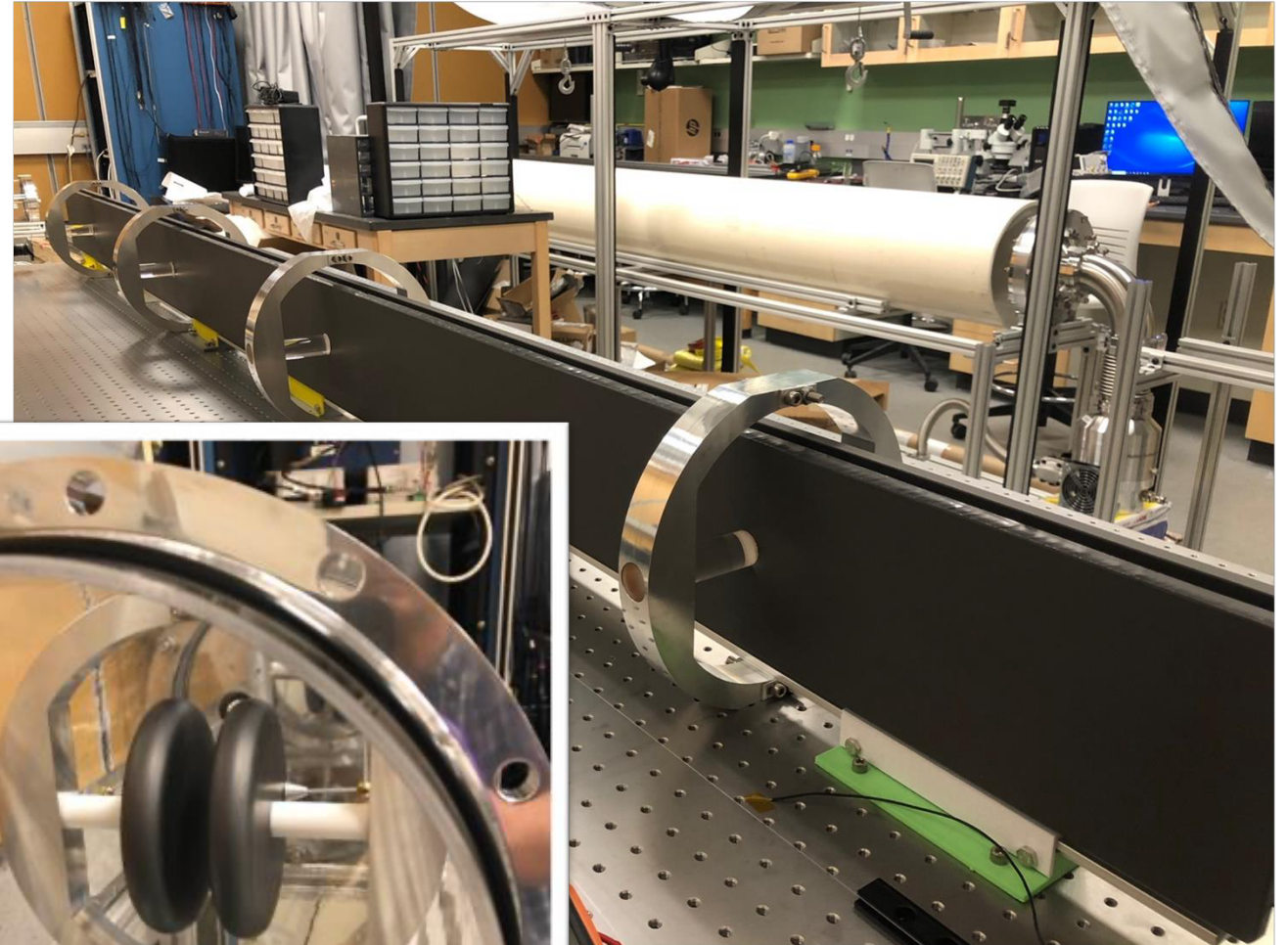
Interaction Region



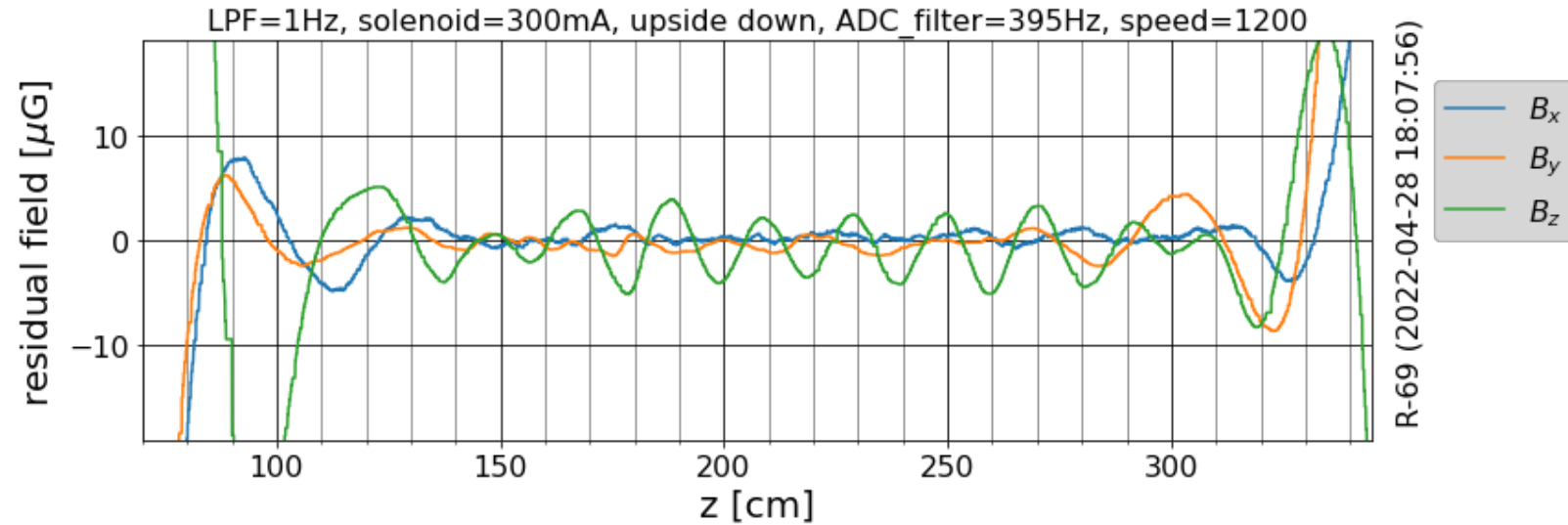
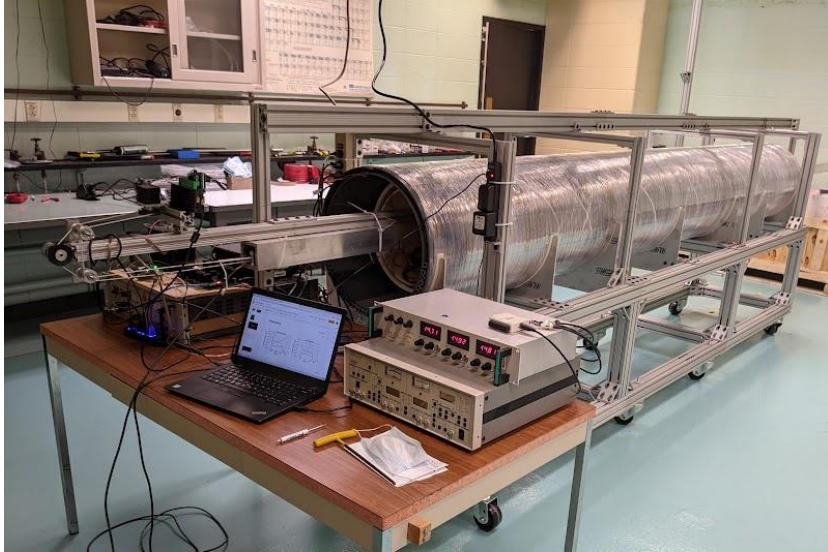
- Try to minimize magnetic Johnson noise
 - 3.0 m long glass machined with Rogowski profile
 - Coated with conductive graphite coating (Aquadag)
 - 2 cm apart, +30 kV or -30 kV on each plate
 - 3.5 m long, 25 cm diam. quartz vacuum chamber
- Ramsey SOF sequence



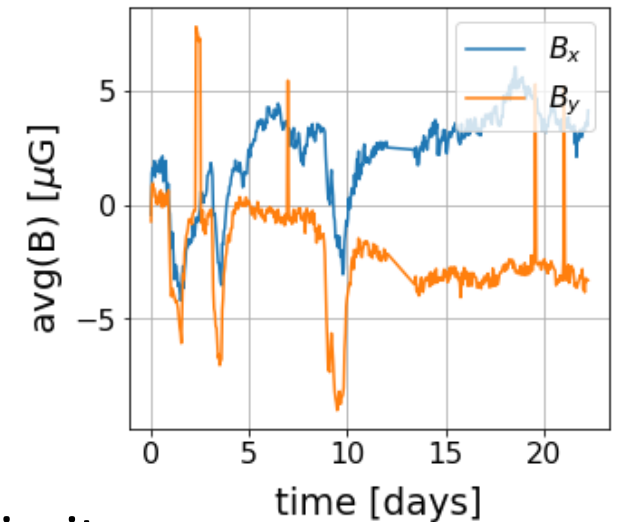
Interaction Region



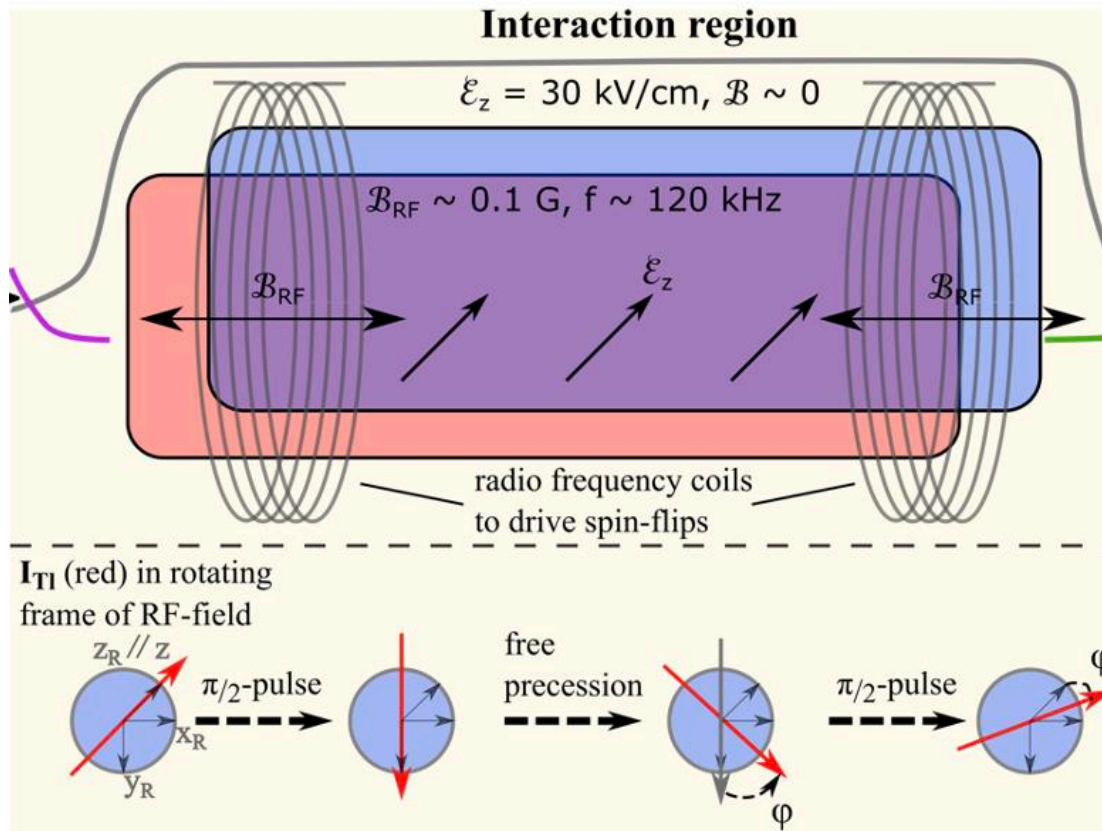
Magnetic Shielding of Interaction Region



- Spin-rotation generates internal magnetic field
 - Must shield external magnetic field
- 4 shielding layers: 3 layers Metglass, 1 layer mu-metal
- 80 shim coils
- Achieved $<10 \mu\text{G}$ over the interaction region
 - Required to keep anticipated systematics below the statistical limit



Ramsey Separated Oscillatory Fields



(1) Create TI nucleus \uparrow/\downarrow superposition with RF field ($\frac{\pi}{2}$ pulse)

(2) Free spin precession for time T , accumulate phase difference:

$$\phi \simeq \left(-\mu_{\text{TI}} B_{\text{int}} \text{sgn}(m_{\text{J}}) + C_{\text{S}} m_{I_2} + 2W_{\text{S}} S P \text{sgn}(E_{\text{MI}}) \right) T / \hbar$$

(3) After second RF $\pi/2$ pulse, probability of $\uparrow \rightarrow \downarrow$:

$$P_{\uparrow \rightarrow \downarrow} = \sin^2 \left(\frac{1}{2} \Omega_{\text{RF}} \tau \right) \cos^2 \frac{1}{2} (\phi_{\text{CPV}} + \phi_{\text{SOF}})$$

where $\phi_{\text{CPV}} = 2W_{\text{S}} S P \text{sgn}(E_{\text{MI}}) T / \hbar = 2\Delta_{\text{CPV}} T / \hbar$ and $\phi_{\text{SOF}} = \pm \pi / 2$

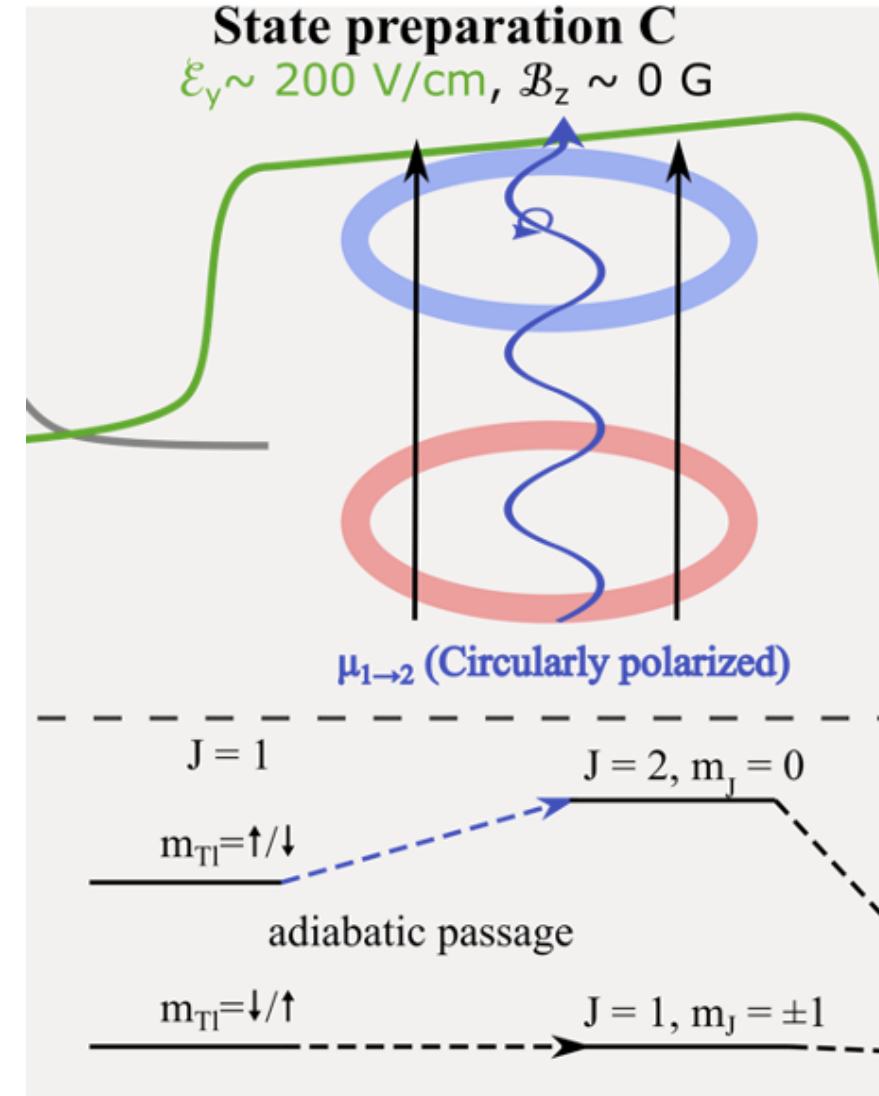
(4) Signal: $S_{\text{SOF}} = P_{\uparrow \rightarrow \downarrow}(\phi_{\text{SOF}} = +\pi/2) - P_{\uparrow \rightarrow \downarrow}(\phi_{\text{SOF}} = -\pi/2)$

State Preparation C: Detection of TI Nuclear Spin State

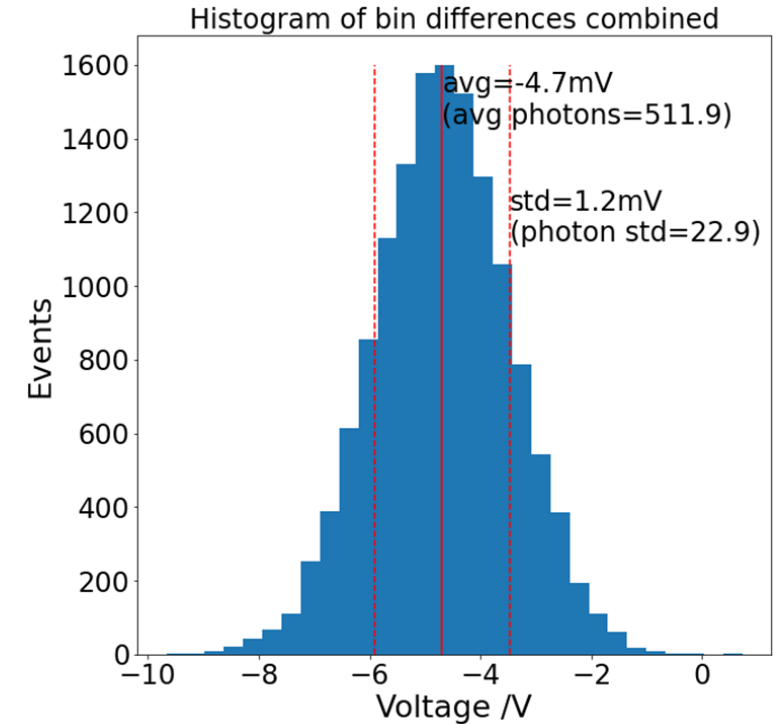
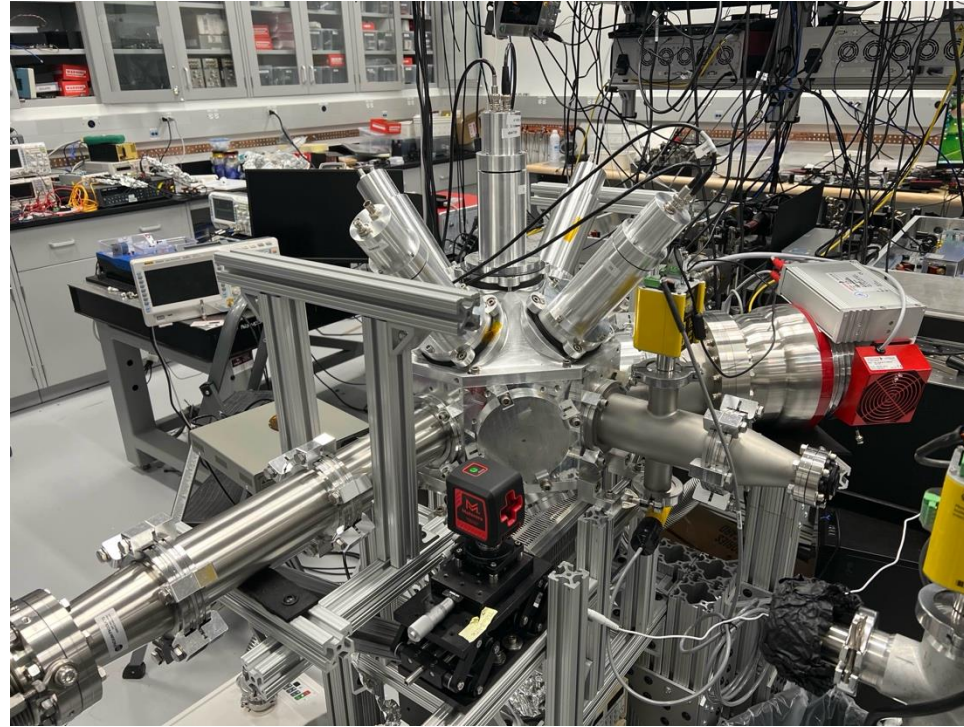
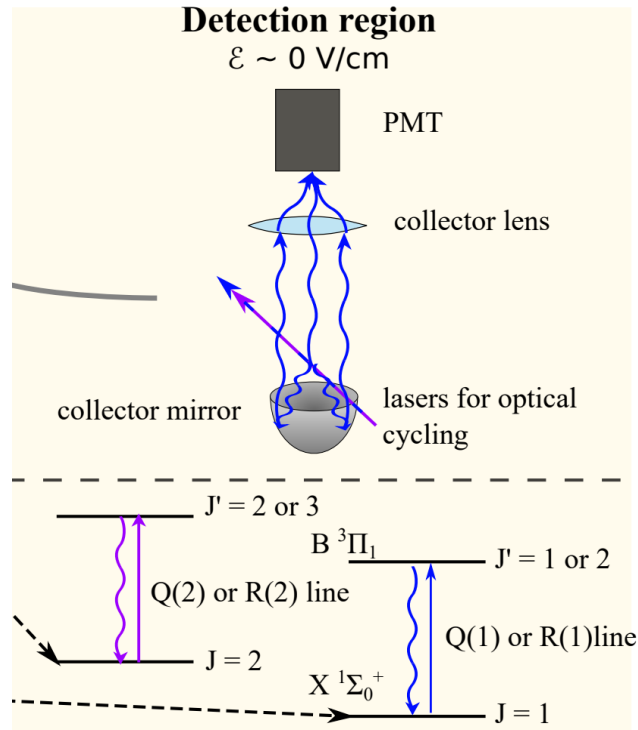
- After interaction region molecules in:

$$|J = 1, m_J, m_{I1} = +1/2, m_2\rangle \text{ and } |J = 1, m_J, m_{I1} = -1/2, m_2\rangle$$

- Thallium \uparrow & \downarrow population in different hyperfine levels < 200 kHz apart
- HF splitting \leq natural linewidth $\Gamma = 1.6$ MHz
 - Can't resolve \uparrow & \downarrow with optical readout
- Move \uparrow or \downarrow to different rotational states
- Microwave driven adiabatic passage like State Prep. B

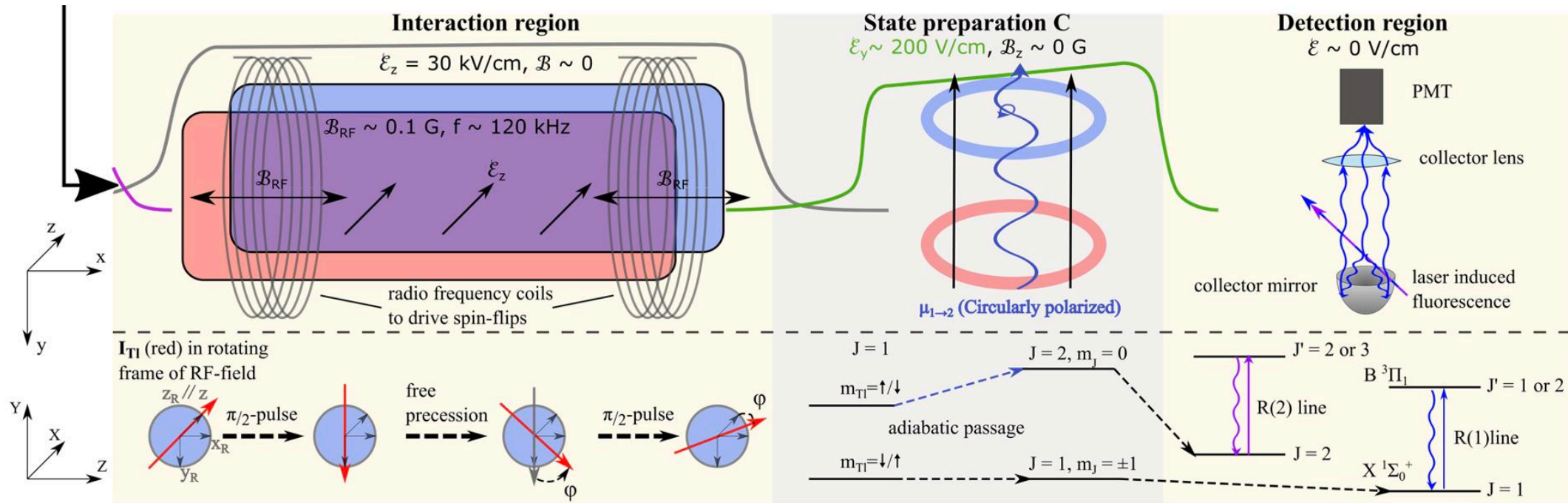


Detection of TI Nuclear Spin State



- Laser induced fluorescence to read out molecules
- Use two UV lasers at 271.8 nm (offset by relevant rotational splittings)
- Excite and detect at same wavelength so must reduce scattered light
- R(1) and R(2) transition to read out \uparrow & \downarrow populations
 - Rapidly switch between transitions in a single pulse using AOMs

Detection of Phase Shift sensitive to CP-Violation



- Construct asymmetry signal

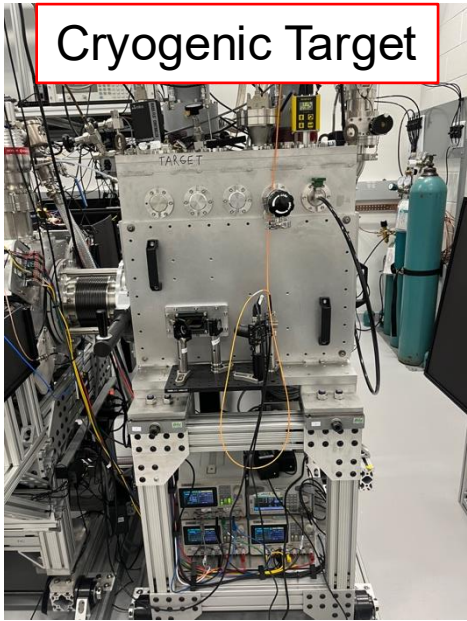
$$A = \frac{S_{\uparrow} - S_{\downarrow}}{S_{\uparrow} + S_{\downarrow}}$$

- With SOF on resonance

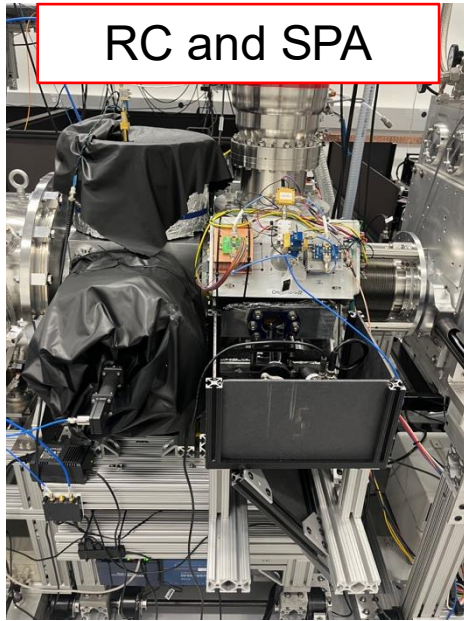
$$A \simeq 1 - 2 \sin^2 \Omega_{RF} \tau \cos^2 \frac{1}{2} (\phi_{CPV} + \phi_{SOF})$$

- With $\phi_{SOF} = \pm\pi/2$ and $\Omega_{RF} \tau = \pi/2$: $A \simeq \text{sgn}(\phi_{SOF}) \sin \phi_{CPV} \sim \pm\phi_{CPV}$

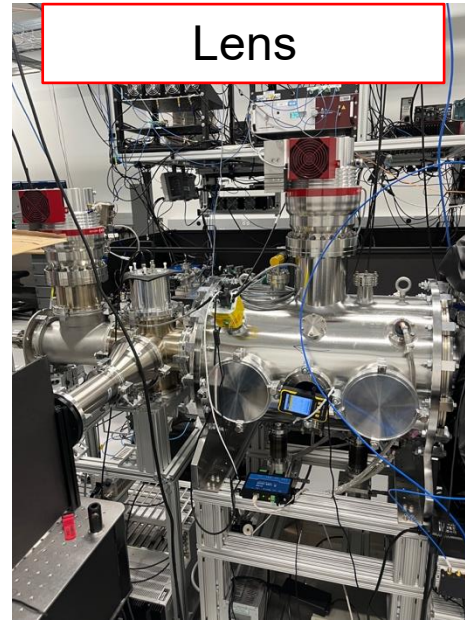
Cryogenic Target



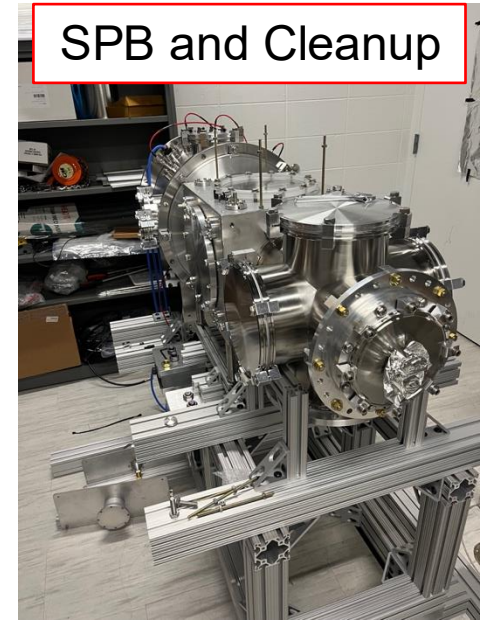
RC and SPA



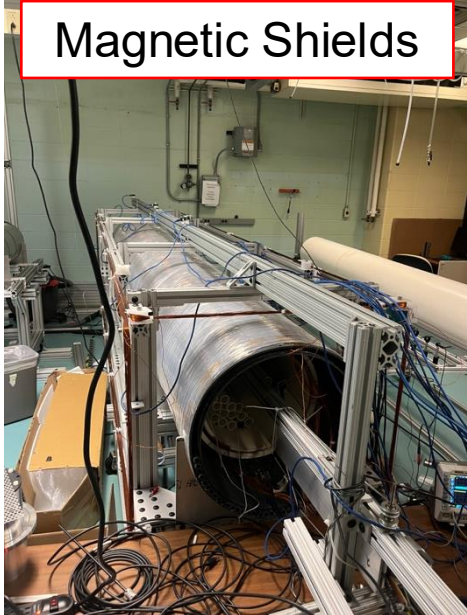
Lens



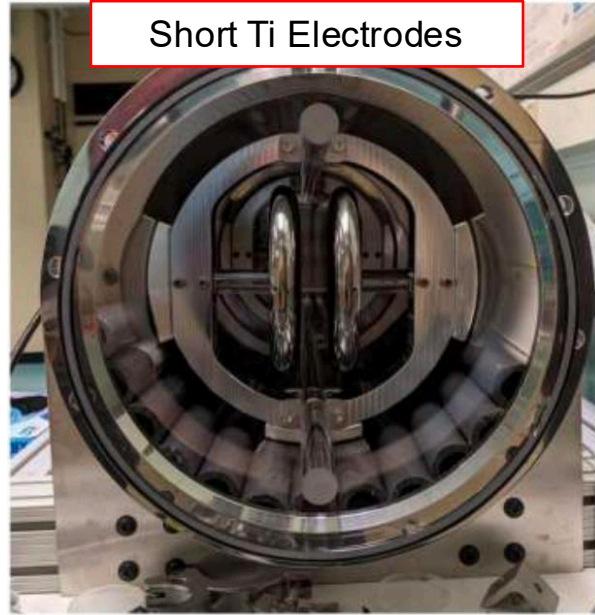
SPB and Cleanup



Magnetic Shields



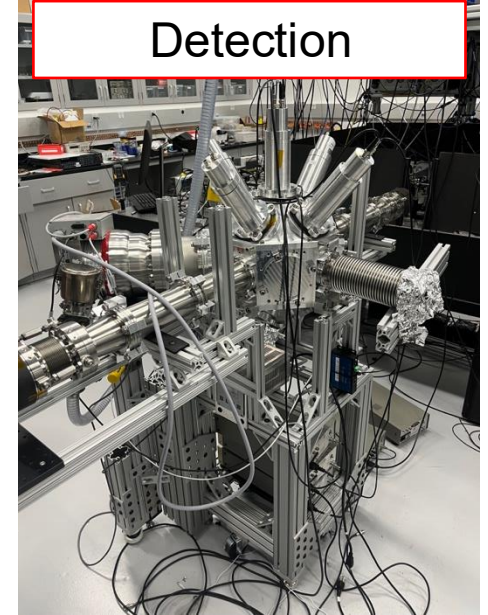
Short Ti Electrodes



Long Electrode Prep



Detection



^{205}TlF ground state energy levels at high electric field

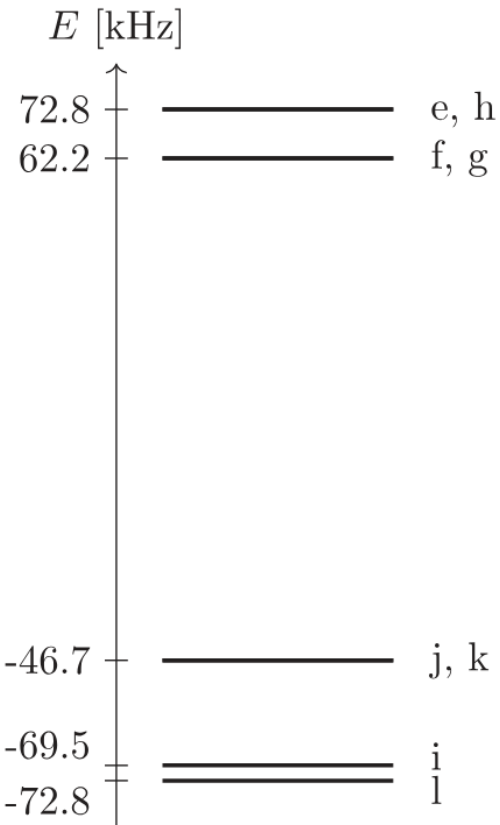


Table 3. All non-degenerate pairs of $|m_j| = 1$ states in the $\tilde{J} = 1$ manifold at $\mathcal{E}_{\text{MI}} = 30 \text{ kV cm}^{-1}$ that do not involve the states $|i\rangle$ and $|l\rangle$ or a flip of m_j . The quantum numbers given are that of the largest decoupled-basis component. State labels l are as in [32] and figure 11. The quantities $df_0/d\mathcal{B}_z$ and $df_0/d\mathcal{E}_z$ give the slope of the resonance frequency with respect to the external magnetic field and electric field, respectively. Shift \mathcal{B}_{mot} indicates the resonance frequency shift, due to the motional field that accompanies \mathcal{E} reversal, with respect to a stray field component \mathcal{B}_y . S denotes the sensitivity to the NSM relative to the maximum possible value; it is given by $|\langle I_{1,z} \rangle_1 - \langle I_{1,z} \rangle_2|$ for the transition between states 1 and 2. f_0 indicates the transition frequency between the two states. $|\langle \cdot | \mathcal{H}_Z | \cdot \rangle|$ indicates the magnitude of the transition dipole moment between states 1 and 2. All shifts are calculated from diagonalization of the ground-state Hamiltonian (equation (7)).

What flips?	State 1				State 2				f_0 kHz	$df_0/d\mathcal{B}_z$ [mHz/ μG]	$df_0/d\mathcal{E}_z$ [mHz/(V/cm)]	Shift \mathcal{B}_{mot} [mHz/ μG]	S	$ \langle \cdot \mathcal{H}_Z \cdot \rangle $ [kHz]		
	l	m_j	m_{I_1}	m_{I_2}	l	m_j	m_{I_1}	m_{I_2}						x, y	z	
m_{I_1}	e, h	e	-	-	-	j	-	+	-	119.52	+2.49	$+4.66 \times 10^{-5}$	0.95	1.33	0.00	
		h	+	+	+	k	+	-	+	-2.49	$+5.22 \times 10^{-5}$					
m_{I_1}, m_{I_2}	j, k	f	+	+	-	k	+	-	+	108.92	+1.52	-1.17×10^{-4}	0.99	0.00	0.09	
		g	-	-	+	j	-	+	-	-1.52	-1.23×10^{-4}					
m_{I_2}	i	e	-	-	-	g	-	-	+	10.59	+4.00	$+1.69 \times 10^{-4}$	0.04	1.88	0.00	
		h	+	+	+	f	+	+	-	-4.00						

- EDM search uses e+j and/or h+k states in which TI spin flips
- (e+j) and (h+k) have opposite signs of internal B field
- Need molecules in $J=1$, high electric field

Some systematics to consider

Potential issues:

- Not at resonance frequency, deviation from exact phase yields extra phase shift: $\phi_{\text{CPV}} + \phi'$
- cancel by E-field reversal which reverses ϕ_{CPV}
- switching e-j vs h-k changes sign of ϕ_{CPV}
- switching sign ϕ_{SOF} , changes sign of asymmetry
- make small changes to RF frequency

- Spatially varying fields -> transitions to undesired states, loss of sensitivity, losses might not be spatially uniform and so get inhomogeneous beam cross-section, will couple with gradients in IR E-field
- Imperfect E-field reversal: TI spin up/down splitting changes with E (2nd order spin-spin, spin-rotation to other J), e-j, h-k get freq shift upon reversal, -31.5 mHz/(V/cm) should cancel
- Stray B-fields: keep below 10 μG with magnetic shielding
- B-fields along E gives different freq for e-j, h-k pairs
- Comagnetometer: use e-g, f-h in which F spin flips – expect no CPV, these states more sensitive to B field but need RF=10.6 kHz
- f-k, g-j flip both spins

Some systematics to consider

- Measuring frequency shifts in 10^{-8} Hz range, many systematic effects

Motional Magnetic Fields

- Particles moving with velocity \vec{v} through electric field \vec{E} feel motional magnetic field: $\vec{B}_m = \frac{\vec{v}}{c} \times \vec{E}$
- Mimics and EDM signal if \vec{E} and \vec{B}_0 misaligned

Leakage Currents

- High voltages can lead to uncontrolled leakage currents
- These currents make magnetic fields that reverse with electric field reversal

Geometric (Berry) Phases

- Inhomogeneous magnetic fields combined with particle trajectories create false frequency shifts

Projected sensitivity

	²⁰⁵ TlF (projected)	¹⁹⁹ Hg	¹²⁹ Xe	²²⁵ Ra	¹⁷¹ Yb	Neutron
Energy shift $\delta\nu$ (Hz)	1×10^{-7}	7×10^{-12}	5×10^{-10}	4×10^{-3}	5×10^{-7}	3×10^{-8}
δS ($e \text{ fm}^3$) or δd ($e \text{ cm}$)	3×10^{-14}	1×10^{-13}	2×10^{-10}	3×10^{-6}	8×10^{-10}	1×10^{-26}
$\delta\bar{\theta}_{QCD}$	1×10^{-12}	6×10^{-11}	3×10^{-8}	3×10^{-6}	–	8×10^{-11}
quark c-EDMs $\alpha\tilde{d}_u + \beta\tilde{d}_d$	$0.8\tilde{d}_d + 0.6\tilde{d}_u$	\tilde{d}_d	\tilde{d}_d	$0.7\tilde{d}_u - 0.7\tilde{d}_d$	–	–
$\delta(\alpha\tilde{d}_u + \beta\tilde{d}_d)$ (cm^{-1})	3×10^{-28}	2×10^{-27}	3×10^{-24}	3×10^{-23}	–	1×10^{-26}
NSM or EDM in terms of d_p or d_n	d_p	$d_n + 0.1d_p$	$d_n + 0.2d_p$	–	–	d_n
δ in nucleon EDM ($e \text{ cm}$)	8×10^{-27}	1×10^{-26}	3×10^{-23}	–	–	1×10^{-26}

values indicated with – not found in literature

Abel et al. Phys. Rev. Lett. 124, 081803 (2020)

Graner et al. Phys. Rev. Lett. 116, 161601 (2016)

Sachdeva et al. Phys. Rev. Lett. 123, 143003 (2019)

Parker et al. Phys. Rev. Lett. 114, 233002 (2015)

Zheng et al. Phys. Rev. Lett. 129, 083001 (2022)

Petrov et al. Phys. Rev. Lett. 88, 073001 (2002)

Dzuba et al. Phys. Rev. A 01211 (2002)

Pospelov et al. Nucl. Phys. B 573, 177 (2000)

Flambaum et al. Phys. Rev. A 101, 042504 (2020)

Current Status

- State Preparation B and C nearing completion
- Small (1m) interaction region with Ti electrodes ready to go
- Alignment of beamline is challenging!
- Coating and alignment of 3.0 m long electrodes over next few months

- First science data in 2026 ?

Advanced Cold Molecule *Electron EDM* (ACME) III collaboration



Johns Hopkins University/ University of Chicago

David DeMille (PI)
Zhen Han (grad student)
Peiran Hu (grad student)

Northwestern University

Gerald Gabrielse (PI)
Xing Fan (postdoc)
Siyuan Liu (grad student)
Collin Diver (grad student)
Maya Watts (grad student)
Daniel Ang
(Harvard grad student)
Cole Meisenhelder
(Harvard grad student)

Harvard University

John Doyle (PI)

Okayama University

Ayami Hiramoto (postdoc)
Takahiko Masuda (PI)
Koji Yoshimura
Noboru Sasao
Satoshi Uetake

Other collaborators

Cris Panda (Berkeley)
Nick Hutzler (Caltech)
Xing Wu (Michigan St.)



David DeMille



John Doyle



Gerald Gabrielse



Daniel Ang



Cole Meisenhelder



Siyuan Liu



John Mitchell



Zhen Han



Peiran Hu



Xing Wu



Zack Lasner



Collin Diver



Maya Watts



Xing Fan



Koji Yoshimura



Satoshi Uetake



Noboru Sasao



Takahiko Masuda



Ayami Hiramoto

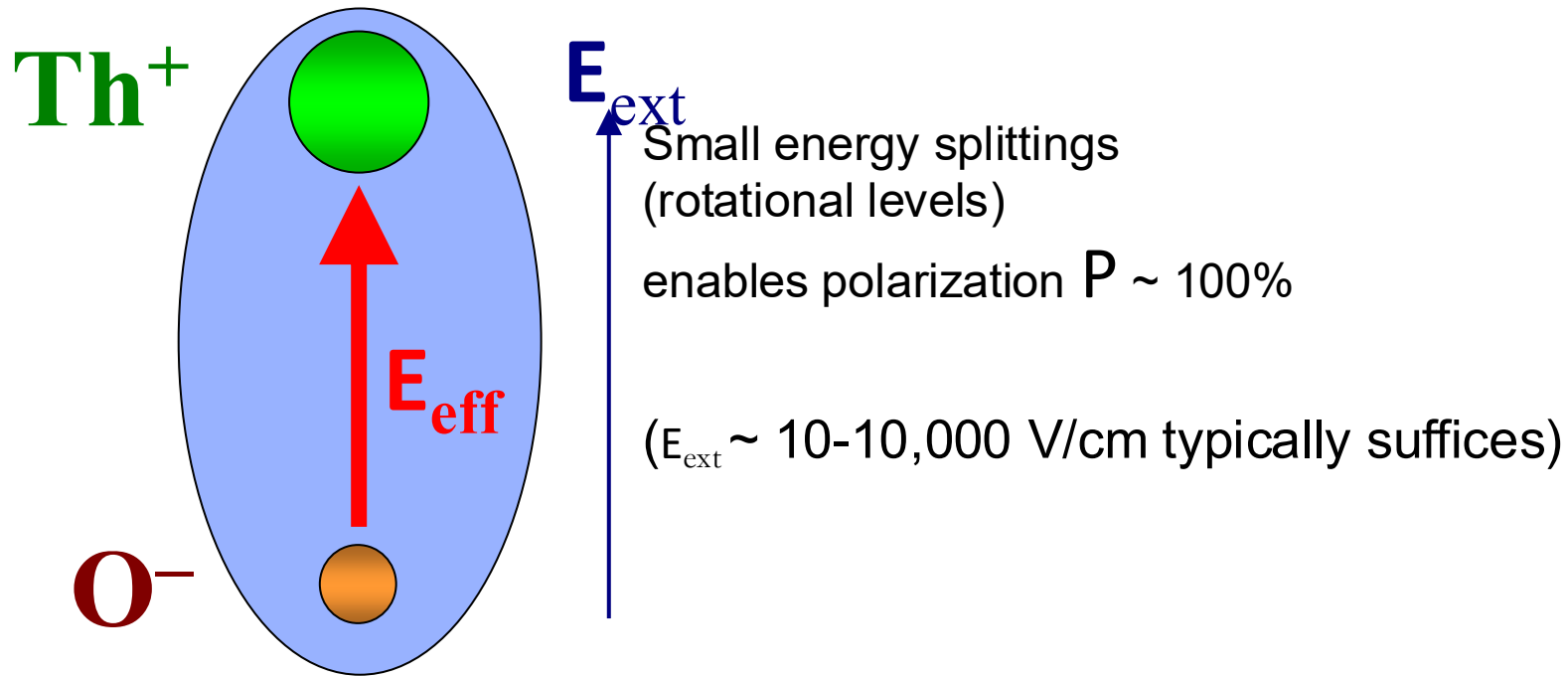


Cris Panda



Nick Hutzler

Amplified electric field E in polar molecules



Inside molecule, electron EDM acted on by $E_{\text{eff}} \sim P (\alpha^2 Z^2) Ze/a_0^2$

P. Sandars
1965

$E_{\text{eff}} \cong 80$ GV/cm for ThO* [near theoretical maximum]

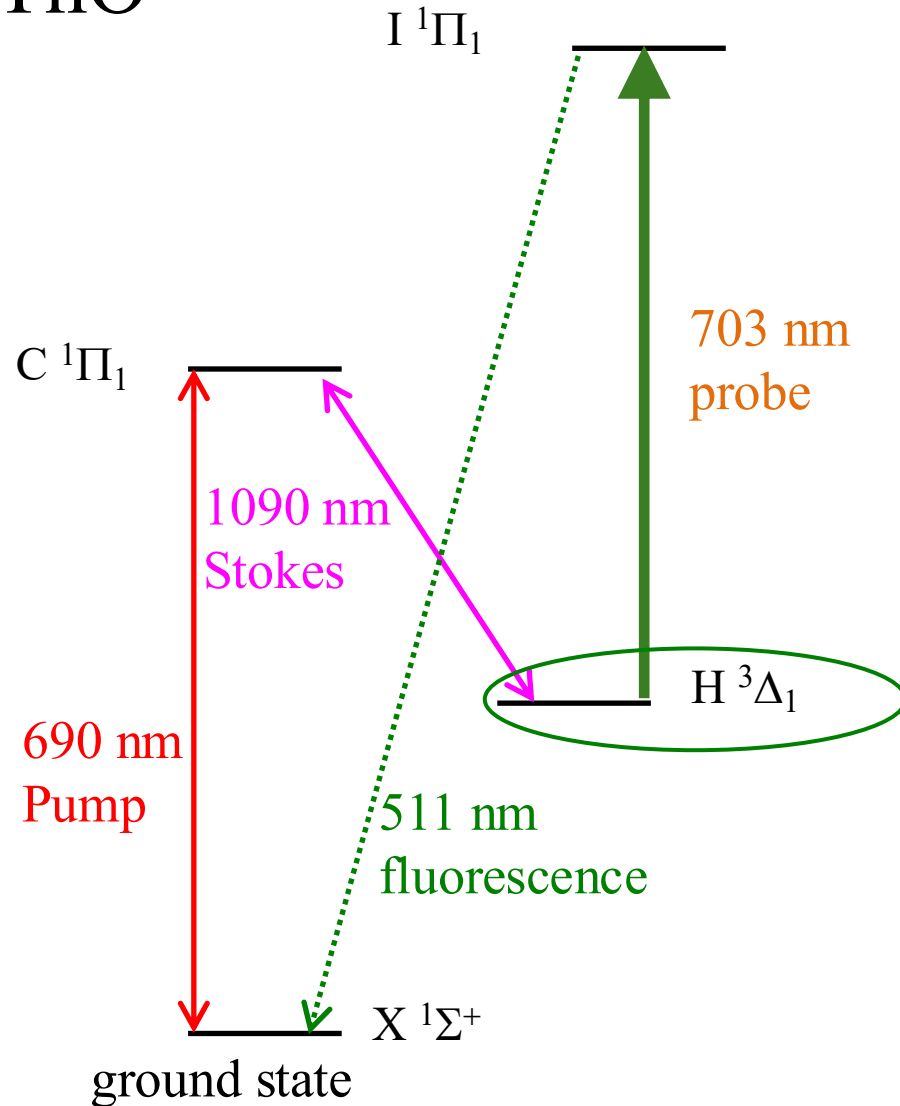
Initial: Meyer & Bohn (2008); $\pm 5\%$: Skripnikov *et al.* (2016), Fleig *et al.* (2016), ...

Requires unpaired electron spin(s): chemical free radical

Molecular species for ACME: ThO^*

[A.C. Vutha *et al.* J. Phys B 2010]

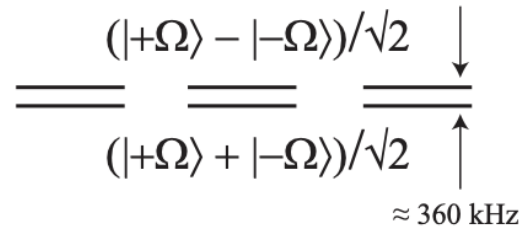
ThO



- **Sufficient coherence time for measurement** in metastable state $H\ ^3\Delta_1$
- **Largest effective internal E:** $\sim 80\ \text{GV/cm}$
- **Suppressed magnetic moment**
 $< 0.01\ \mu_B$ in $H\ ^3\Delta_1$ reduces B -field systematics
[Idea: Meyer, Bohn, Cornell *et al.* (JILA);
Measured: A.C. Vutha *et al.*, PRA 2011]
- **Omega-doublet co-magnetometer**
suppresses many possible systematics
& requires only very modest polarizing E-field
- All spectroscopic data previously known
- State preparation and readout
w/standard, robust diode & fiber lasers
- Blue-shifted fluorescence from probe laser
 \Rightarrow no problem with backgrounds
- **High beam source yield**

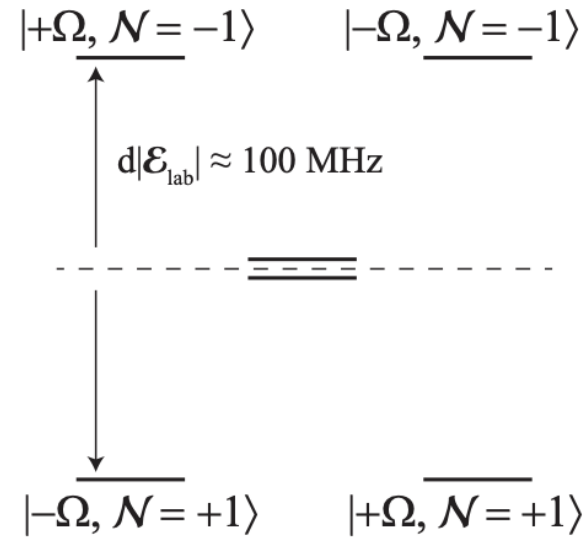
Level Structure of $H^3\Delta_1$ $J=1$ state of ThO

$$\mathcal{E}_{\text{lab}} = 0, \mathcal{B}_{\text{lab}} = 0, \mathbf{d}_e = 0$$



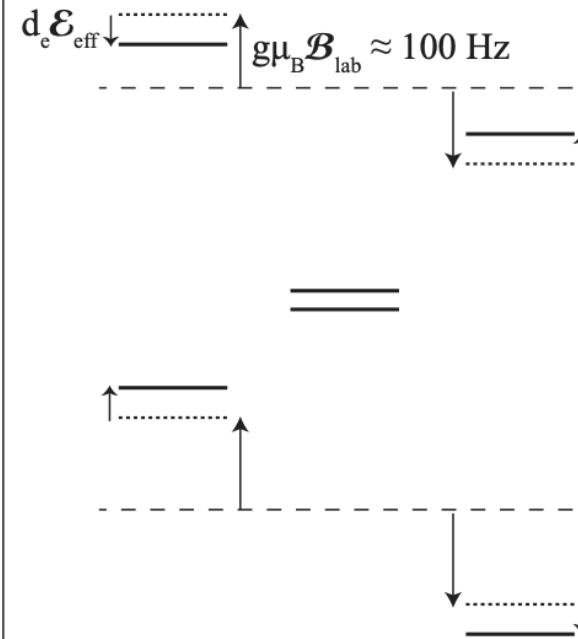
M = -1 M = 0 M = +1

$$\mathcal{E}_{\text{lab}} \neq 0, \mathcal{B}_{\text{lab}} = 0, \mathbf{d}_e = 0$$



M = -1 M = 0 M = +1

$$\mathcal{E}_{\text{lab}} \neq 0, \mathcal{B}_{\text{lab}} \neq 0, \mathbf{d}_e \neq 0$$



M = -1 M = 0 M = +1

- Spacing of levels of opposite parity $\sim 360 \text{ kHz}$!
- Completely polarized in fields of 100 V/cm

(Figure 2.1 from Nick Hutzler's Thesis)

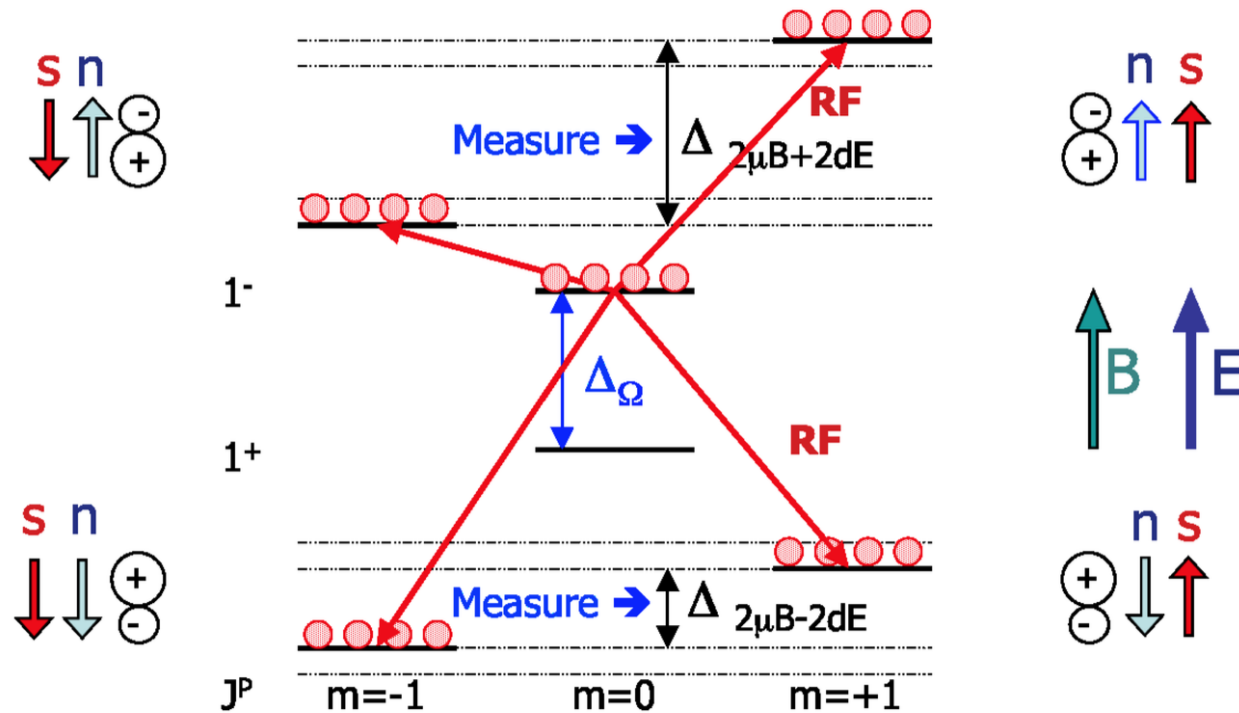
Small magnetic moment in $H^3\Delta_1$ $J=1$ state of ThO

$$\begin{array}{rcccl}
 & \xrightarrow{\Lambda = +2} & + & \xleftarrow{\Sigma = -1} & = & \xrightarrow{\Omega = +1} \\
 \boxed{{}^3\Delta_1} & & & & & \\
 & \xleftarrow{\mu_L = g_L \Lambda \mu_B = -2\mu_B} & + & \xrightarrow{\mu_S = g_S \Sigma \mu_B \approx +2\mu_B} & = & \mu \approx 0
 \end{array}$$

- -cancellation between magnetic moment from electron orbital angular momentum and electron spin
- -Magnetic moment of order $|g\mu_B| < 0.01 \mu_B$!!!
- -tremendous reduction in sensitivity to magnetic fields

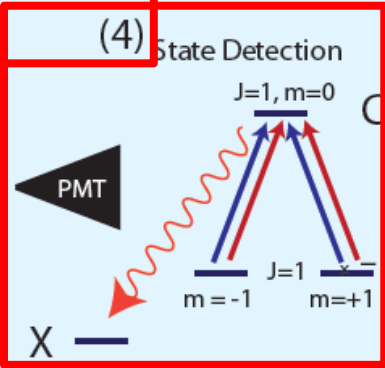
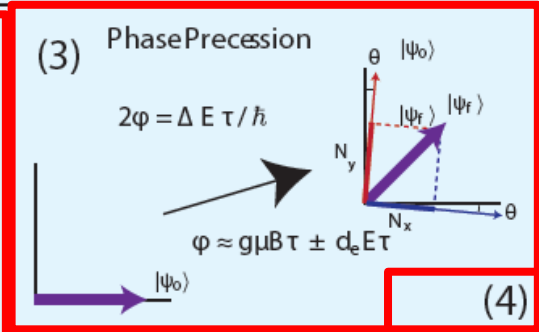
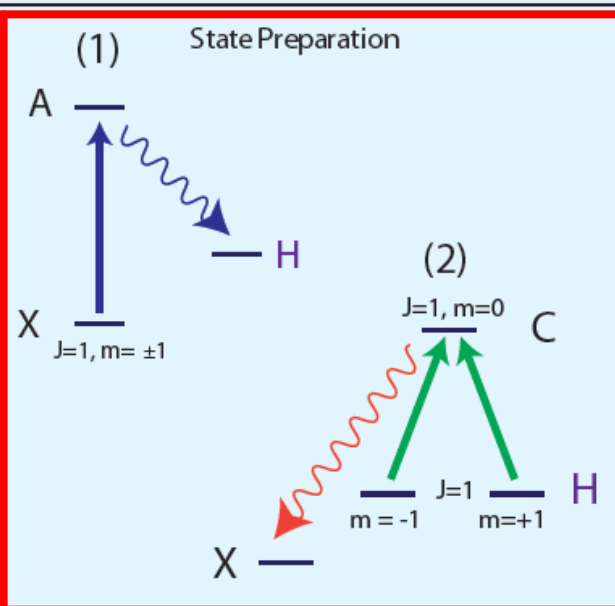
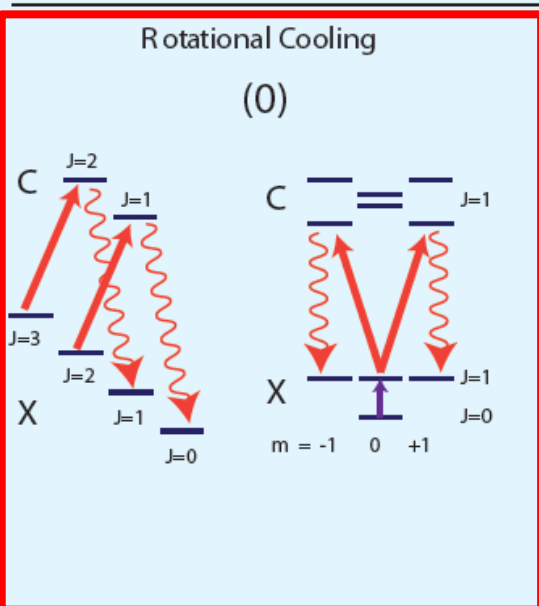
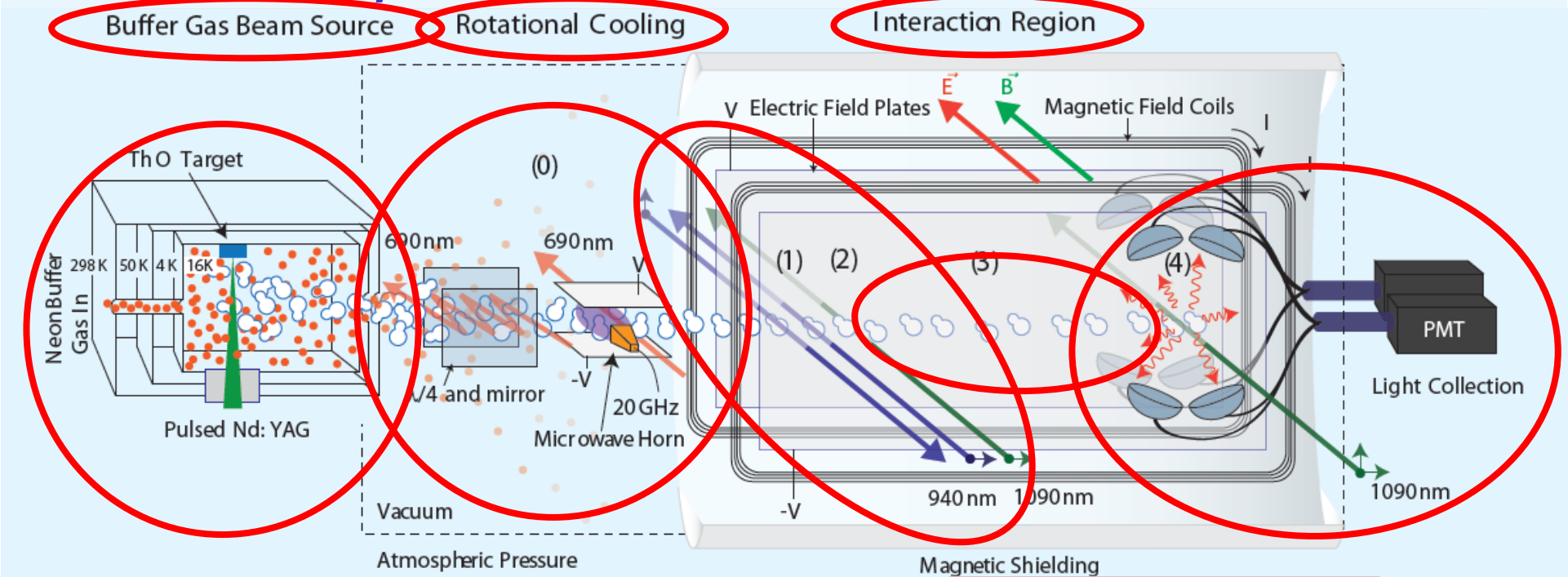
(Figure 2.2 from Nick Hutzler's Thesis)

Electron EDM search in Hund's case (c) Polar Molecule



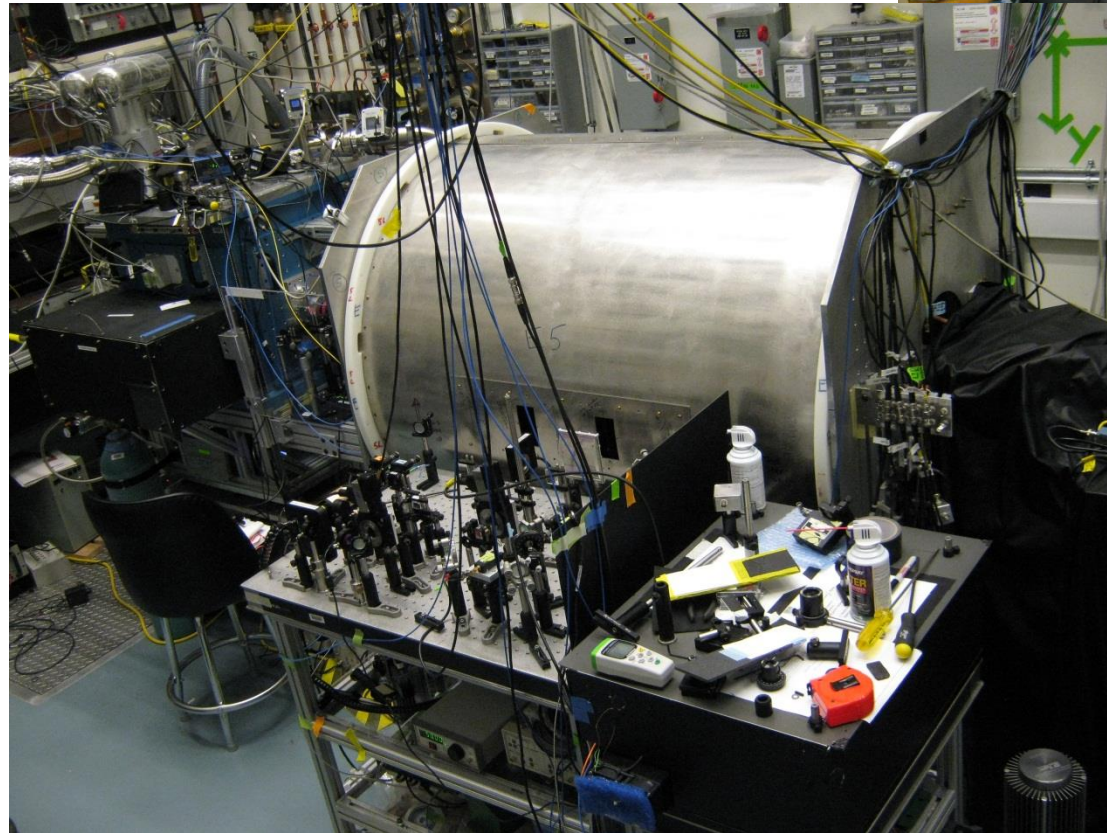
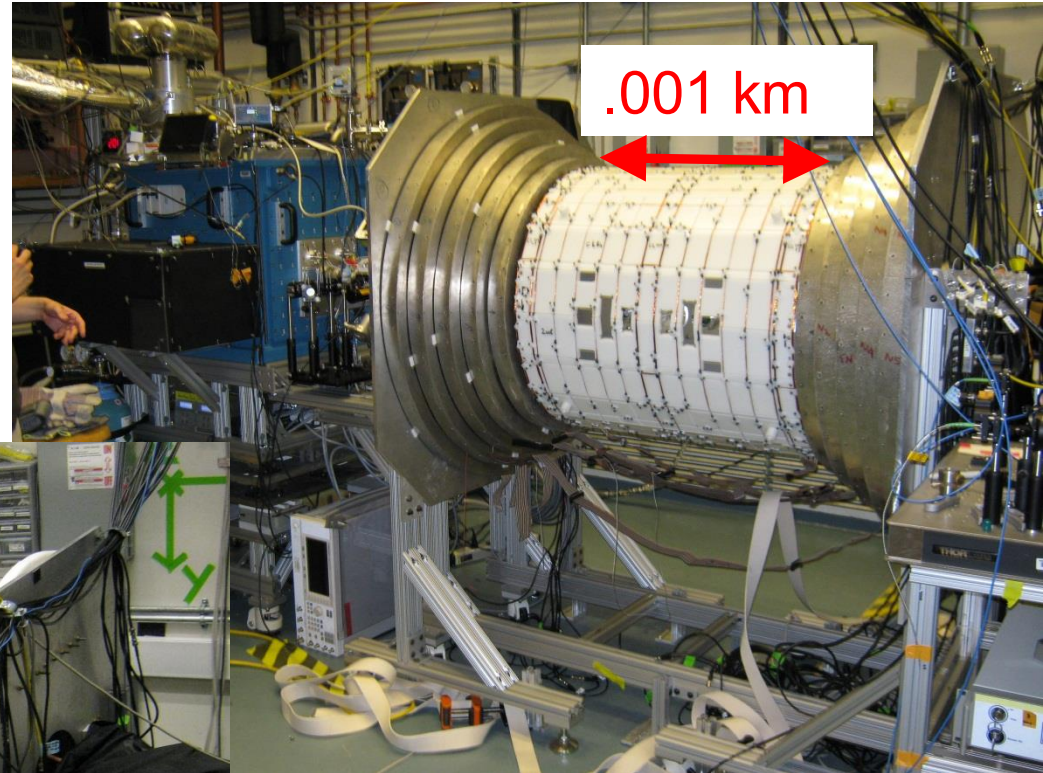
- Prepare superposition : $|\psi_N(t = 0)\rangle = \frac{1}{\sqrt{2}} [|M = 1, N\rangle + |M = -1, N\rangle]$
- $M = \pm 1$ levels have different energies in B , E fields, acquire relative phase shifts
- $\phi_E \approx d_e \mathcal{E}_{\text{eff}} N t$, $\phi_B \approx g_J \mu_B B t$
- After time τ , components acquire relative phase shifts :
 $|\psi_N(t = \tau)\rangle = \frac{1}{\sqrt{2}} [e^{i\phi} |M = 1, N\rangle + e^{-i\phi} |M = -1, N\rangle]$
- Detect projection of spin on \hat{x} and \hat{y} axes, look for E -field dependent shift

ACME I experimental schematic



ACME I apparatus

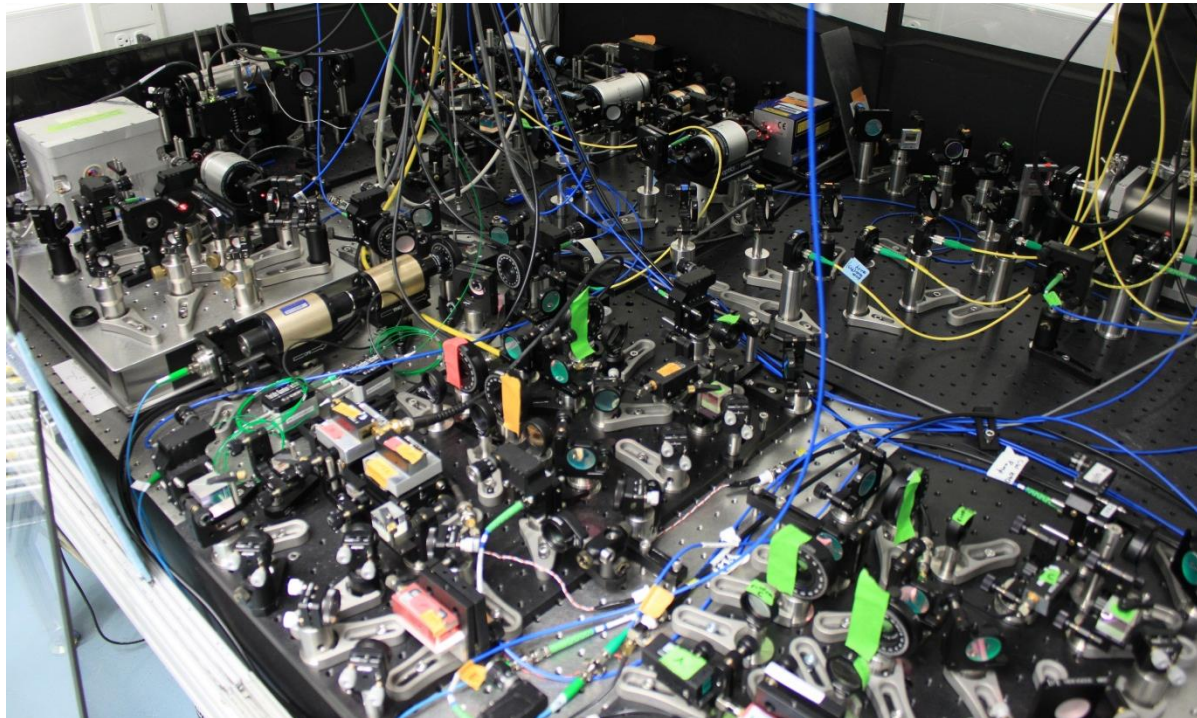
Magnetic field coils
(3 orthogonal components
& all first-order gradients)



Complete
beam source
& magnetic shields
& last-stage optics

ACME I apparatus

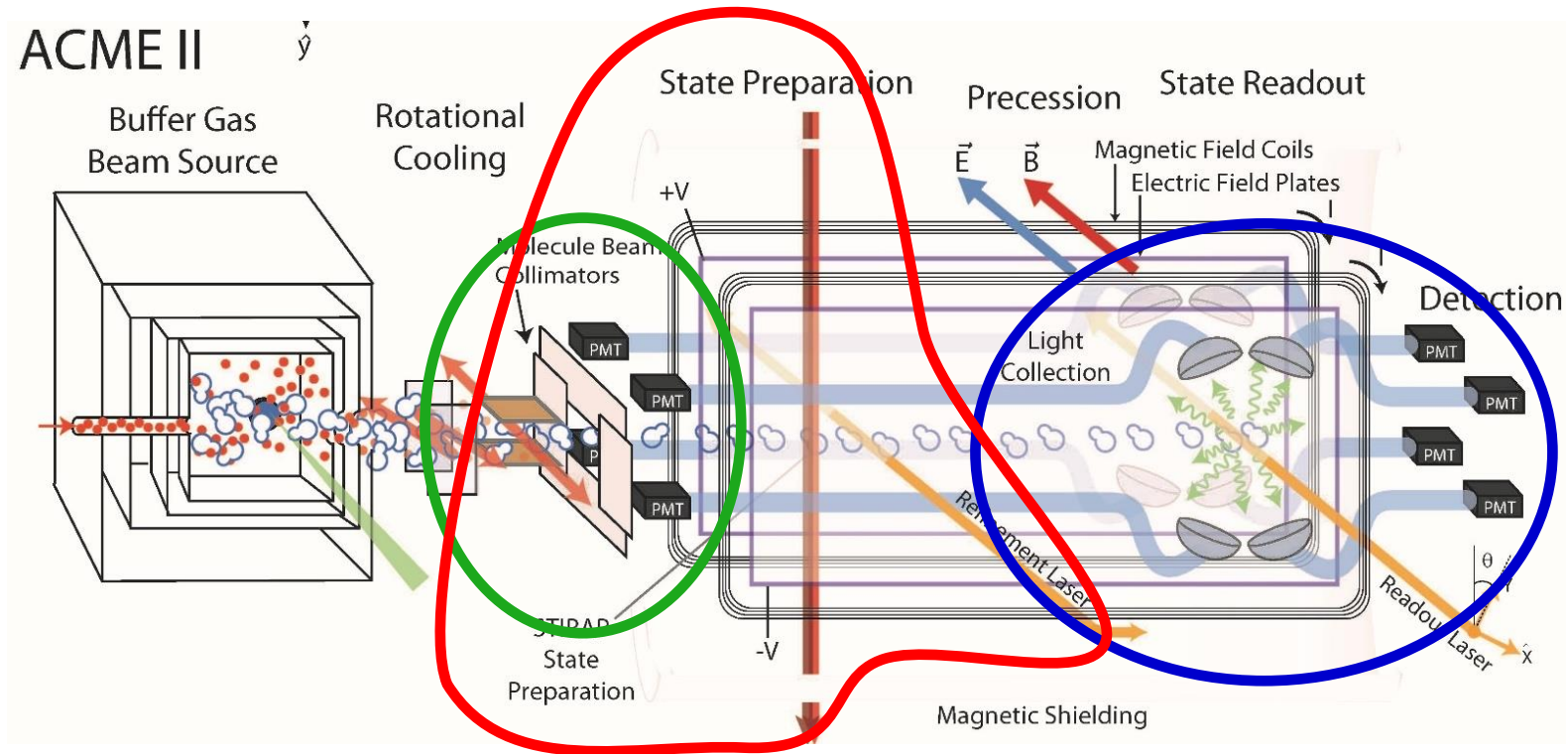
One of several optical tables w/
~ten lasers, dozens of modulators,
hundreds of meters of optical fiber, etc.
split between two rooms in two buildings



“control room”



ACME II upgrades to increase signal

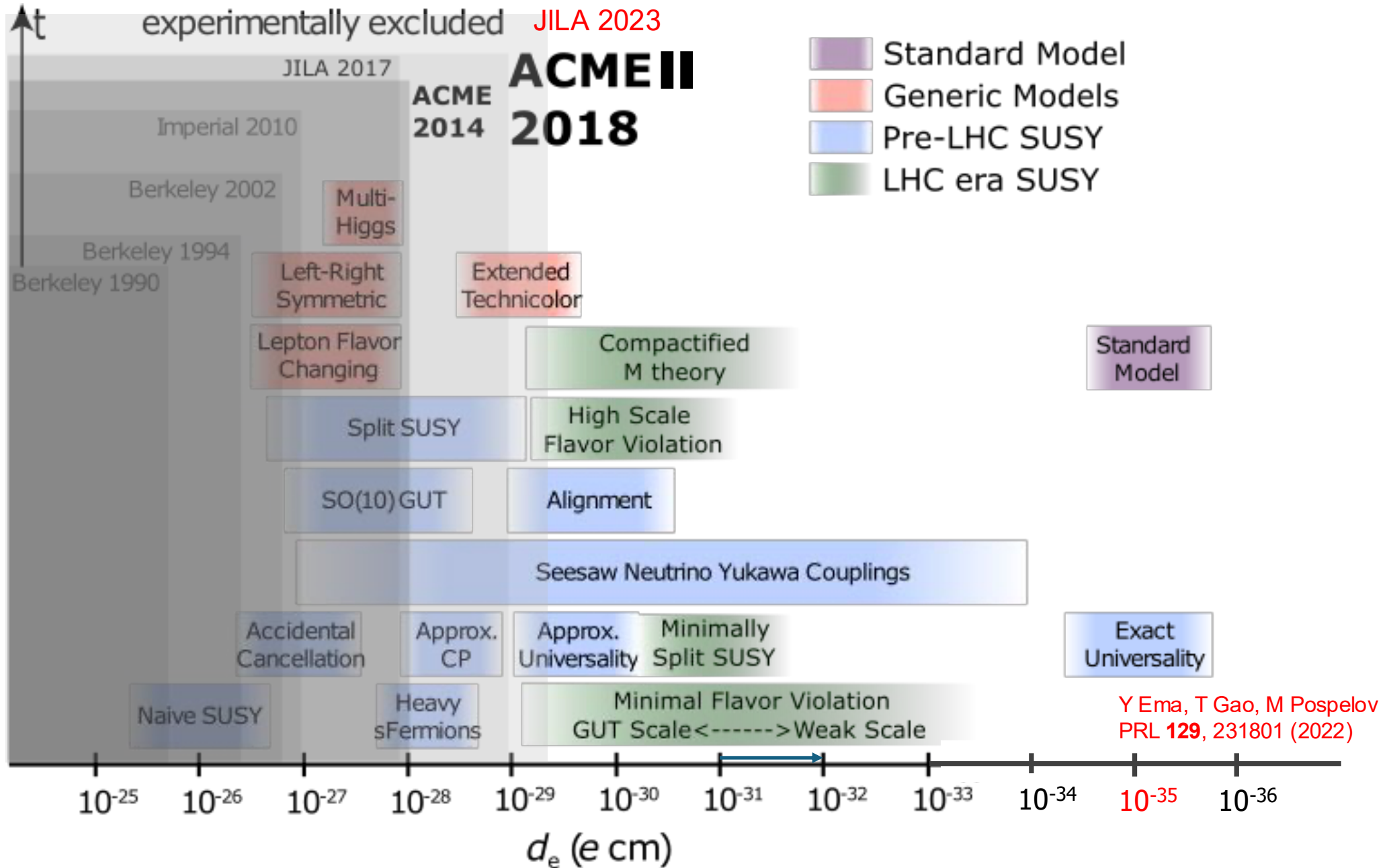


- Coherent (STIRAP) state prep. \Rightarrow x12 Signal
- Larger detection area \Rightarrow x8 Signal
- New probe transition, better PMTs, improved optics \Rightarrow x4 Signal

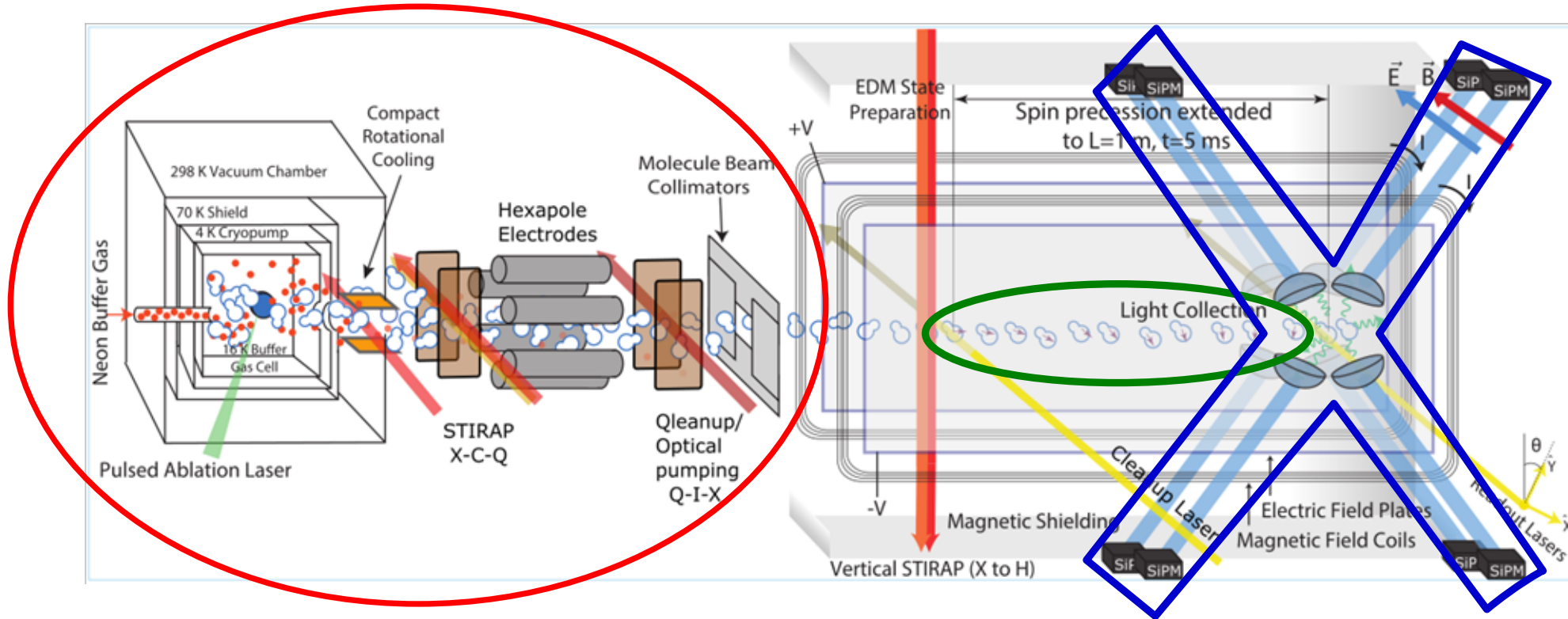
C. Panda *et al.*,
PRA (2016)

Bottom line: $\sim 10\times$ improved sensitivity vs. ACME I

Search for new physics via electron EDM



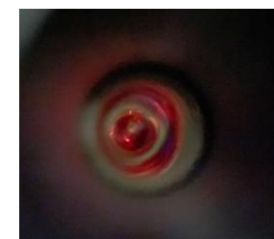
ACME III upgrades for statistical sensitivity + systematics control



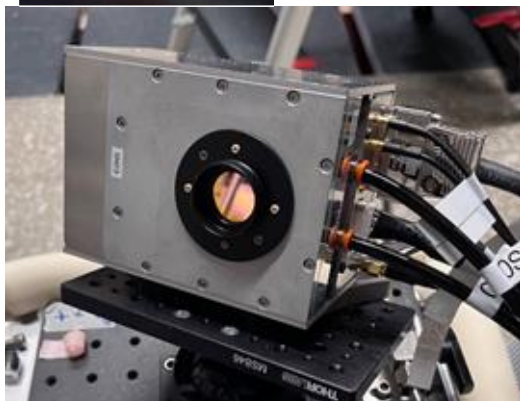
- More useful molecules via molecular lens [NJP 2022], improved beam source, etc.
- ~5x longer interaction time via improved state lifetime info [$\tau_H = 4.2(5)$ ms: PRA 2022]
- Better detection efficiency: optimized SiPM detectors [Opt Exp 2023, NIM-A 2023] & collection optics
- Additional technical improvements to reduce noise & systematic errors
[improved magnetic shields, in situ magnetometry with “new” molecular state, low birefringence optics, etc...]

Bottom line: ~30× anticipated improvement in statistical sensitivity vs. ACME II

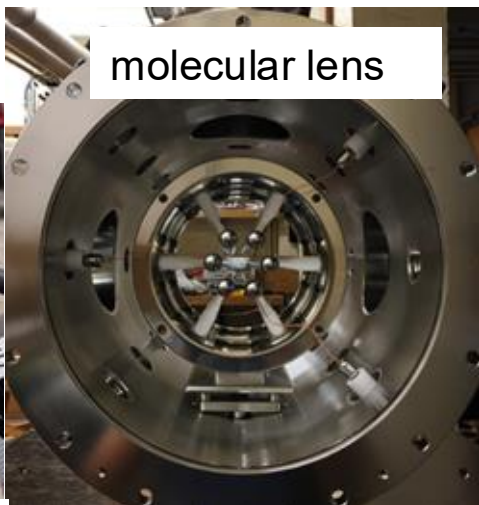
ACME III: fully operational, systematics studies nearly complete



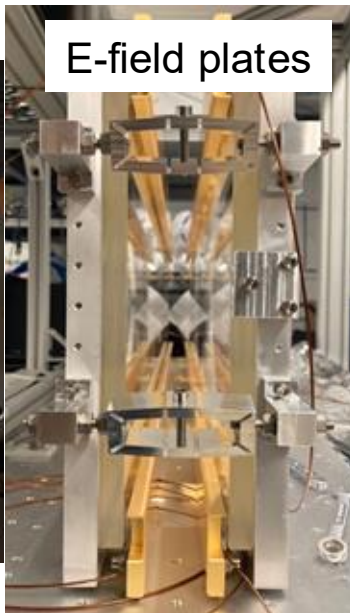
naked-eye
visible
fluorescence



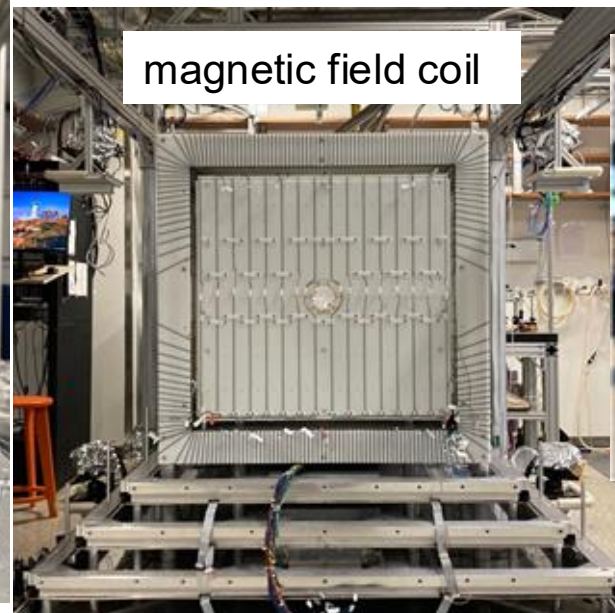
Silicon Photomultiplier



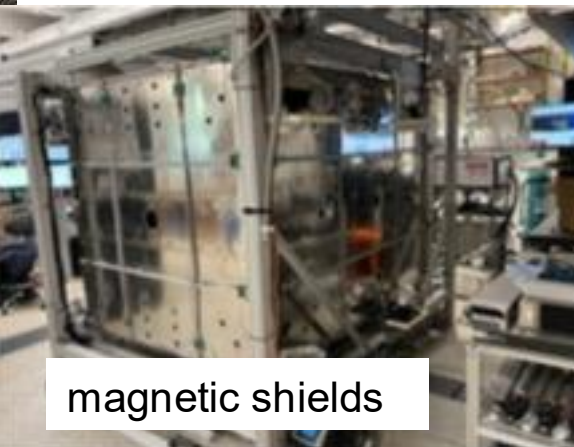
molecular lens



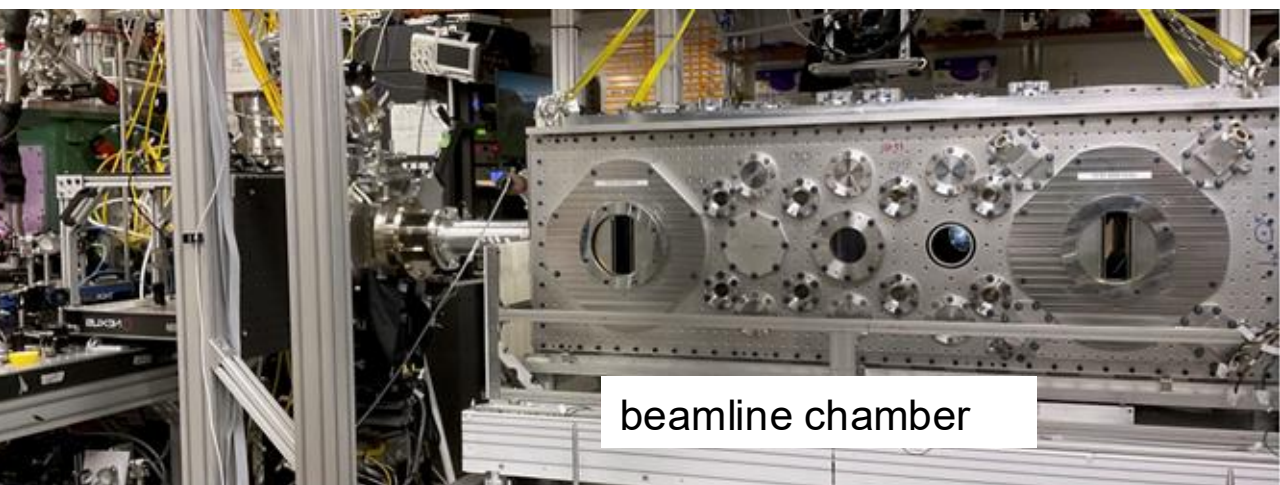
E-field plates



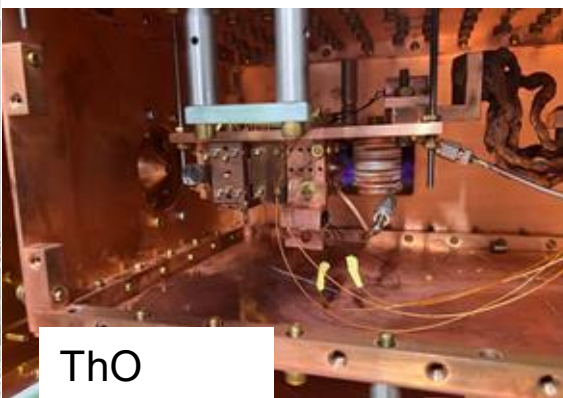
magnetic field coil



magnetic shields



beamline chamber



ThO
source



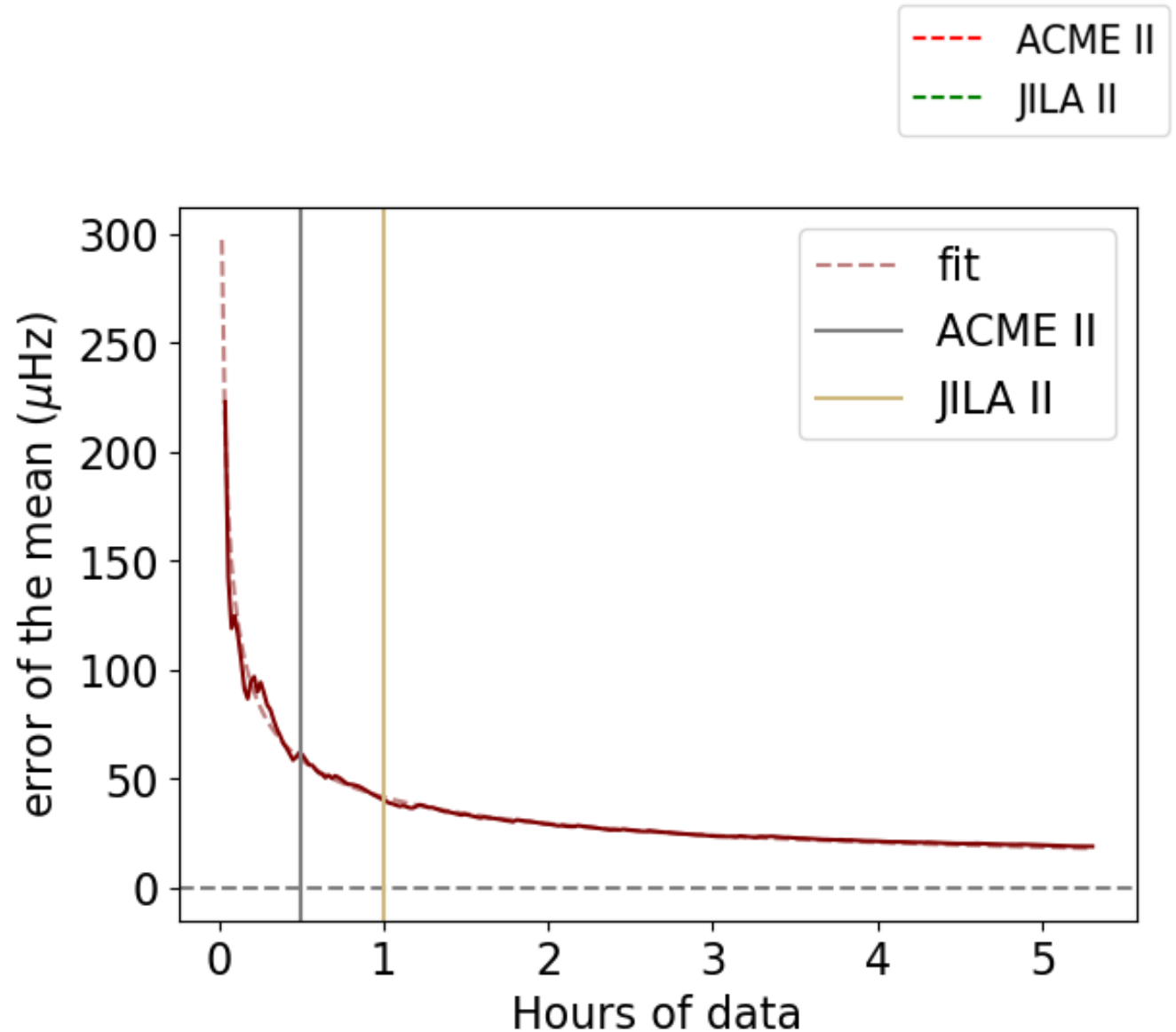
control station

Status of ACME III

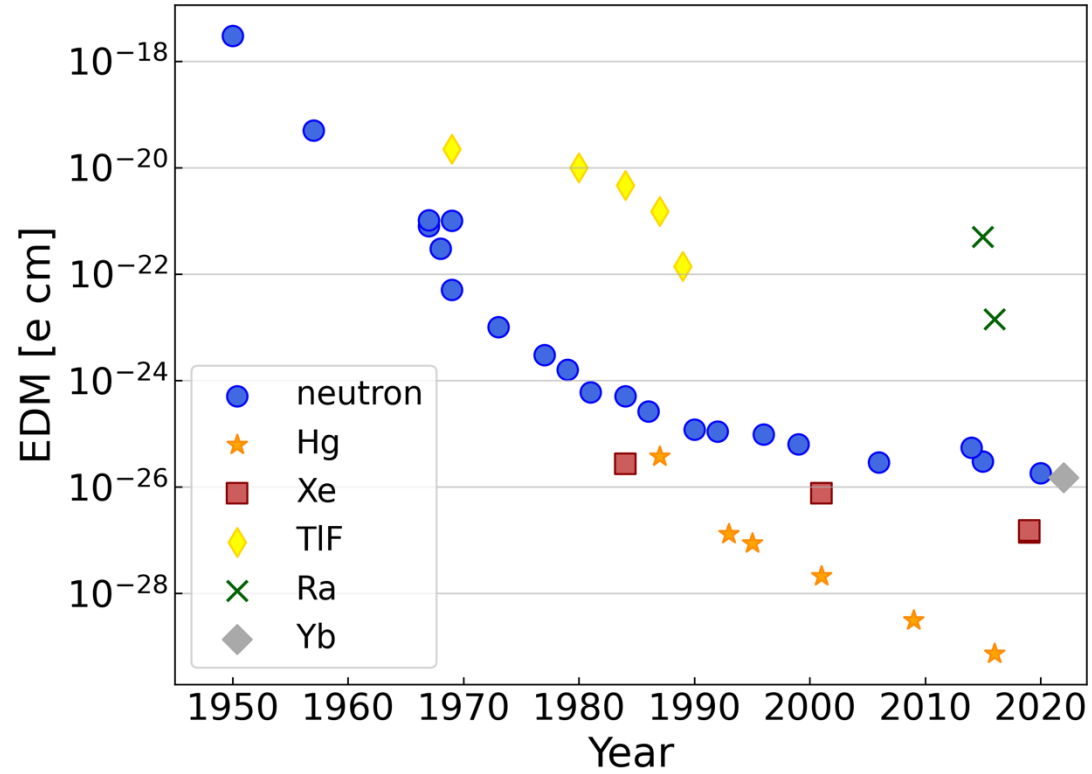
- ACME III apparatus fully operational at new location (Northwestern Univ.)

- Detection rate as anticipated, typical S/N = 1 JILA @ 1 hour

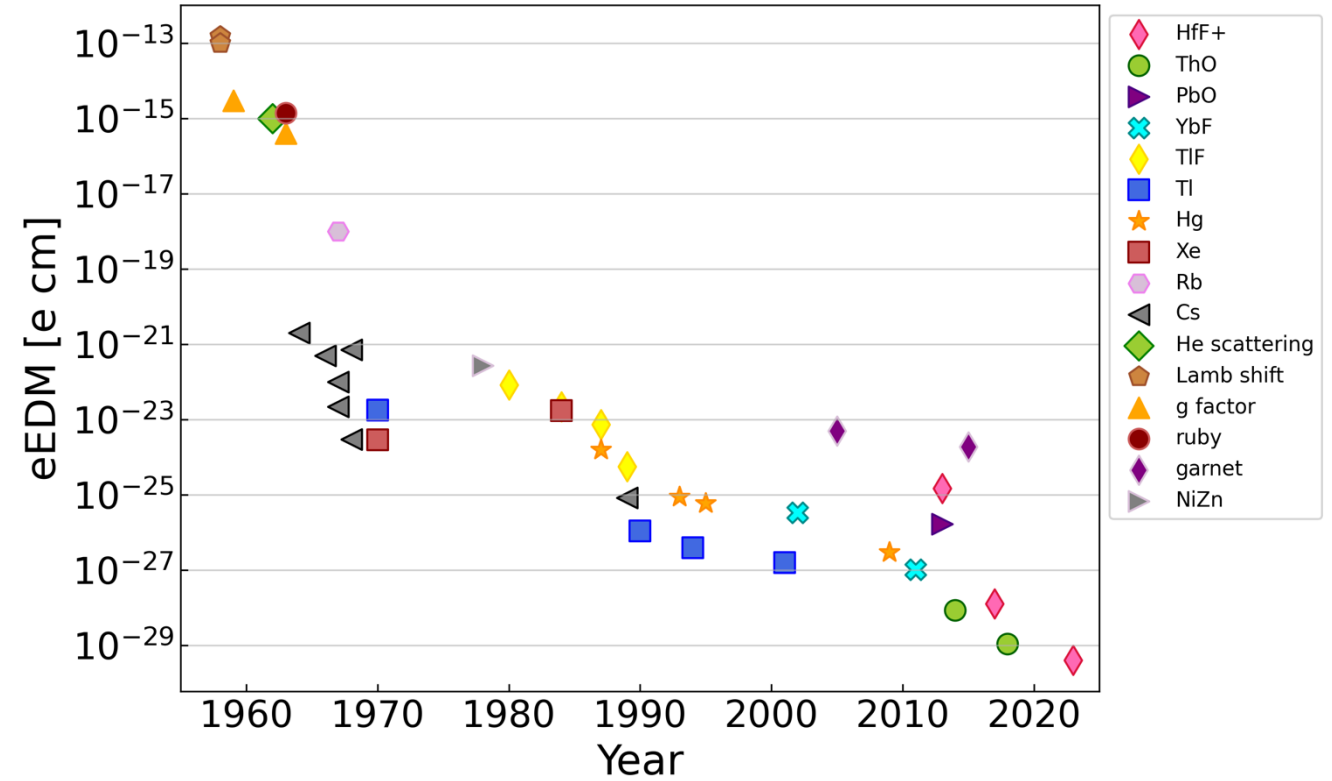
- Systematic error studies nearing conclusion
- Control of previously *known* systematics sufficient for 20x improvement vs JILA sensitivity (*B*- and *E*-field gradients, birefringence gradients)



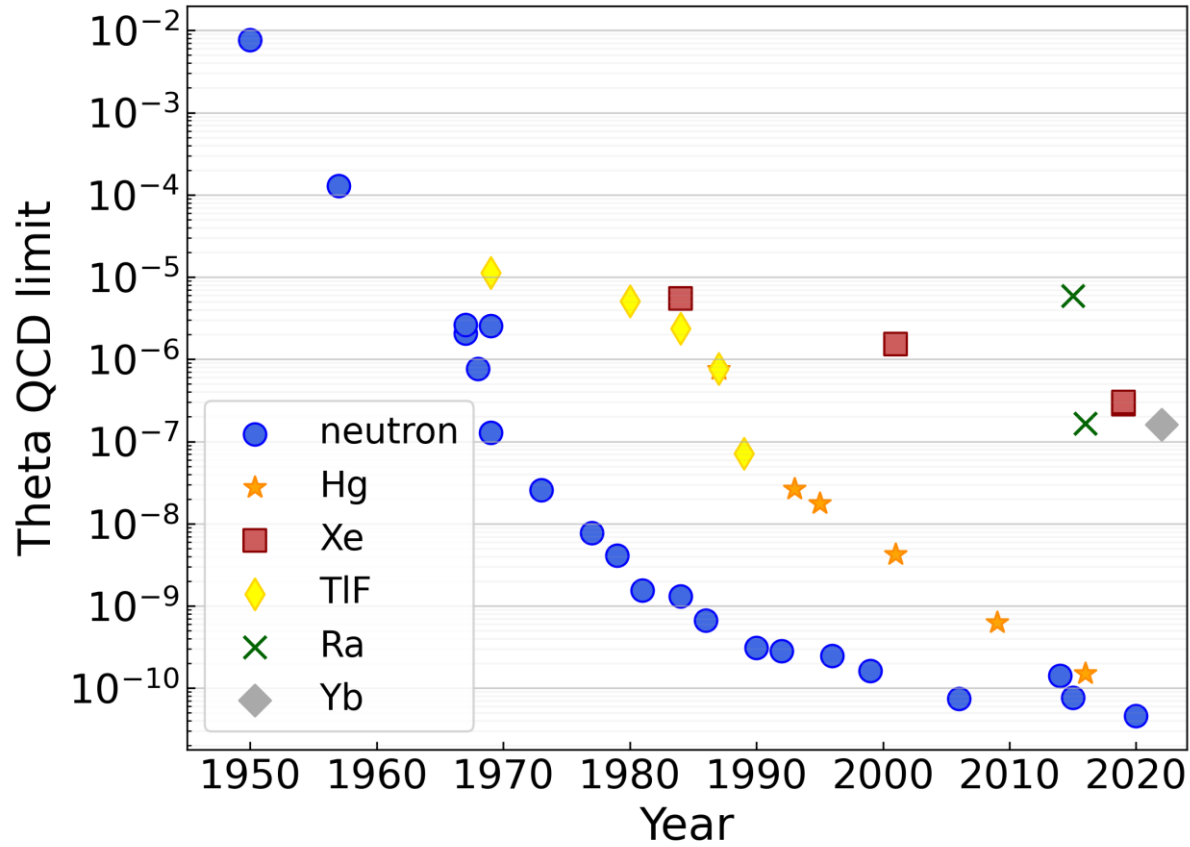
Hadronic EDMs



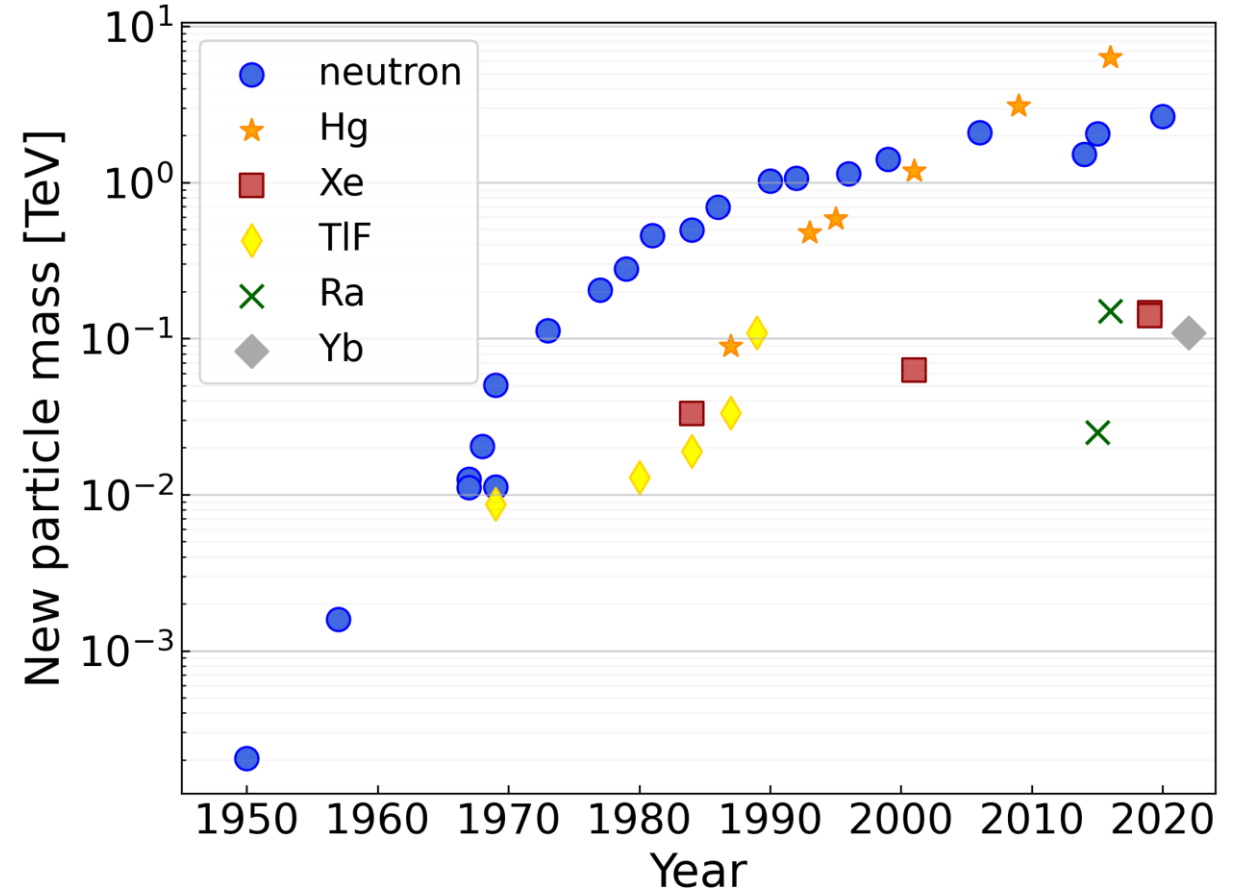
Electron EDM limits



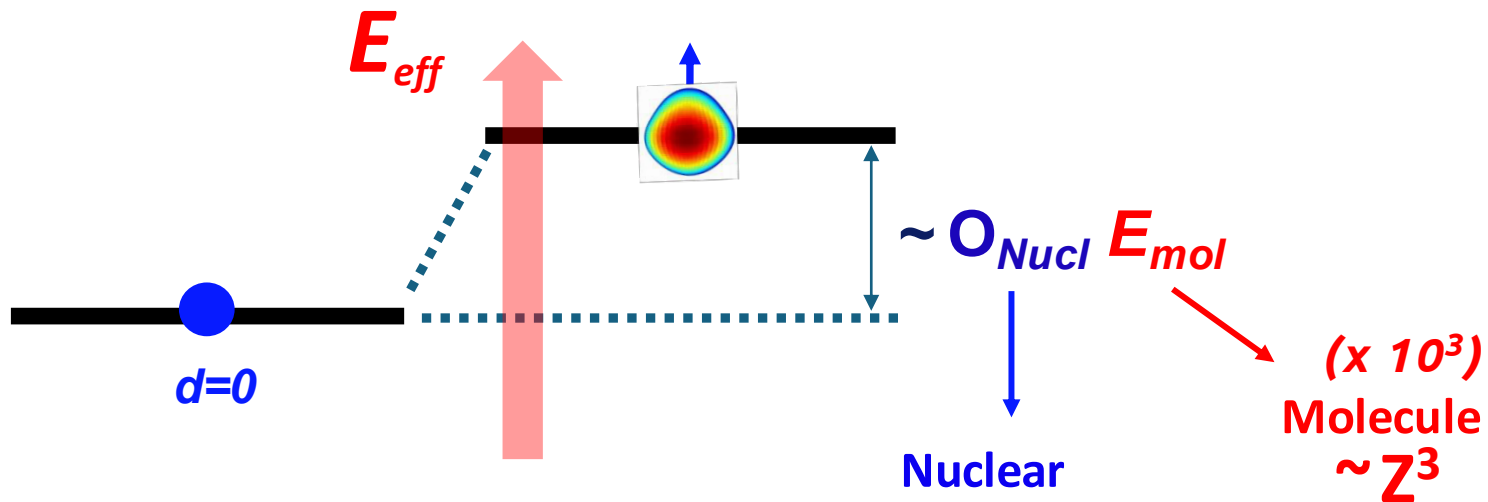
Theta QCD bounds



New particle mass reach



Why Radioactive Molecules?



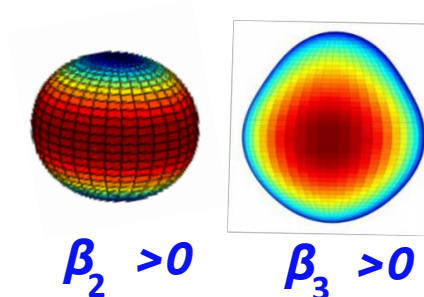
^{225}Ra ($Z=88$, $N=137$)
 $T_{1/2} = 15$ days



[Gaffney et al. Nature 497, 199 (2013)]

$$\sim Z A^{2/3} \beta_2 \beta_3^2 / (E_+^N - E_-^N)$$

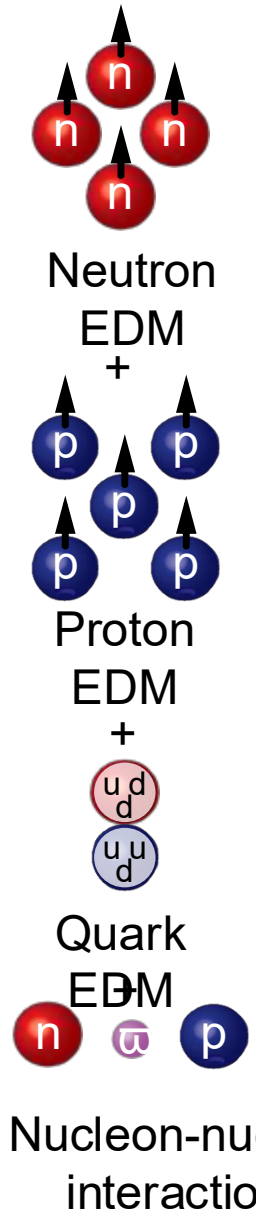
protons nuclear mass nuclear deformation nuclear levels



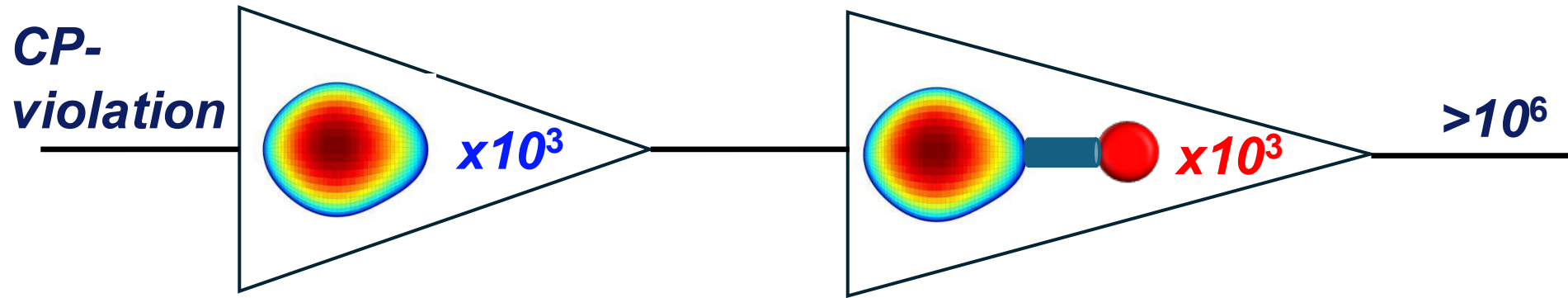
- ✓ Large Z, A
- ✓ Nuclear spin $I > 0$
- ✓ $\beta_2, \beta_3 > 0$

Enhanced in actinide, short-lived nuclei:
Fr ($Z=87$), Ra ($Z=88$), Th ($Z=90$), ...
($T_{1/2} \sim 22$ min) ($T_{1/2} \sim 15$ d) ($T_{1/2} \sim 19$ d)

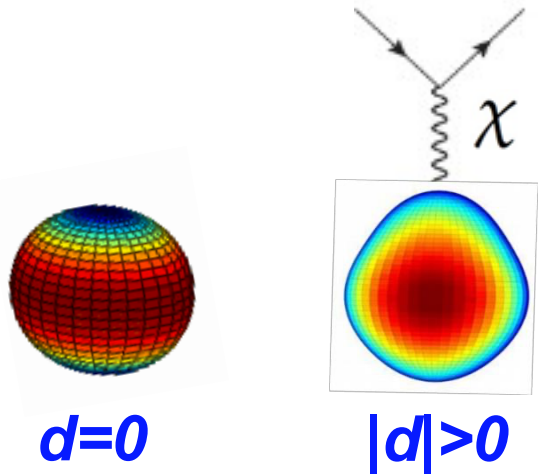
Radioactive Molecules => Best of both worlds!



Nuclear \times **Molecule**
 $(\times 10^3)$ $(\times 10^3)$

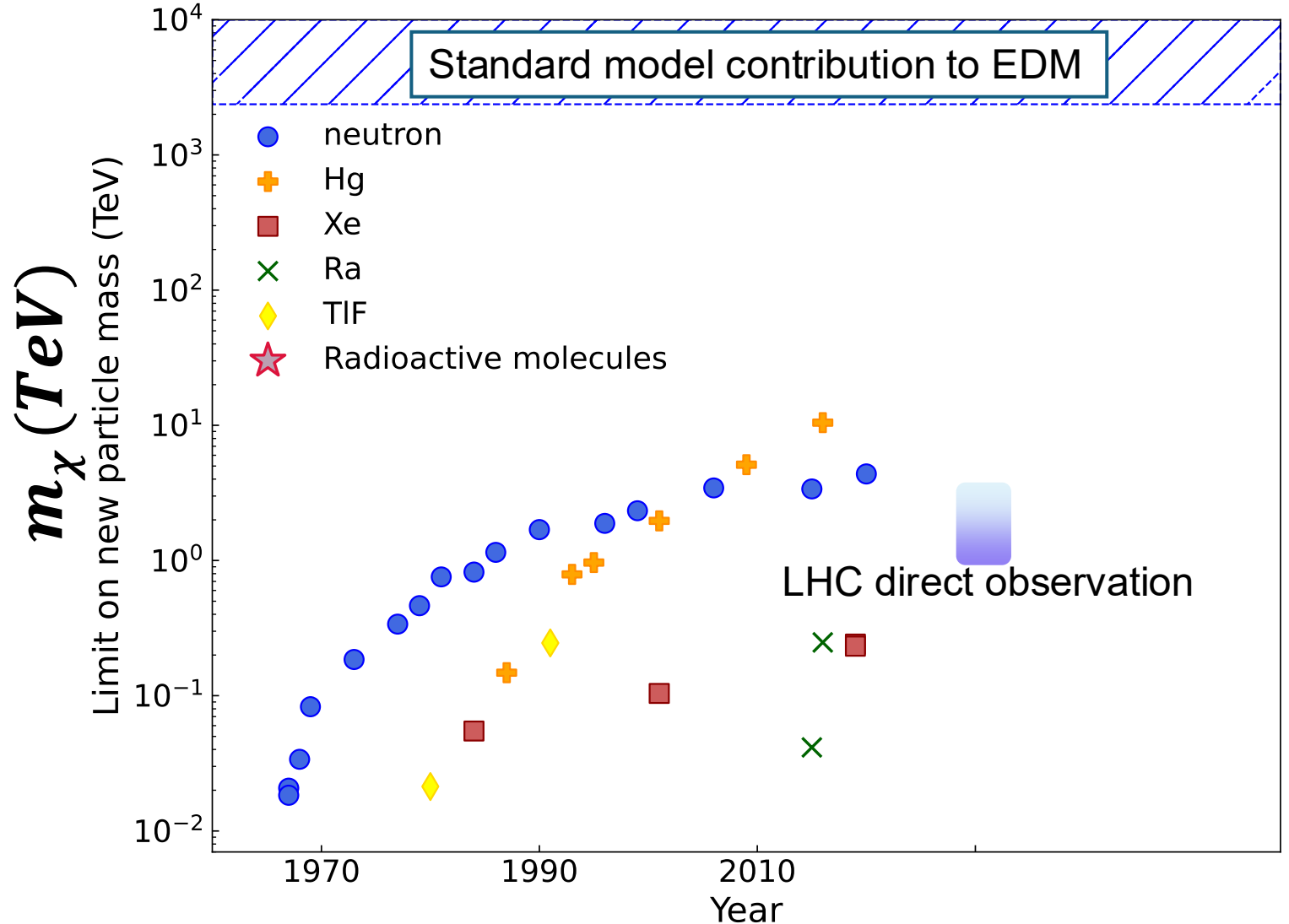


Molecules as Laboratories of Nuclear & Particle Physics

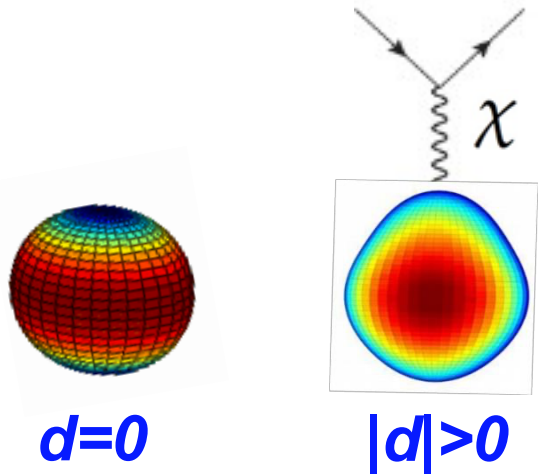


$$d_f \sim \frac{m_f}{m_\chi^2} g^2 \sin \phi_{CP}$$

$$m_\chi \sim \frac{1}{\sqrt{d_f}}$$



Molecules as Laboratories of Nuclear & Particle Physics



$$d_f \sim \frac{m_f}{m_\chi^2} g^2 \sin \phi_{CP}$$

$$m_\chi \sim \frac{1}{\sqrt{d_f}}$$

$$\Delta \sim \frac{1}{(d E_{mol} \tau \sqrt{N})}$$

